Gapless Topological Phases and Symmetry-Enriched Quantum Criticality

Ruben Verresen[1], Ryan Thorngren,[1,2,3] Nick G. Jones[4,5] and Frank Pollmann[6,7]

[1]*Department of Physics, Harvard University, Cambridge, Massachusetts 02138, USA*
[2]*Center of Mathematical Sciences and Applications, Harvard University,*
Cambridge, Massachusetts 02138, USA
[3]*Department of Physics, Massachusetts Institute of Technology, Cambridge, Massachusetts 02139, USA*
[4]*Mathematical Institute, University of Oxford, Oxford OX2 6GG, United Kingdom*
[5]*The Heilbronn Institute for Mathematical Research, Bristol BS8 1UG, United Kingdom*
[6]*Department of Physics, T42, Technische Universität München, 85748 Garching, Germany*
[7]*Munich Center for Quantum Science and Technology (MCQST), 80799 Munich, Germany*

We introduce topological invariants for gapless systems and study the associated boundary phenomena. More generally, the symmetry properties of the low-energy conformal field theory (CFT) provide discrete invariants establishing the notion of symmetry-enriched quantum criticality. The charges of nonlocal scaling operators, or more generally, of symmetry defects, are topological and imply the presence of localized edge modes. We primarily focus on the $1 + 1d$ case where the edge has a topological degeneracy, whose finite-size splitting can be exponential or algebraic in system size depending on the involvement of additional gapped sectors. An example of the exponential case is given by tuning the spin-1 Heisenberg chain to a symmetry-breaking Ising phase. An example of the algebraic case arises between the gapped Ising and cluster phases: This symmetry-enriched Ising CFT has an edge mode with finite-size splitting scaling as $1/L^{14}$. In addition to such new cases, our formalism unifies various examples previously studied in the literature. Similar to gapped symmetry-protected topological phases, a given CFT can split into several distinct symmetry-enriched CFTs. This raises the question of classification, to which we give a partial answer—including a complete characterization of symmetry-enriched $1 + 1d$ Ising CFTs. Nontrivial topological invariants can also be constructed in higher dimensions, which we illustrate for a symmetry-enriched $2 + 1d$ CFT without gapped sectors.

Subject Areas: Condensed Matter Physics,
Quantum Physics, Statistical Physics

I. INTRODUCTION

Topological phases of quantum matter are fascinating emergent phenomena, commonly characterized by non-local order parameters in the bulk and exotic behavior at the boundary. A subclass of gapped topological phases are the so-called symmetry-protected topological (SPT) phases, which are only nontrivial in the presence of certain global symmetries [1–8]. In one dimension, SPT phases have ground-state degeneracies associated with their boundaries called zero-energy edge modes [9,10]. These edge modes are often exponentially localized with the same length scale as the bulk correlation length, seemingly suggesting that the bulk gap is essential. However, in recent years, studies have shown the existence of critical chains that nevertheless host topologically protected edge modes, with either algebraic or exponential finite-size splitting [11–36]. Our work provides a unifying framework for this phenomenon, placing it into the more general context of symmetry-enriched quantum criticality. The idea is simple: A given universality class can split into various distinct classes when additional symmetries are imposed. These can be distinguished by symmetry properties of either local or nonlocal operators. The latter nonlocal case serves as a topological invariant and can imply emergent edge modes.

Our work unifies in two respects. First, as already mentioned, it offers a framework that incorporates previously studied examples, giving a common explanation for the observed edge modes at criticality while also introducing qualitatively novel cases. Second, the invariants we introduce are direct generalizations of those studied in the gapped case, protecting edge modes in both settings. In particular, gapped SPT and spontaneously symmetry-breaking (SSB) phases correspond to the special cases where the bulk universality class is chosen to be trivial

(i.e., there are no low-energy degrees of freedom). This puts in perspective how much is left to be explored: One can repeat the study and classification for any choice of universality class. In this work, we focus on universality classes described by conformal field theories (CFTs).

Examples of symmetry-enriched criticality are hiding in plain sight. These tend to occur at phase transitions where all neighboring gapped phases are nontrivial (either SPT or SSB). For example, a paradigmatic SPT phase is the Haldane phase realized in the spin-1 Heisenberg chain [3,10,37–40]. By introducing an easy-axis anisotropy, the SPT phase can be driven to an Ising phase:

$$H_{XXZ} = J\sum_n (S_n^x S_{n+1}^x + S_n^y S_{n+1}^y + \Delta S_n^z S_{n+1}^z). \quad (1)$$

These two gapped phases are separated by an Ising critical point at $\Delta_c \approx 1.1856$ [41]. We point out that, although the bulk correlation length diverges, a twofold degeneracy with open boundaries remains exponentially localized, shown in Fig. 1. We show that this Ising CFT is topologically enriched by π rotations around the principal axes (a $\mathbb{Z}_2 \times \mathbb{Z}_2$ group), explaining the observed edge modes.

The concepts developed in this work apply to symmetry-enriched CFTs with a general on-site symmetry group G; we refer to them also as G-enriched CFTs, or G-CFTs for short. This is not only relevant for condensed matter systems, such as the example described above, but also to high-energy physics; in particular, G-CFTs can be related to discrete torsion of orbifold CFTs arising in string theory [42–45], although edge modes have not yet been pointed out in that context. While we introduce our framework for general symmetry groups G and discuss a variety of examples, for clarity we illustrate these concepts in detail for two particular symmetry groups: the unitary
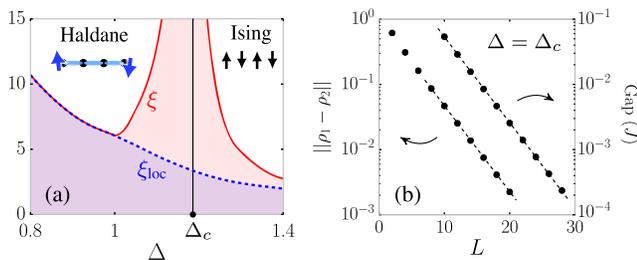
group $\mathbb{Z}_2 \times \mathbb{Z}_2$ and the antiunitary $\mathbb{Z}_2 \times \mathbb{Z}_2^T$ (where complex conjugation is defined relative to an on-site basis). In particular, for the Ising CFT, the former (latter) symmetry group gives rise to edge modes whose finite-size splitting is exponentially (algebraically) small in system size. For the algebraic splitting, we show that the power is remarkably high, scaling as $1/L^{14}$. This is derived by studying the symmetry properties of descendant operators in the CFT. To emphasize the generality of our approach, we present examples for other symmetry groups, including $U(1) \times \mathbb{Z}_2 \times \mathbb{Z}_2^T$, $U(1) \rtimes \mathbb{Z}_2^T$, and $\mathbb{Z}_3 \times \mathbb{Z}_3$. We also discuss the classification of such symmetry-enriched CFTs, providing a complete answer in the case of the Ising CFT for a general symmetry group G. The topological invariants we introduce can also be generalized to higher dimensions, which we illustrate at the end of this work.

The remainder of this paper is organized as follows. Since the essential concepts can be readily understood, we give an overview in Sec. II. This provides a self-contained summary for the reader in a hurry and can serve as a guide to the other sections. In particular, it introduces and motivates the notion of symmetry flux: This is the key player throughout this work and allows us to define topological invariants at criticality. Moreover, Sec. II gives a sense of how this invariant protects edge modes at criticality. Symmetry fluxes and edge modes are discussed more systematically in Secs. III and IV, respectively. Section V concerns the classification of G-enriched CFTs. A $\mathbb{Z}_3 \times \mathbb{Z}_3$ and a fermionic $\mathbb{Z}_2^f \times \mathbb{Z}_2^T$ example are presented in Sec. VI, and in Sec. VII we show how previous works fit into our framework. Finally, Sec. VIII discusses generalizations to higher dimensions.

II. A CONCEPTUAL OVERVIEW

This section functions as a primer, motivating concepts introduced in greater generality in subsequent sections. The reader seeking a taste of symmetry-enriched criticality may choose to read only this section. Alternatively, readers preferring generality and not requiring motivational examples may skip this section altogether and continue to Sec. III.

We first review the known order parameters for gapped phases in 1D, which are either local (SSB) or non-local (SPT). In Sec. II B, we show that, similarly, critical points can also host local and nonlocal order parameters. Nontrivial nonlocal order parameters can be related to the existence of edge modes discussed in Sec. II C. Comments on the classification of such symmetry-enriched critical points, fermionic versions, and higher-dimensional generalizations can be found in Secs. II D, II E and II G. These subsections serve as pointers to the main sections of this paper.

In order to present some of the key concepts of this work in a simple manner, in this overview we fix the symmetry

FIG. 1. Persistent edge mode in a spin-1 XXZ chain at criticality. (a) The bulk correlation length ξ blows up, whereas the edge mode localization length ξ_{loc} stays finite. (b) The latter can be measured in two ways: the two ground states $|\uparrow_l \downarrow_r\rangle \pm |\downarrow_l \uparrow_r\rangle$ have a splitting which is exponentially small in system size L, or, equivalently, the two states differ by an operator which is exponentially localized near the edges (L is the region we trace out near an edge before calculating the distance of the two density matrices). The dashed lines are proportional to $\exp(-L/\xi_{loc})$ with $\xi_{loc} \approx 3.3$.

group $G = \mathbb{Z}_2 \times \mathbb{Z}_2^T$ as an illustrative example ($\mathbb{Z}_2^T$ denotes the group generated by an antiunitary symmetry that squares to the identity). Other symmetry groups encountered in this work include $\mathbb{Z}_2 \times \mathbb{Z}_2$ (Sec. III), $\mathbb{Z}_3 \times \mathbb{Z}_3$ and $\mathbb{Z}_2^f \times \mathbb{Z}_2^T$ (Sec. VI), $U(1) \times \mathbb{Z}_2 \times \mathbb{Z}_2^T$, $U(1) \rtimes \mathbb{Z}_2^T$ (Sec. VII), and $\mathbb{Z}_2 \times \mathbb{Z}_2 \times \mathbb{Z}_2$ (Sec. VIII). Below, we consider spin-1/2 chains, denoting the Pauli matrices by X, Y, and Z, and representing the symmetry group $\mathbb{Z}_2 \times \mathbb{Z}_2^T$ by the spin-flip $P \equiv \prod_n X_n$ and an antiunitary symmetry given by complex conjugation in this basis, $T \equiv K$.

A. Local and nonlocal order parameters for gapped phases

Naturally, phases that spontaneously break a symmetry can be diagnosed by long-range order of some local operator with a nontrivial charge (i.e., the operator does not commute with the symmetry). The standard example is the Ising chain $H_{\text{Ising}} = -\sum_n Z_n Z_{n+1}$, where the ground state has $\lim_{|n-m|\to\infty} \langle Z_m Z_n \rangle \neq 0$. Since Z_n has charge -1 under the $\mathbb{Z}_2$ Ising symmetry P, this is distinct from the trivial phase, which can have long-range correlations only for operators with charge $+1$. Moreover, a physical state (i.e., without long-range cat-state-like entanglement) will obey clustering: $\lim_{|n-m|\to\infty} \langle Z_m Z_n \rangle = \langle Z_m \rangle \langle Z_n \rangle$. We conclude that $\langle Z_n \rangle \neq 0$, which means the ground state is no longer invariant under the $\mathbb{Z}_2$ symmetry (otherwise, $\langle Z_n \rangle = \langle Z_n P \rangle = -\langle P Z_n \rangle = -\langle Z_n \rangle \Rightarrow \langle Z_n \rangle = 0$), implying a ground-state degeneracy.

In the presence of $\mathbb{Z}_2$ symmetry there is only one symmetry-breaking "Ising" phase. If we additionally impose complex conjugation symmetry $\mathbb{Z}_2^T$, then this single Ising phase subdivides into two distinct phases. Indeed, consider $H'_{\text{Ising}} = -\sum_n Y_n Y_{n+1}$. If we preserve only $\mathbb{Z}_2$, one can smoothly connect H_{Ising} to H'_{Ising} without closing a gap by rotating Y_n into Z_n. However, the Ising order parameter Y_n is imaginary, whereas Z_n is real. Hence, these two Hamiltonians cannot be connected while preserving $\mathbb{Z}_2 \times \mathbb{Z}_2^T$. They must be separated by a quantum phase transition. (In fact, a direct phase transition between the two (e.g., the XX chain) would be an example of a deconfined quantum critical point in one dimension [46–48].) We see in Sec. II B that if the system is gapless, the charges of local operators can distinguish phases even in the absence of symmetry breaking.

A SPT phase, on the other hand, cannot be probed by any local observable. Instead, one can associate with any (this is simplest for on-site symmetries; for other cases, see Ref. [49]) unbroken symmetry a string order parameter (this is derived using the concept of symmetry fractionalization [2,40] as we discuss in Sec. III and review in the Appendix A 3). For instance, the trivial paramagnet $H_{\text{triv}} = -\sum_n X_n$ has long-range order $\lim_{|n-m|\to\infty} \langle X_m X_{m+1} \cdots X_{n-1} X_n \rangle \neq 0$, whereas the paradigmatic cluster SPT model [50–54]

$$H_{\text{cluster}} = -\sum_n Z_{n-1} X_n Z_{n+1} \tag{2}$$

has long-range order

$$\lim_{|n-m|\to\infty} \langle Z_{m-1} Y_m X_{m+1} \cdots X_{n-1} Y_n Z_{n+1} \rangle \neq 0. \tag{3}$$

(the simplest way of deriving this is by noting that it equals the product $\prod_{k=m}^n Z_{k-1} X_k Z_{k+1}$, and $Z_{k-1} X_k Z_{k+1} = +1$ in the ground state). We see that in both cases, the string is made out of the unbroken $\mathbb{Z}_2$ symmetry P. However, their end-point operators are distinct: In the trivial (nontrivial) case it is real (imaginary). As before, these discretely distinct charges mean that the two Hamiltonians must be separated by a quantum phase transition.

In the SSB case, the long-range order of a local operator together with the clustering property allows us to derive a bulk degeneracy. This does not work for stringlike objects since there is no natural way of factorizing the correlation function. However, if we consider the system with open boundaries, then it is well defined to consider a string with a single end point (i.e., the other end disappears into the boundary). More precisely, consider the long-range order with the end points of the strings close to the left and right boundary; now act with the global symmetry $\prod_n X_n$ and apply clustering. It is for this reason that SPT phases come with protected zero-energy edge modes. In the case of the above cluster model, there is a protected qubit (a Kramers pair) at each edge, giving a global fourfold degeneracy with open boundaries [50–54].

More generally, the string order parameter [49,55] for an on-site symmetry $\prod_n U_n$ has the form

$$\mathcal{S}_n = \cdots U_{n-2} U_{n-1} \mathcal{O}_n, \tag{4}$$

where $\mathcal{O}_n$ is some local operator such that $\langle \mathcal{S}_m^\dagger \mathcal{S}_n \rangle$ has long-range order, as in Eq. (3). In this work, we use the term "symmetry flux" for such a string operator. In principle, one could use this terminology more broadly for any string operator of the form of Eq. (4), since it acts like a source of flux for operators charged under the symmetry (see Sec. II G). We use this term in the more restrictive sense (i.e., for end-point operators that give rise to long-range order) since it is the symmetry properties of its end-point operator $\mathcal{O}_n$ which encode the projective representation (or, equivalently, the second group cohomology class) labeling the gapped phase [49,55]. (Relatedly, it has been appreciated how SPT phases can be diagnosed by what happens when you gauge the global symmetry, in which case, these symmetry fluxes become local operators [56]; see also Refs. [57,58].) In this work, we generalize these string order parameters (equivalently, symmetry fluxes) to cases where long-range order is replaced by "longest-range order" as we discuss now.

B. Generalized order parameters for gapless phases

We see that for gapped phases the key idea is that symmetry properties of both local and nonlocal operators allow us to define discrete invariants. We now show that this generalizes to gapless phases.

Let us note that we do not consider the trivial instance where the symmetry group of interest acts exclusively on gapped degrees of freedom (i.e., gapless modes would be uncharged). For instance, if one stacks a gapped SPT phase on top of a critical chain such that all the symmetries protecting the former act trivially on the latter, then the SPT phase is automatically stable by virtue of, e.g., there not being any symmetry-allowed way of coupling the SPT edge mode operators to the critical bulk. We exclude such cases, instead focusing on situations where (part of) the protecting symmetry acts on the gapless low-energy theory—making the gaplessness an essential piece of the physics at play. Remarkably, there are still local and nonlocal order parameters in this case.

The simplest example—with a local order parameter—is given by the two critical Ising chains:

$$H = -\sum_n (Z_n Z_{n+1} + X_n),$$
$$H' = -\sum_n (Y_n Y_{n+1} + X_n). \tag{5}$$

These are at a phase transition between the trivial paramagnet and the above H_{Ising} and H'_{Ising}, respectively. Both are described by the Ising universality class, or, equivalently, the CFT with central charge $c = 1/2$ [59]. This universality class has a unique local operator $\sigma(x)$ with scaling dimension $\Delta_\sigma = 1/8$ [meaning that $\langle \sigma(x)\sigma(0)\rangle \sim 1/x^{2\Delta_\sigma}$] [59]. The lattice operators that have overlap with this continuum field σ are naturally given by the Ising order parameters of the nearby phases, i.e., $\sigma(x) \sim Z_n$ for H and $\sigma(x) \sim Y_n$ for H' [60]. We observe that these two operators transform differently under complex conjugation T. We say that these two Ising CFTs are enriched by the $\mathbb{Z}_2^T$ symmetry T, with the former CFT obeying $T\sigma T = +\sigma$ and the latter $T\sigma T = -\sigma$. Indeed, one can argue that this charge is always discrete, i.e., $T\sigma T = \pm\sigma$, and that it is well defined; i.e., all choices of lattice operators that generate σ in the low-energy effective theory have the same charge (or sign) if T is an unbroken symmetry. [Both statements follow from that the fact that if $\mathcal{O}_1$ and $\mathcal{O}_2$ both generate σ, then $\langle \mathcal{O}_1 \mathcal{O}_2 \rangle \neq 0$ (following from the fusion rule $\sigma \times \sigma = 1 + \varepsilon$), which must be real if T is unbroken.] This discrete invariant cannot change as long as we stay within the Ising universality class.

What is the consequence of such an invariant? It means that any G-symmetric path (here $G = \mathbb{Z}_2 \times \mathbb{Z}_2^T$) of gapless Hamiltonians connecting H and H' must at some point go through a different universality class. For example, consider the interpolation $\lambda H + (1 - \lambda)H'$ (with $0 \leq \lambda \leq 1$):

This is everywhere in the Ising universality class except at the halfway point $\lambda = 1/2$, where the system passes through a multicritical point (with a dynamical critical exponent $z_{\text{dyn}} = 2$). Alternatively, $\lambda H - (1 - \lambda)H'$ passes through a Gaussian fixed point (central charge $c = 1$) at $\lambda = 1/2$. It is at these non-Ising points that the property $T\sigma T = \pm\sigma$ changes. Of course, the G symmetry of the path is key: H and H' are unitarily equivalent by a rotation around the x axis $e^{-i\alpha \sum_n X_n}$ ($0 \leq \alpha \leq \pi/4$), but this path violates complex conjugation symmetry T. This is similar to how we see that the nearby gapped phases H_{Ising} and H'_{Ising} are distinguished by the additional symmetry.

The above examples could be distinguished by symmetry properties of local operators. A more interesting case is when two enriched critical points can be distinguished only by the symmetry properties of nonlocal operators. An example is given by

$$H = -\sum_n (Z_n Z_{n+1} + X_n),$$
$$H'' = -\sum_n (Z_n Z_{n+1} + Z_{n-1} X_n Z_{n+1}). \tag{6}$$

The former (latter) is a phase transition between the trivial phase and the Ising (cluster SPT) phase that we encounter above. These two systems H and H'' cannot be distinguished by a local operator; in particular, both are described by the Ising universality class with $\sigma(x) \sim Z_n$ [61], implying $T\sigma T = +\sigma$. In previous work, H and H'' were shown to be topologically distinct by mapping them to free-fermion chains and then appealing to a winding number [33,61]. In this work, we go significantly beyond this by identifying a topological invariant which is well defined in the presence of interactions. Indeed, the Ising CFT also has a nonlocal operator $\mu(x)$ with scaling dimension $\Delta_\mu = 1/8$—this is related to the local $\sigma(x)$ under Kramers-Wannier duality. For the usual critical Ising chain, this is known to be the string operator $\mu(x) \sim \cdots X_{n-2}X_{n-1}X_n$ at any position n. For H'', however, one can show that $\mu(x) \sim \cdots X_{n-2}X_{n-1}Y_n Z_{n+1}$ [61]. [Note that in both cases, the nearby symmetry-preserving phase [62] has long-range order $\lim_{|x-y|\to\infty}\langle \mu(x)\mu(y)\rangle \neq 0$—see, e.g., Eq. (3)—as expected by Kramers-Wannier duality.] This suggests that the two models are two distinct G-enriched Ising CFTs distinguished by $T\mu T = \pm\mu$. To establish this, we need to ensure that the charge of μ is well defined; i.e., that it is independent of our choice of operator on the lattice. This requires us to generalize the notion of symmetry flux or string order parameter (which we review in the previous subsection) to gapless cases.

The symmetry flux of $P = \prod_n X_n$ is a string operator consisting of the same on-site unitaries as P, i.e., $S_n = (\prod_{m<n} X_m)\mathcal{O}_n$, with a condition on the end-point operator $\mathcal{O}_n$. In the gapped case, we can choose the latter

such that the string operator has long-range order. In the gapless case, we generalize this condition by demanding that $\mathcal{O}_n$ is chosen such that $\langle \mathcal{S}_m^\dagger \mathcal{S}_n \rangle$ has the slowest possible algebraic decay. For the Ising CFT, it is known that $\Delta = 1/8$ is the smallest possible scaling dimension [59]. Hence, the above discussion about μ tells us that the symmetry flux of P has the end-point operator $\mathcal{O}_n = X_n$ for H and $\mathcal{O}_n = Y_n Z_{n+1}$ for H''; note that their charges under T are distinct. One can argue—as we do in Sec. III— that once one fixes the $\mathbb{Z}_2$ symmetry under consideration (here P), then the Ising universality class has a unique symmetry flux, even in the presence of additional gapped degrees of freedom [63]. This means that we have a well-defined charge $T\mu T = \pm\mu$. We say that the above two models H and H'' realize two distinct $(\mathbb{Z}_2 \times \mathbb{Z}_2^T)$-enriched Ising CFTs. Moreover, since this is based on charges of nonlocal operators, we say that they are topologically distinct.

We thus propose that distinct symmetry-enriched CFTs can be distinguished by how symmetry fluxes of $g \in G$ are charged under the other symmetries in G. For the models in Eq. (6), the discrete invariant is the sign picked up when conjugating the symmetry flux of P by T. A nice feature of this definition of symmetry flux is that in the gapped case it reduces to the usual string order parameter. Indeed, in that case, asking for the slowest possible decay is asking for long-range order. Moreover, in the gapped symmetry-preserving case, one can argue that the symmetry flux is always unique in one spatial dimension; this follows from the principle of symmetry fractionalization [1,2]. Indeed, the symmetry properties of its end-point operator $\mathcal{O}_n$ encode the projective representation (or, equivalently, the second group cohomology class) labeling the gapped phase. In the gapless case, the uniqueness or degeneracy of the symmetry flux depends on the particular CFT, as we discuss in detail in Sec. III.

C. Edge modes from charged symmetry fluxes

If a symmetry flux has a nontrivial charge under another symmetry, then this can be linked to ground-state degeneracies in the presence of open boundary conditions. This is well known for the case with a bulk gap [49], and in this work we show that it extends to the gapless case. We argue this more generally in Sec. V; here we illustrate this for the lattice model H'' in Eq. (6), taking a half-infinite system with sites $n = 1, 2, \ldots$. We show that the boundary of this critical chain spontaneously magnetizes (see Ref. [28] for a related system with $G = \mathbb{Z}_2 \times \mathbb{Z}_2$). Indeed, on the lattice we see that Z_1 commutes with H''; the spontaneous edge magnetization $Z_1 = \pm 1$ thus gives a twofold degeneracy. To see that this magnetization is not a mere artifact of our fine-tuned model, we can study its stability in the Ising CFT starting with $\langle \sigma(x \approx 0) \rangle \neq 0$ (with the boundary at $x = 0$). If we add the P-symmetry flux $\mu(0)$ to the Hamiltonian, this would connect the two ordering directions and hence

destabilize them. This is what would happen for the usual Ising chain H, where the symmetry flux is condensed near the boundary ($\langle \mu(0) \rangle \neq 0$), giving us a symmetry-preserving boundary condition ($\langle \sigma(0) \rangle = 0$) [64]. However, if $T\mu T = -\mu$, the $\mathbb{Z}_2^T$ symmetry prevents us from adding this perturbation, and, remarkably, the edge magnetization is stable. Indeed, in Sec. IV we show that all *symmetry-allowed* perturbations correspond to operators with scaling dimension greater than one, implying that they are irrelevant for the boundary RG flow. In summary, the zero-dimensional edge spontaneously breaks P symmetry stabilized by the $(\mathbb{Z}_2 \times \mathbb{Z}_2^T)$-enriched bulk CFT.

It is important to note that this degeneracy crucially relies on the presence of an edge. The key reason for this is that, while $\mu(x)$ is nonlocal in the bulk, it is local near a boundary. I.e., its string can terminate [note that terminating its string in the bulk would effectively lead to a two-point operator $\mu(x)\mu(y)$]; see Sec. IV for how this enters the general argument. Indeed, H'' has a unique ground state with periodic boundary conditions. In fact, in that case H and H'' are related by the unitary transformation $U = \prod_n (CZ)_{n,n+1}$, where CZ is the control-Z gate, and it is well established that the critical Ising chain H has a unique ground state. This unitary transformation also relates the trivial gapped phase to the nontrivial gapped cluster phase [51].

Thus far, we have focused on a single end, giving the complete story for a half-infinite system. For a finite system of length L, we need to consider the finite-size splitting of the symmetry-preserving states which entangle both edges:

$$| \uparrow_l \uparrow_r \rangle \pm |\downarrow_l \downarrow_r \rangle \quad \text{and} \quad | \uparrow_l \downarrow_r \rangle \pm |\downarrow_l \uparrow_r \rangle. \qquad (7)$$

In general, to analytically determine such finite-size splitting, it is useful to start in the scale-invariant RG fixed-point limit and then consider what additional perturbations are necessary to distinguish the states. For example, if the system is gapped, then all four states in Eq. (7) are degenerate in the fixed-point limit. The only way a local perturbation can then couple the two edges is at Lth order in perturbation theory. Indeed, for gapped SPT phases, the finite-size splitting is exponentially small in system size [54]. For critical systems, however, the RG fixed-point limit is richer, being described by a CFT. In particular, it is known [65] that the two antiferromagnetic states in Eq. (7) are split from the ferromagnetic ones at the energy scale $1/L$, the same as the finite-size bulk gap. This is due to the spontaneous boundary magnetizations sensing their (mis) alignment through the critical bulk. The remaining two states $| \uparrow_l \uparrow_r \rangle \pm |\downarrow_l \downarrow_r \rangle$ are exactly degenerate within the CFT. They can be split by perturbing away from the fixed-point limit by adding RG-irrelevant perturbations. The splitting can already occur at second order in perturbation theory (intuitively, each edge has to couple to the critical bulk). Nevertheless, we show that the

dominant contribution has a surprisingly large power, scaling as $1/L^{14}$, caused by the so-called seventh descendant of μ; see Sec. IV for a derivation.

The above twofold degeneracy with open boundaries is the generic result for a topologically nontrivial symmetry-enriched Ising CFT. The nature of its finite-size splitting depends on the protecting symmetry. In the above case, where μ is odd under an antiunitary symmetry, we find an algebraic splitting of order $1/L^{14}$. In other scenarios, μ may be odd under a symmetry associated with additional gapped degrees of freedom, which by the same perturbative argument would lead to an exponentially small finite-size splitting. The latter case is in agreement with the observations in Ref. [28] and is also what we observe in Fig. 1. Both scenarios are discussed in detail in Sec. IV.

Since algebraically localized edge modes are not common in the current literature (exceptions being systems with long-range interactions [66–69]), one might wonder to what extent they are, in fact, localized. The key feature that makes an edge mode meaningful is normalizability. Indeed, this is what allows one to make statements of the type "90% of the weight is contained in the first five sites." Algebraic modes can still be normalizable. For instance, suppose one has a Majorana edge mode of the form $\gamma_L \sim \sum_n (1/n^\alpha)\gamma_n$ (where γ_n is a Hermitian Majorana mode on site n, satisfying $\{\gamma_n, \gamma_m\} = 2\delta_{n,m}$), by which we mean [70] that if $|\psi\rangle$ is a ground state, then so is $\gamma_L|\psi\rangle$. Then, $\gamma_L^2 = \frac{1}{2}\{\gamma_L, \gamma_L\} \sim \sum_n (1/n^{2\alpha})$, which is finite if $\alpha > 1/2$; i.e., the operator is normalizable. Relatedly, an algebraic edge mode has a localization length. One way of understanding this is by noting that their localization is determined by perturbations which are irrelevant in the renormalization-group flow, and such operators naturally have a length scale. To the best of our knowledge, this work contains the first example of an algebraically localized edge mode that cannot be destroyed while preserving the symmetry and universality class.

D. Classifying G-CFTs

In Sec. II B, we define discrete invariants. Two natural questions arise: Given a universality class, how many distinct invariants can one realize, and are these invariants complete? More precisely, if all local operators and symmetry fluxes have the same symmetry properties, can the models be smoothly connected while preserving their universality class? We explore this in Sec. V, arguing that these invariants are indeed complete for the Ising CFT. In particular, we discuss the case of the symmetry group $G = \mathbb{Z}_2 \times \mathbb{Z}_2$ for illustrative purposes. We first recall the six distinct gapped phases in this symmetry class, after which we study the universality classes that naturally arise at the direct transitions between these phases. In particular, we find nine distinct $(\mathbb{Z}_2 \times \mathbb{Z}_2)$-enriched Ising $(c = 1/2)$ universality classes, whereas we show that all $(\mathbb{Z}_2 \times \mathbb{Z}_2)$-enriched Gaussian $(c = 1)$

transitions can be connected (if they have minimal codimension, as we explain in Sec. V). For the $c = 1$ case, we construct exactly solvable models that allow us to connect symmetry-enriched CFTs which have seemingly distinct symmetry properties. This is possible since—unlike for the Ising CFT—there is a connected family of different $c = 1$ universality classes along which scaling dimensions can cross, such that the symmetry properties of symmetry fluxes need not be invariant for $c = 1$. However, as we discuss in Secs. V and VII, there are still nontrivial G-CFTs for $c \geq 1$.

E. Majorana edge modes at criticality

The edge mode encountered in the spin chain H'' in Eq. (6) is rather unusual from the gapped perspective. First, the ground state is unique with periodic boundary conditions, and twofold degenerate with open boundaries (we do not count the states whose finite-size splitting scales as the bulk gap of order $1/L$). There is no gapped bosonic SPT phase with this property. Moreover, while the ground states $|\uparrow_l \uparrow_r\rangle \pm |\downarrow_l \downarrow_r\rangle$ can be toggled by a local edge mode operator $Z_1 \sim \sigma(0)$, such cat states are unstable, and the system would collapse into $|\uparrow_l \uparrow_r\rangle$ or $|\downarrow_l \downarrow_r\rangle$ (i.e., the zero-dimensional edges exhibit spontaneous symmetry breaking, which is not possible in the absence of a bulk). In this collapsed basis, one would need an extensive operator P to toggle between them.

In Sec. VI B we show that under a Jordan-Wigner transformation, the above becomes a fermionic example where the edge mode is more conventional: The bulk is a free Majorana $c = \frac{1}{2}$ CFT, and each boundary hosts a localized zero-energy Majorana edge mode. This system has the same ground-state degeneracy as the usual gapped Kitaev chain [71]. Moreover, similar to the latter, there is an edge Majorana operator that toggles between the two (stable) ground states. The system is characterized by the symmetry flux of fermionic parity symmetry being odd under spinless time-reversal symmetry.

This critical Majorana chain arises as a phase transition from the gapped phase with two Majorana modes (per edge) protected by spinless time reversal, to the Kitaev chain phase with one Majorana mode (per edge); at the transition, one edge mode delocalizes, becoming the bulk critical mode, whereas the other mode remains localized [33]. Mapping this back to the spin-chain language, starting from the gapped cluster phase, two of the four degenerate ground states with open boundary conditions have a splitting that is determined by the bulk correlation length: These become delocalized at the critical point toward the Ising phase, with only the above twofold degeneracy remaining. Entering the gapped Ising phase, we have an edge magnetization which gradually merges with the bulk magnetization as we go deeper into the phase; see also Ref. [72] where an analogous case with gapped degrees of freedom is discussed.

F. A unified language

There is already a considerable body of work on critical one-dimensional systems with topological edge modes [11–36]. Section VII is devoted to demonstrating how our formalism allows us to unify previous works. We illustrate this for Refs. [11,16,19,28,33], showing how the models introduced therein can be interpreted as G-enriched Ising or Gaussian CFTs. This automatically identifies novel discrete bulk invariants for these systems in terms of their symmetry fluxes, ensuring the presence of protected edge modes.

G. Generalization to arbitrary dimensions: Twisted sectors

While the present work focuses on one spatial dimension, these concepts can be generalized to higher dimensions, which is the focus of Sec. VIII. To this end, we first reformulate the topological invariant in the one-dimensional case. Any string operator associated with an on-site symmetry U can be interpreted as creating a flux for that symmetry. To see this, one can imagine inserting this operator in spacetime, then any operator charged under U will pick up a phase factor when encircling the end point of the string—the defining characteristic of a flux. More precisely, in Sec. VIII we explain how the operator-state correspondence relates the symmetry flux operator defined above (i.e., the slowest-decaying string operator) to a Hamiltonian in the presence of an external flux (i.e., certain terms in the Hamiltonian have been "twisted" by phase factors). In particular, the charge of the end-point operator of the symmetry flux naturally coincides with the charge attached to the external flux. This gives a different perspective on the topological invariant for both gapped and gapless models. In the gapped case, this coincides with a well-known approach for detecting and classifying SPT phases in terms of the response functions of external flux insertions [5,6,57,58,73–82]. For a simple illustration of detecting the SPT invariant for the cluster chain by inserting fluxes (i.e., twisting certain terms), see Eqs. (31) and (32) in Sec. VIII.

We show how this approach of encoding SPT invariants in the charges of external fluxes can generalize to the gapless case in general dimensions. In particular, we consider two-dimensional systems where the Hamiltonian has been twisted along a one-dimensional line (i.e., flux threads through the system). If the corresponding ground state is unique and its charge is distinct from the untwisted case, it provides a bulk topological invariant even in the gapless case, which can moreover be linked to edge modes. This idea is broadly applicable, and we illustrate it in detail for several copies of the $2 + 1D$ Ising CFT with a nontrivial topological invariant protected by $\mathbb{Z}_2^3$ symmetry; this constitutes an example which does not rely on any gapped sector.

III. SYMMETRY FLUXES AND TOPOLOGICAL INVARIANTS

In this section, we explain how to define discrete topological invariants for both gapped and gapless systems in one spatial dimension (higher-dimensional generalizations are discussed in Sec. VIII). We do this by introducing the notion of symmetry fluxes; their charges will be the invariants. In Sec. III B, we illustrate how this indeed associates a topological invariant with the Ising critical point of the spin-1 XXZ chain encountered in Fig. 1. These invariants constrain the possible structure of phase diagrams, as we illustrate in Sec. III C. This section is devoted to bulk properties; the related phenomenon of topological edge modes is discussed in Sec. IV.

A. Defining symmetry fluxes and their charges

Consider a symmetry element $g \in G$, where G is the symmetry group of the Hamiltonian. If this is represented on the lattice by an unbroken on-site unitary operator $U^g = \prod_n U_n^g$, we can associate with it a symmetry flux. This is defined to be a (half-infinite) string operator of the form $\mathcal{S}_n^g \equiv \cdots U_{n-3}^g U_{n-2}^g U_{n-1}^g \mathcal{O}_n^g$ where the local end-point operator $\mathcal{O}_n^g$ is chosen such that the resulting correlator

$$\langle \mathcal{S}_m^{g\dagger} \mathcal{S}_n^g \rangle = \langle \mathcal{O}_m^{g\dagger} U_m^g U_{m+1}^g \cdots U_{n-1}^g \mathcal{O}_n^g \rangle \qquad (8)$$

has the slowest possible decay as a function of $|n - m|$. In practice, the correlator in Eq. (8) has two possible functional forms depending on whether or not U^g is associated with gapped degrees of freedom—meaning that all particles charged under this symmetry are massive. If this is the case, its symmetry flux has long-range order (i.e., it tends to a finite positive value). Otherwise, there is algebraic decay, $\langle \mathcal{S}_m^{g\dagger} \mathcal{S}_n^g \rangle \sim 1/|n - m|^{2\Delta_g}$. (Note that any decay faster than algebraic would imply symmetry breaking.) The exponent Δ_g is called the scaling dimension of $\mathcal{S}_g$ and is by definition as small as possible; long-range order can be seen as the special case $\Delta_g = 0$. The universality class of the system determines the value of Δ_g.

An obvious and important question is whether—for a given model—the above definition specifies a unique symmetry flux. Note that we want to avoid trivial overcounting: Multiplying any symmetry flux by, e.g., a phase factor e^{ikn} will again give a symmetry flux. For this reason, we consider only nonoscillatory symmetry fluxes; i.e., $\lim_{|n-m|\to\infty} |n - m|^{2\Delta_g} \langle \mathcal{S}_m^{g\dagger} \mathcal{S}_n^g \rangle$ should be a well-defined finite value. Moreover, if $\mathcal{S}^g$ and $\tilde{\mathcal{S}}^g$ differ only by subleading correlations, then we do not want to count them as being distinct. In other words, we define an equivalence class where $\mathcal{S}^g$ and $\tilde{\mathcal{S}}^g$ are in the same class if and only if $\mathcal{S}^g - \tilde{\mathcal{S}}^g$ is not a symmetry flux (i.e., its two-point correlator decays faster than $1/|n - m|^{2\Delta}$). We then naturally have a vector space spanned by the (classes

of) symmetry fluxes of $g \in G$, and its dimension D_g is a property of the universality class, as we soon discuss. For instance, we see that this space is one dimensional for gapped systems and for the Ising universality class, which simplifies things considerably. We now discuss the action of the symmetry group G on this vector space of symmetry fluxes.

1. Charges of symmetry fluxes

The group G has a natural action on symmetry fluxes via conjugation:

$$U^h \mathcal{S}^g U^{h\dagger} = \cdots U_{n-2}^{hgh^{-1}} U_{n-1}^{hgh^{-1}} (U^h \mathcal{O}_n^g U^{h\dagger}). \qquad (9)$$

It is easy to see [83] that this is a symmetry flux for hgh^{-1}. It is hence natural to take h to be an element of the subgroup of all elements commuting with g—the stabilizer $C(g)$—which implies that $U^h \mathcal{S}^g U^{h\dagger}$ is again a symmetry flux for g.

Let us consider the case where the space of symmetry fluxes of g is one dimensional. Then the new flux $U^h \mathcal{S}^g U^{h\dagger}$ and $\mathcal{S}^g$ must be linearly dependent. We define the relative phase to be the charge of the symmetry flux of g under h. In general, the charge $\chi_g(h) \in U(1)$ is given by the pre-factor in $U^h \mathcal{S}^g U^{h\dagger} = \chi_g(h)\mathcal{S}^g + \mathcal{S}_{\text{sub}}^g$, where $\mathcal{S}_{\text{sub}}^g$ is the subdominant (i.e., faster-decaying) piece. This charge is well defined, i.e., independent of the choice of symmetry flux (within a given class), since this choice would affect only the subdominant piece. However, in practice one chooses the end-point operator $\mathcal{O}^g$ to transform nicely under $C(g)$, in which case we can directly read off the charge from $U^h \mathcal{S}^g U^{h\dagger} = \chi_g(h)\mathcal{S}^g$. If G is Abelian, it can be shown that these charges are classified by $H^2(G, U(1))$; see Appendix A for details.

The charges under antiunitary symmetries are slightly more subtle, since they seemingly change if we redefine $\mathcal{S}^g \rightarrow i\mathcal{S}^g$. Here we show how to properly define such a charge for a symmetry flux of a unitary symmetry g of order 2 [i.e., $(U^g)^2 = 1$], which will be enough for all the antiunitary cases studied in this work. The key point is that a unitary that squares to unity must necessarily be Hermitian: $U^g = U^{g\dagger}$. Using this, one can show that one can always choose the end-point operator $\mathcal{O}^g$ of its symmetry flux to be Hermitian [84], in which case, its charge under an antiunitary symmetry is well defined (alternatively, one can combine the antiunitary symmetry with taking the dagger to get an effective unitary action).

This framework of symmetry fluxes applies to finite and continuous groups alike. However, in practice it is often sufficient to consider the charge of discrete subgroups. This is already well known for gapped SPT phases [e.g., the Haldane phase can be said to be protected by the SO(3) group of spin rotations, but just as well by its $\mathbb{Z}_2 \times \mathbb{Z}_2$ subgroup of π rotations [38]]. The reason for this is simple to understand: The symmetry flux is well defined for any

element g of a continuous group, but usually the charges under its stabilizer $C(g)$ are trivial. For instance, for a generic rotation in SO(3), the only elements that commute with it are other rotations along the same axis, and one can argue that these always lead to trivial charges. It is only at special high-symmetry points of SO(3), namely. at π rotations, where the stabilizer contains nontrivial elements (such as π rotations along orthogonal axes).

The above shows that charges are straightforwardly defined if the symmetry flux is unique, directly giving access to discrete invariants. We now show that this uniqueness is indeed guaranteed if, for example, the bulk is gapped or described by the Ising universality class. We also touch upon the more general case where the space of symmetry fluxes is higher dimensional; in this case, one can also obtain discrete invariants.

2. Symmetry fluxes for gapped phases

In the gapped case, the symmetry flux for any unbroken symmetry $g \in G$ is unique; i.e., any two symmetry fluxes are linearly dependent. This follows from the concept of symmetry fractionalization (see Appendix A 3 for a proof). Indeed, in this case the above definition of the symmetry flux coincides with the well-known notion of a string order parameter characterizing the phase [49,55]. Note that this uniqueness applies even to critical systems as long as U^g acts nontrivially on gapped degrees of freedom only, at least if we restrict ourselves to cases without bulk degeneracies (from the perspective of conformal field theory, this means that we assume that there is only a single local operator of scaling dimension zero). The uniqueness of this symmetry flux implies we have well-defined charges $\chi_g(h)$.

It is known that gapped phases are classified by topologically distinct projective representations of G which are labeled by a so-called cocycle $\omega \in H^2(G, U(1))$ [1–3]. The above charges $\chi_g(h)$ can be expressed in terms of this cocycle (see Appendix A 3). The converse is also true, e.g., for Abelian groups G: In Appendix A 3 we prove that the cocycle can be reconstructed from knowing the charges. This is not true for arbitrary groups G. Nevertheless, in practice, knowing the charges is often equivalent to knowing the projective representations (the simplest known counterexample involves a group of 128 elements [49]).

3. Symmetry fluxes for the Ising universality class

We now show that if one is given a G-symmetric lattice model where some degrees of freedom are described by the Ising universality class and other degrees of freedom (if present) are gapped, then any $g \in G$ has a unique symmetry flux $\mathcal{S}^g$. First, the Ising CFT is known to have an emergent $\mathbb{Z}_2$ symmetry (i.e., this makes no reference to what the symmetries of the lattice model might be), and it is known that this has a unique symmetry flux μ which moreover has scaling dimension $\Delta_\mu = 1/8$ [59] (it is unique because the partition function in the sector twisted by the emergent $\mathbb{Z}_2$

symmetry has a unique ground state; see Sec. VIII). Second, this is the only unitary on-site symmetry of the Ising CFT [85]; hence, any lattice symmetry which acts nontrivially on the local degrees of freedom of the CFT must coincide—for the gapless part of the spectrum—with the emergent $\mathbb{Z}_2$ symmetry, thereby inheriting the uniqueness of its symmetry flux. A part of the symmetry can of course also act nontrivially on additional gapped degrees of freedom, but as we argue in Sec. III A 2, this does not affect the conclusion of uniqueness.

In summary, for any $g \in G$ we have a unique symmetry flux. Its scaling dimension is $\Delta_g = 1/8$ if g acts nontrivially on the CFT, otherwise $\Delta_g = 0$. As we describe in Sec. III A 1, this uniqueness gives us well-defined charges $\chi_g(h) \in \mathrm{U}(1)$ under any symmetry h that commutes with g. These charges form a discrete invariant of the symmetry-enriched Ising CFT. We see an example of this in Sec. III B.

4. Symmetry fluxes for general universality classes

In the above two cases, for each $g \in G$, the vector space of symmetry fluxes happened to be one dimensional. More generally, it might have some dimension D_g, such that each basis of symmetry fluxes $\mathcal{S}_\alpha^g$ come with an additional label $\alpha = 1, \ldots, D_g$. Hence, the subgroup of elements that commute with g (the stabilizer of g) has a higher-dimensional representation on this space of fluxes, $U^h[\mathcal{S}_\alpha^g]U^{h\dagger} = R_{\alpha,\beta}^g(h)[\mathcal{S}_\beta^g]$, where $[\mathcal{S}^g]$ denotes the equivalence class defined above. For example, $D_g > 1$ generically happens at transitions between distinct SPT phases (or between G-CFTs), where the different symmetry fluxes become degenerate.

A higher-dimensional representation can of course still come with discrete labels (in particular, there are cases where all degenerate fluxes have the same charges; see Sec. VII), but extra care has to be taken before one can conclude that these give invariants of the G-enriched CFT. In particular, in rare cases, some CFTs allow for marginal perturbations which can change D_g. For example, the $c = 1$ $\mathbb{Z}_2$-orbifold CFT allows for one-dimensional vector spaces of symmetry fluxes ($D_g = 1$), but this CFT can be smoothly tuned to a compact boson CFT where this representation becomes two dimensional. Such a process is explored in a lattice model in Sec. V where we use this to connect apparently distinct G-CFTs with $c = 1$.

5. Implications for phase diagrams

Identifying discrete invariants for symmetry-enriched universality classes has strong implications for the possible structure of phase diagrams. In particular, if two models are described by the same CFT at low energies but by distinct symmetry-enriched CFTs, then these two transitions cannot be smoothly connected in a larger phase diagram. This means that any path attempting to connect them must have an intermediate point where the universality class

discontinuously changes—either to a distinct CFT (necessarily of higher central charge) or to something that is not a CFT (e.g., a gapless point with dynamical critical exponent $z_{\mathrm{dyn}} \neq 1$). Examples are discussed in Sec. III C.

B. Topological invariant for the critical spin-1 anisotropic Heisenberg chain

Having laid out the general structure of symmetry fluxes, we are now in a good position to apply this to a concrete model: the spin-1 *XXZ* chain. As we mention in the Introduction and as shown in Fig. 1, as one tunes the easy-axis anisotropy Δ (not to be confused with a scaling dimension) from the topological Haldane phase to the symmetry-breaking Ising phase, there remains a localized edge mode at the Ising critical point. Here we identify a bulk topological invariant at criticality, establishing that it indeed forms a novel symmetry-enriched Ising CFT. This invariant also explains its edge behavior, as we discuss in Sec. IV.

The gapped Haldane phase is known to be protected by, for example, the $\mathbb{Z}_2 \times \mathbb{Z}_2$ group of π rotations (represented by $R_\gamma = \prod_n e^{i\pi S_n^\gamma}$ for $\gamma = x, y, z$). This SPT phase has long-range order in $\langle S_i^\gamma \exp(i\pi \sum_{i<k<j} S_k^\gamma) S_j^\gamma \rangle$. The symmetry flux of R_γ is thus $\prod_{m<n} e^{i\pi S_m^\gamma} S_n^\gamma$. Its long-range order is shown in Fig. 2(a) for $\gamma = x$, which indeed vanishes at the critical point $\Delta = \Delta_c$. In the Ising phase for $\Delta > \Delta_c$, we have the local order parameter S_n^z characterizing the spontaneous breaking of R_x and R_y.

Despite the vanishing of the long-range order of these order parameters, they still play an important role at criticality: They are identified by their scaling dimension $1/8$, as shown in Fig. 2(b). We thus conclude that—similar to the known gapped case—the symmetry flux of R_x at criticality is still the Haldane string order parameter. As we
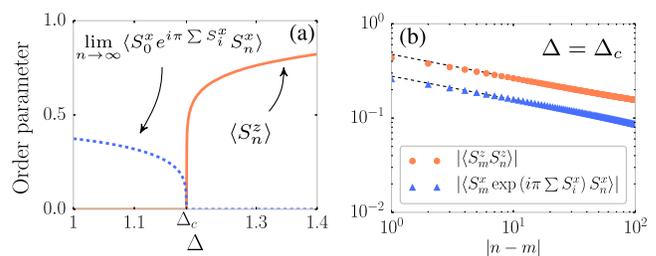

FIG. 2. Order parameters and symmetry fluxes for the spin-1 *XXZ* chain. (a) The Haldane string order parameter and Ising order parameter have long-range order in the SPT and symmetry-breaking phase, respectively. (b) At criticality, the long-range order is replaced by algebraic decay. Both operators have the same scaling dimension (i.e., their correlators decay as $1/|n-m|^{2\Delta}$ with $\Delta = 1/8$; the dashed lines are a guide to the eye) and in the continuum limit correspond to the μ and σ operators of the Ising CFT, respectively. We conclude that μ has nontrivial charge under other symmetries, which functions as a topological invariant.

discuss in Sec. III A 3, this means that the Ising critical point is nontrivially enriched by $\mathbb{Z}_2 \times \mathbb{Z}_2$ symmetry. More concretely, if we denote the symmetry flux of R_x by μ (using the traditional notation of scaling operators of the Ising CFT) [86], we have the nontrivial charge $R_z \mu R_z = -\mu$.

One can also consider the symmetry flux for R_z. In fact, since the local fields of the Ising transition are all neutral under R_z, this symmetry remains gapped. As a consequence, the topological string order parameter for R_z has long-range order throughout this whole region of the phase diagram. This thus also functions as a topological invariant. This is a general feature of gapless SPT phases which are (partially) protected by gapped degrees of freedom. The case without such an additional gapped sector is thus arguably the most novel: There is no long-range order to appeal to, making the CFT-based approach essential. This is the case, for example, for H'' encountered in Sec. II, and as we see in Sec. IV, this difference has an important consequence for the edge modes.

We note that the gapped Haldane phase is also known to be protected by time-reversal symmetry $T_{\mathrm{spin}} = R_y K$ (where K is complex conjugation in the local z basis). Similarly, the Ising criticality at $\Delta = \Delta_c$ is enriched by the $\mathbb{Z}_2 \times \mathbb{Z}_2^T$ symmetry generated by R_x and T_{spin}. Indeed, we see that $T_{\mathrm{spin}} \mu T_{\mathrm{spin}} = -\mu$. It would be interesting to define a notion of symmetry flux for antiunitary symmetries, which in this case would have to be charged under the unitary symmetries R_γ as well as under itself.

C. Implications for phase diagrams: Bond-alternating spin-1 Heisenberg chain

Having identified the discrete invariant $R_z \mu R_z = -\mu$ for the spin-1 XXZ chain at criticality, we can distinguish it from a trivial Ising criticality where $R_z \mu R_z = \mu$. Whereas the former appears at a phase transition between an Ising phase and a nontrivial SPT phase, the latter appears as one tunes from/to a trivial SPT phase (condensing μ would lead to a symmetric gapped phase, with its symmetry properties determining its phase). The discreteness of $R_z \mu R_z = \pm\mu$ means that these two Ising criticalities cannot be smoothly connected, constraining the possible structure of phase diagrams containing such Ising transitions. This can be illustrated by adding, e.g., bond alternation:

$$H = J\sum_n [1 - \delta(-1)^n](S_n^x S_{n+1}^x + S_n^y S_{n+1}^y + \Delta S_n^z S_{n+1}^z).$$

(10)

The two-parameter phase diagram obtained with iDMRG [87,88] is shown in Fig. 3(a) (see also Refs. [89,90]). For large δ, we can realize a trivial Ising CFT where the symmetry flux of R_x is not charged, being given by $\mu \sim e^{i\pi \sum_{m<n} S_m^x}$. We observe that the two topologically
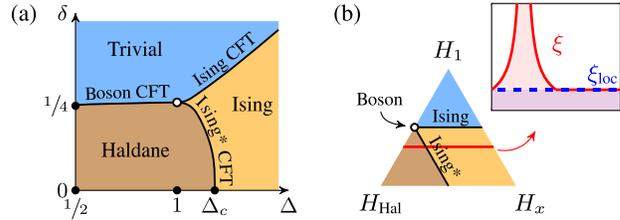

FIG. 3. Transitions between topologically distinct Ising universality classes. (a) Phase diagram of the bond-alternating $S = 1$ XXZ chain. There is a $c = 1$ transition between the topologically distinct $c = 1/2$ transitions. The tricritical point (hollow marker) is a Wess-Zumino-Witten $SU(2)_1$ CFT, where the trivial and Haldane string order parameters both have scaling dimension $1/8$. (b) Similar phase diagram for an exactly solvable $S = 1/2$ model; in this case, the $c = 1$ boson CFT is in the free Dirac universality class [inset, analog of Fig. 1(a)].

distinct symmetry-enriched Ising CFTs (with central charge $c = 1/2$) are separated by a point where the universality class changes (hollow white marker). In this case, this "transition of transitions" is described by the Wess-Zumino-Witten $SU(2)_1$ CFT with central charge $c = 1$. Here, the symmetry flux of R_x still has scaling dimension $\Delta_{R_x} = 1/8$, but this space is now two dimensional (i.e., there are two linearly independent symmetry fluxes of R_x). Indeed, one symmetry flux is nontrivial $e^{i\pi \sum_{m<n} S_m^x} S_n^x$ and the other, trivial $e^{i\pi \sum_{m<n} S_m^x}$. This degeneracy of symmetry fluxes is in fact true along the whole line of $c = 1$ CFTs separating the trivial and Haldane SPT phase, which is natural given the emergent duality symmetry at this transition.

Similar phenomenology can already be observed in an exactly solvable spin-1/2 chain which realizes the same three gapped phases, as shown in Fig. 3(b). In this case, the two topologically distinct Ising CFTs are now separated by the $c = 1$ free Dirac CFT, where the two symmetry fluxes of R_x again become degenerate (now with scaling dimension $\Delta_{R_x} = 1/4$). The Hamiltonians for these spin-1/2 chains are introduced and discussed in detail in Sec. V, and the phase diagram is calculated in Appendix B.

IV. EDGE MODES AT CRITICALITY

In the previous section, we introduce the notion of a symmetry flux and its corresponding charge. In this section, we relate this bulk property to degeneracies in the presence of open boundary conditions. This section is naturally divided in two: In Sec. IV A, we focus on a single boundary of a half-infinite system, where we explain how a charged symmetry flux can lead to the boundary spontaneously breaking a symmetry; in Sec. IV B, we study the coupling between such boundary magnetizations and calculate the finite-size splitting of the degeneracy. Throughout this section, we use the Ising CFT as an illustrative example, but the method which we lay out is generally applicable.

In fact, at the end of every subsection, we indicate what the necessary analysis would be for a general CFT.

A. Half-infinite chain: A single boundary

Let us consider a half-infinite system, allowing us to study a single edge. We furthermore presume that the system is described by the Ising universality class. To study what happens near its boundary, we use the fact that all possible boundary RG fixed points describing the $(0 + 1)$-dimensional edge of this CFT are known [65,91]. There are three distinct fixed points, as sketched in Fig. 4; these have different behavior with respect to the $\mathbb{Z}_2$ symmetry intrinsic to the Ising CFT.

(i) The free boundary fixed point: This preserves the $\mathbb{Z}_2$ symmetry. The symmetry flux of this $\mathbb{Z}_2$ symmetry denoted by $\mu(x)$ can be said to have condensed. Indeed, $\langle \mu(x_{\text{boundary}}) \rangle \neq 0$ [64]. Note that in the bulk, the one-point function of $\mu(x)$ is not well defined due to it being nonlocal. However, near the boundary, $\mu(x)$ becomes local.

(ii) The (explicitly) fixed$^{\pm}$ boundary fixed point: This requires explicitly breaking the $\mathbb{Z}_2$ Ising symmetry at the level of the Hamiltonian (near its boundary). The local spin operator $\sigma(x)$ points up or down near the edge $\langle \sigma(x_{\text{boundary}}) \rangle \neq 0$; its sign depends on the explicit breaking of the $\mathbb{Z}_2$ symmetry. This fixed point is excluded by enforcing $\mathbb{Z}_2$ symmetry of the Hamiltonian.

(iii) The spontaneously fixed boundary fixed point: The symmetry is not broken at the level of the Hamiltonian, but the ground state spontaneously magnetizes. More precisely, it is a two-dimensional Hilbert space which is the direct sum of the two symmetry-broken orderings.

The latter fixed point (note that this is not a Cardy state in the boundary conformal field theory) is not often mentioned in the literature, but this is for a good reason: It is usually an unstable [92] RG fixed point. A generic perturbation would condense $\mu(x)$ near the boundary,

flowing to the free fixed point. From the RG perspective, this is due to the boundary scaling dimension of $\mu(x_{\text{boundary}})$ being $1/2$; this is smaller than 1, implying it is relevant for $(0 + 1)$-dimensional RG flows. However, if $\mu(x)$ is charged under some additional symmetry, then this RG flow is prohibited, and the spontaneous fixed boundary condition—along with its twofold degeneracy—is stabilized. The above is summarized in Fig. 4. This explains the edge modes observed in Sec. II and in Fig. 1, confirming that these are not fine-tuned features.

One can in principle repeat the above analysis for any CFT. The necessary information to set up the problem is the list of possible conformal boundary conditions, as well as the boundary condition changing operators and their (boundary) scaling dimensions. Supplemented by the symmetry properties of these operators, one can study which boundary RG fixed points are stable and (non) degenerate.

B. Finite-size splitting: Coupled boundaries

As we argue in the previous subsection, if the $\mathbb{Z}_2$-symmetry flux $\mu(x)$ of the Ising CFT is charged under an additional symmetry, the boundary spontaneously magnetizes. We now investigate the resulting degeneracy and its finite-size splitting for a finite chain of length L (with $x \in [0, L]$). Since the bulk gap vanishes as $1/L$, we can only meaningfully speak of degeneracies whose finite-size splitting decays faster than this. There are four candidate degenerate ground states labeled by their boundary magnetizations:

$$| \uparrow_l \uparrow_r \rangle, | \uparrow_l \downarrow_r \rangle, |\downarrow_l \uparrow_r \rangle, |\downarrow_l \downarrow_r \rangle. \qquad (11)$$

However, presuming the model under consideration has a ferromagnetic sign, the antiferromagnetic states in Eq. (11) are split from the ferromagnetic ones at the scale of $1/L$ [65,91]. Intuitively, this is because the edges can sense their (mis)alignment through the critical bulk. We thus have only two ground states: $| \uparrow_l \uparrow_r \rangle$ and $|\downarrow_l \downarrow_r \rangle$. In fact, within the CFT, these are exactly degenerate eigenstates. This does not mean that they have no splitting in realistic systems: By definition, a CFT has no length scales; hence, the only quantity with units of energy is $1/L$. If we perturb the CFT with RG-irrelevant perturbations present in any realistic system, then the twofold degeneracy could be split by the smaller energy scales of order $\xi^{\alpha}/L^{1+\alpha}$ or of order $\exp(-L/\xi)$ (where ξ is a constant with units of length). As a consistency check, note that in the RG fixed-point limit, $\xi/L \to 0$, confirming that splittings which are faster than $1/L$ are indeed not visible in the CFT.

The purpose of this section is to determine whether the finite-size splitting of the aforementioned twofold degeneracy is algebraic or exponential in system size. This comes down to analyzing the possible perturbations
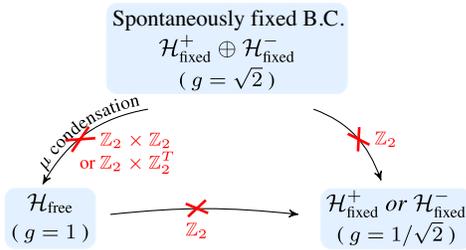

FIG. 4. Topologically protected edge modes in the Ising CFT. Boundary RG flow for the Ising CFT: Usually the free boundary condition (B.C.) is stable (when preserving global $\mathbb{Z}_2$), but it can be prevented when μ is charged under additional symmetries. In that case, the spontaneously fixed boundary condition (with a global twofold degeneracy) is stable.

V one can add to the CFT Hamiltonian $H = H_{\text{CFT}} + V$ mixing $|\uparrow_l \uparrow_r\rangle \leftrightarrow |\downarrow_l \downarrow_r\rangle$. To connect these two states which break the Ising symmetry, we need to perturb with the corresponding symmetry flux. Indeed, $\mu(x_{\text{boundary}})$ is known to be a boundary-condition-changing (BCC) operator toggling between the two fixed$^\pm$ boundary conditions [65,91]. We already established that we cannot add $\mu(x)$ due to it being charged under an additional symmetry. However, there is a whole tower of BCC operators: the descendants of $\mu(x)$, with scaling dimensions $\Delta_n = 1/2 + n$ (where $n = 1, 2, 3, \ldots$). Note that since $\Delta_n > 1$, these are RG irrelevant for the $(0 + 1)$-dimensional edge. This means they do not affect the analysis in Fig. 4, but they can indeed contribute to finite-size splitting. Whether it is possible to add such descendants of $\mu(x)$ depends on the protecting or enriching symmetry. Determining which descendant— if any—is allowed, determines whether the splitting is exponential or algebraic (along with its power), as we explain now.

1. Exponential splitting

If $\mu(x)$ is charged under a symmetry U which is associated with gapped degrees of freedom (d.o.f.), then all its descendants have the same nontrivial charge. To see this, note that the descendants are created by applying the local Virasoro generators L_n to $\mu(x)$, and U acts trivially on local gapless d.o.f. In conclusion, there is no perturbation within the low-energy CFT that can couple $|\uparrow_l \uparrow_r\rangle \leftrightarrow |\downarrow_l \downarrow_r\rangle$. Any effective interaction must hence be mediated through gapped d.o.f., which can lead at most to a finite-size splitting of order $\exp(-L/\xi)$. This applies whenever the protecting symmetry is unitary: The only unitary symmetry of the Ising CFT is its $\mathbb{Z}_2$ symmetry [85], such that any additional unitary symmetry must be associated with gapped d.o.f.. A case in point is the critical spin-1 XXZ chain, where $\mu(x)$ is charged under R_z (see Sec. III B). This explains the exponentially localized edge mode observed in Fig. 1. A similar conclusion was drawn in the work by Scaffidi et al. [28], where the gapped degrees of freedom stabilized a spontaneous boundary magnetization in a critical Ising chain.

2. Algebraic splitting

In case $\mu(x)$ is charged under an antiunitary symmetry T, then the charge of its descendants can be different. More generally, if $\mathcal{O}_n$ is the lattice operator for a continuum operator $\varphi(x)$, then its first descendants can be realized by $\partial_x \varphi(x) \sim \mathcal{O}_{n+1} - \mathcal{O}_n$ and $\partial_t \varphi(x) \sim i[H, \mathcal{O}_n]$. Hence, we see that $\partial_x \varphi(x)$ has the same charge under T as $\varphi(x)$, whereas it is opposite for $\partial_t \varphi(x)$. For the boundary operator $\mu(0)$, we have only the timelike derivative; i.e., $\mu(0)$ has a unique first descendant with charge $T\partial_t \mu(0) T = +\partial_t \mu(0)$.

We are hence allowed to add a perturbation $H = H_{\text{CFT}} + \lambda \partial_t \mu(0)$. Remarkably, however, this descendant cannot split the twofold ground-state degeneracy. Indeed,

the perturbation disappears after a well-chosen change of basis:

$$H = H_{\text{CFT}} + i\lambda[H, \mu(0)] = \underbrace{e^{-i\lambda\mu(0)} H_{\text{CFT}} e^{i\lambda\mu(0)}}_{\equiv \tilde{H}_{\text{CFT}}} + O(\lambda^2).$$

(12)

Note that since $T\mu(0)T = -\mu(0)$, our rotated Hamiltonian $\tilde{H}_{\text{CFT}}$ is still symmetric: $T\tilde{H}_{\text{CFT}}T = \tilde{H}_{\text{CFT}}$. Equation (12) tells us that the perturbed Hamiltonian H is equivalent to a Hamiltonian with the same spectrum as the unperturbed case [plus perturbations given by higher descendants at order $O(\lambda^2)$]. In particular, the ground state degeneracy is not split by the first descendant.

To summarize the above: The zeroth descendant [i.e., $\mu(0)$] was not allowed by symmetry, whereas the symmetry-allowed first descendant could be "rotated" away using the zeroth descendant. Interestingly, this pattern continues for a while, but not indefinitely. First, it can be shown that any even descendant is T-odd [93] and is hence excluded by symmetry. Second, while all odd descendants are allowed by symmetry, many of them can be removed by using the fact that even descendants generate symmetry-preserving rotations. More precisely, if we denote the number of nth descendants of $\mu(0)$ as N_n (which have scaling dimension $\Delta_n = 1/2 + n$), then only $N_{2m+1} - N_{2m}$ descendants [94] at level $2m + 1$ cannot be rotated away and can hence actually cause a finite-size splitting. We thus need to determine the smallest odd n such that $N_n > N_{n-1}$. Fortunately, the number of descendants of $\mu(0)$ can be read off from the (chiral) partition function, i.e., $\sum_n N_n q^n = q^{-\frac{23}{48}}\chi_{1,2}(q)$ [59], where

$$q^{-\frac{23}{48}}\chi_{1,2}(q) = (1 + q + q^2 + q^3 \\ + 2q^4 + 2q^5 + 3q^6 + 4q^7 + \cdots).$$ (13)

We see that $N_7 - N_6 = 4 - 3 = 1$, leaving us with a single symmetry-allowed seventh descendant of $\mu(0)$, which we denote by $\mu^{(7)}(0)$, that cannot be rotated away. We conclude that the perturbation $V = \lambda(\mu^{(7)}(0) + \mu^{(7)}(L))$ can split the degeneracy. Since we need to flip both edges in order to couple $|\uparrow_l \uparrow_r\rangle \leftrightarrow |\downarrow_l \downarrow_r\rangle$, we have to go to second order in λ to observe a splitting, i.e., λ^2/L^β. Since this has to have units of energy, we can conclude that $\beta = 1-2[\lambda]$, where the unit of λ is $[\lambda] = 1 - \Delta_7$. In summary, we find an algebraic splitting with power $\beta = 2\Delta_7 - 1 = 14$.

This remarkably fast algebraic decay can be confirmed in the spin model $H'' = -\sum_{n=1}^{L-1} Z_n Z_{n+1} - \sum_{n=1}^{L-2} Z_n X_{n+1} Z_{n+2}$ introduced in Sec. II. This fine-tuned model has exact boundary magnetizations $Z_1 = \pm 1 = Z_L$. For this system,

$$\mu(x) \sim \cdots X_{n-2} X_{n-1} Y_n Z_{n+1},$$
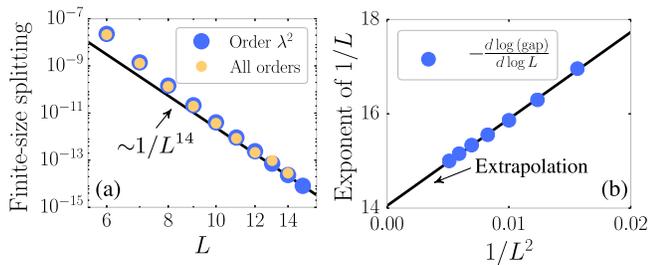$$\partial_t \mu(x) \sim \cdots X_{n-2} X_{n-1} X_n.$$ (14)

FIG. 5. Finite-size splitting of edge mode in the Ising CFT. If a unitary symmetry protects the edge mode, finite-size splitting is exponentially small in system size. For an antiunitary symmetry, however, the field theory analysis in the main text suggests a splitting of order $1/L^{14}$. (a) We confirm the latter numerically in a spin-chain model where μ is charged under $\mathbb{Z}_2^T$. Note that for $L = 15$, the gap is around machine precision. (b) To separate out higher-order corrections present in (a), we extrapolate the leading exponent of $1/L$; the data agree with the predicted splitting of order $1/L^{14} \times (1 + \alpha/L^2)$.

In particular, we see that $\partial_t \mu(0) \sim X_1$. This operator is allowed by symmetry but does not contribute to the splitting, as we discuss above. We consider a dressed operator $X_1 Z_2 Z_3$, which should generically contain all possible descendants of $\mu(0)$ which are T-even. Our perturbed Hamiltonian is thus $H = H'' + \lambda(X_1 Z_2 Z_3 + Z_{L-2} Z_{L-1} X_L)$. In Fig. 5(a), we see the finite-size splitting obtained with exact diagonalization for $\lambda = 0.1$. The data are consistent with the CFT prediction of $1/L^{14}$. We can also analytically predict the next-to-leading-order contribution, which arises from acting with the seventh descendant of μ on one end and with the ninth descendant on the other, generating a splitting of order $1/L^{\Delta_7 + \Delta_9 - 1} = 1/L^{16}$. The gap thus scales as $1/L^{14} + \alpha/L^{16}$, which means that the effective exponent of the algebraic decay is L dependent: $-d \log(\text{gap})/d \log L \approx 14 + 2\alpha/L^2$ for large L. The numerical data in Fig. 5(b) show perfect agreement with this formula.

The above focused on the illustrative example of the Ising CFT, but the principle is much more general. Once one has studied the boundary RG flow diagram and concluded the presence of edge modes due to charged symmetry fluxes (as in Sec. IV A), one can study the finite-size splitting by determining the dominant symmetry-allowed BCC operator. In the antiunitary case, one can use the fact that the contributions of descendants can be rotated away by other descendants, which applies to any CFT. One important difference will be the counting appearing in the tower of states such as in Eq. (13).

V. CLASSIFYING G-ENRICHED CFTS IN $1 + 1$D

The previous sections show how a given bulk universality class (with, in particular, a fixed central charge c) can split up into distinct classes when additional symmetries are enforced. The concept of a symmetry flux and its associated

charge allows us to distinguish such symmetry-enriched CFTs. However, there are various invariants one can associate with G-symmetric universality classes.

(i) Spontaneously broken symmetries. At the coarsest level, there is the phenomenon of symmetry breaking. The invariant this allows us to define is the subgroup $G_{\text{eff}} \subset G$ of unbroken symmetries. In particular, the absence of symmetry breaking means $G_{\text{eff}} = G$.

(ii) Charges of symmetry fluxes. As we define and discuss in Sec. III, with any $g \in G_{\text{eff}}$ we can associate a symmetry flux $\mathcal{S}^g$. We can measure the charge of $\mathcal{S}^g$ with respect to any other symmetry $h \in G_{\text{eff}}$ which commutes with g. The universality class tells us whether this charge is an invariant of the phase (e.g., if the space of g-symmetry fluxes is one dimensional).

(iii) Gapped symmetries. Another robust invariant of the phase is the list of the unbroken symmetries which act only on gapped degrees of freedom forming a subgroup $G_{\text{gap}} \subset G_{\text{eff}}$. We refer to symmetries in G_{gap} as being gapped. (Note that having a larger G_{gap} is not necessarily correlated with having a smaller central charge; it does, however, usually imply that the critical degrees of freedom are more unstable.)

(iv) Charges of local scaling operators. Lastly, for any unbroken symmetry $g \in G_{\text{eff}}$ which is not gapped (i.e., $g \notin G_{\text{gap}}$), we can study the charges of local low-energy CFT observables under g. Similar to the charges of symmetry fluxes, these charges can lead to invariants of the phase (e.g., a unique local operator with a particular scaling dimension has an invariant charge). For example, recall the Ising operator σ from Sec. II that was either real or imaginary.

For gapped phases, the third and fourth invariants are trivial (since $G_{\text{gap}} = G_{\text{eff}}$). Indeed, in most practical cases, the first two provide a complete classification of gapped one-dimensional phases protected by an on-site symmetry group G [1–4]. A natural question is whether the above invariants are also complete for G-enriched CFTs. We show that this is the case for the Ising CFT, which we first illustrate for the symmetry group $\mathbb{Z}_2 \times \mathbb{Z}_2$. For Gaussian CFTs, we give a partial answer, showing that the $c = 1$ transitions arising between gapped ($\mathbb{Z}_2 \times \mathbb{Z}_2$)-symmetric phases can all be smoothly connected. We also use the latter case as an instructive example for the more subtle points encountered in Sec. III, showing that G-CFTs with apparently distinct charges for their symmetry fluxes can be part of the same G-CFT. In this section, we limit ourselves to unitary symmetries.

Throughout this section, we discuss the example $G = \mathbb{Z}_2 \times \mathbb{Z}_2$ in the context of a spin-$1/2$ chain, with the symmetries realized by the group of π rotations $R_\gamma = \prod_n R_\gamma^{(n)}$, where

$$R_x^{(n)} = X_{2n-1}X_{2n}, \quad R_y^{(n)} = Y_{2n-1}Y_{2n}, \quad R_z^{(n)} = Z_{2n-1}Z_{2n}.$$

Note that the way we write these symmetries betrays that we have fixed a unit cell, such that the $R_\gamma^{(n)}$ symmetries indeed commute. This property ensures that these operators define a linear, on-site representation of $\mathbb{Z}_2 \times \mathbb{Z}_2$.

In Sec. V A, we recall the six gapped phases that can occur for this symmetry group, along with solvable models which are used in the following two subsections. In Sec. V B, we classify the symmetry-enriched Ising CFTs. In Sec. V C, we discuss the case of the Gaussian CFT.

A. Gapped bulk

To keep this work self-contained, we briefly review the gapped phases with this symmetry group. According to the classification for spin chains with $\mathbb{Z}_2 \times \mathbb{Z}_2$ symmetries, there are exactly two gapped phases where the ground state preserves the full symmetry group [1–4]. These are the trivial phase and the topological Haldane phase, which can be realized in a spin-1/2 chain, respectively, as follows:

$$H_1 = \sum_n (X_{2n-1}X_{2n} + Y_{2n-1}Y_{2n}),$$

$$H_{\text{Hal}} = \sum_n (X_{2n}X_{2n+1} + Y_{2n}Y_{2n+1}).$$

For both Hamiltonians, the ground state is a product of singlets, but for H_1 each singlet is within a unit cell, whereas for the latter, it is across unit cells. The latter is reminiscent of the ground state of the well-known spin-1 Affleck-Kennedy-Lieb-Tasaki (AKLT) model; indeed, by introducing a term that penalizes spin-0 states in each unit cell, H_{Hal} can be adiabatically connected to the AKLT model [9,95] [which in turn can be connected to the spin-1 Heisenberg chain in Eq. (1)]. Relatedly, while both models clearly have a unique ground state for periodic boundary conditions, H_{Hal} has a zero-energy spin-1/2 degree of freedom at each open boundary. (Note that to keep the on-site representation of $\mathbb{Z}_2 \times \mathbb{Z}_2$ well defined, we can cut the chain only between unit cells.) These two symmetric phases can be distinguished by their symmetry fluxes: E.g., for H_1 the symmetry flux of R_x is $\mathcal{S}^x = \cdots R_x^{(n-2)}R_x^{(n-1)}R_x^{(n)}$, whereas for H_{Hal} it is $\mathcal{S}^x = \cdots R_x^{(n-2)}R_x^{(n-1)}X_{2n-1}$. These clearly have different charges under R_y and R_z.

In addition to these two symmetry-preserving phases, there are four symmetry-breaking phases (which can be labeled by G_{eff}). Three of these preserve a $\mathbb{Z}_2$ subgroup generated by one of the $R_{\gamma=x,y,z}$:

$$H_x = \sum_n X_n X_{n+1}, \quad H_y = \sum_n Y_n Y_{n+1}, \quad H_z = \sum_n Z_n Z_{n+1}.$$

We label these three Ising phases as I_x, I_y, and I_z, respectively. The fourth breaks the complete $\mathbb{Z}_2 \times \mathbb{Z}_2$ symmetry group (i.e., $G_{\text{eff}} = \{1\}$) and is realized by

$$H_0 = -\sum_n (X_{2n-1}X_{2n+1} + Y_{2n}Y_{2n+2}). \tag{15}$$

These six Hamiltonians satisfy a very useful duality property: There is a nonlocal change of variables which effectively interchanges $H_x \leftrightarrow H_1$, $H_y \leftrightarrow H_{\text{Hal}}$, and $H_z \leftrightarrow H_0$. We give an explicit lattice construction in Appendix C. Physically, this transformation can be interpreted as gauging R_z (while keeping R_x fixed).

Lastly, we note that phases of matter can be stacked. Two G-symmetric models can be combined into a two-leg ladder; the new on-site symmetry is simply the tensor product of the two individual on-site symmetries. One can then study what phase the stacked model belongs to. E.g., stacking the trivial phase onto any other phase leaves the latter invariant; it acts as the identity element, explaining our notation H_1. Oppositely, stacking any phase onto the phase that breaks all symmetries remains in the latter phase; it hence acts as the zero element explaining the label H_0 (together with the relations $\text{Hal} * \text{Hal} = 1$, $I_\gamma * \text{Hal} = I_\gamma$, and $I_\gamma * I_\gamma = I_\gamma$, the Abelian semigroup of $\mathbb{Z}_2 \times \mathbb{Z}_2$ phases is completely specified).

B. Ising criticality ($c = 1/2$)

We classify ($\mathbb{Z}_2 \times \mathbb{Z}_2$)-enriched Ising CFTs with a straightforward generalization to general symmetry groups G. This will show that the four invariants mentioned above form a complete set of invariants for this universality class. Our principal focus is on symmetry-enriched Ising CFTs which naturally occur as phase transitions between the aforementioned gapped phases. Practically, this means that such Ising CFTs have a single symmetry-allowed bulk perturbation which can open up a gap (a relevant operator). I.e., only one parameter needs to be tuned to achieve criticality; such CFTs are said to have codimension one. Ising CFTs with higher codimension can occur but physically correspond to accidental criticalities in a phase diagram; we discuss them at the end of this subsection. Ising CFTs of codimension one are characterized by having an unbroken symmetry $\mathbb{Z}_2 \subset G_{\text{eff}}$ which anticommutes with the local Ising scaling operator σ (i.e., this $\mathbb{Z}_2 \not\subset G_{\text{gap}}$). Indeed, this nontrivial charge forbids us from adding σ as a perturbation, such that there is only one relevant symmetric operator which can open up a gap (commonly denoted by ε).

We now demonstrate how the four labels we propose allow us to derive that there are at least nine codimension-one Ising CFTs; afterward, we confirm that this list is complete. First, we have to determine the group of unbroken symmetries. If there is symmetry breaking at the critical point, we have $G_{\text{eff}} \cong \mathbb{Z}_2$ (the symmetry group cannot be completely broken if we consider a codimension-one CFT). There are three choices for the unbroken symmetry R_γ ($\gamma = x$, y, z). Note that the remaining invariants are already determined: σ must be odd under this remaining symmetry, and a single bosonic

$\mathbb{Z}_2$ on-site symmetry flux cannot be charged under itself, i.e., $\chi_g(g) = 1$. We can also determine which gapped phases this CFT can be perturbed into. If we condense σ (corresponding to perturbing with, say, $-\varepsilon$), we arrive at the phase breaking all symmetries (labeled by 0), whereas if we condense μ (perturbing with $+\varepsilon$), then we flow to a gapped phase with a single-$\mathbb{Z}_2$ symmetry R_γ, which can be only the Ising phase I_γ. We use the shorthand notation $[0, I_\gamma]$ to denote this transition, which is realized by, for example, the lattice Hamiltonian $H_0 + H_\gamma$.

If there is no symmetry breaking, then $G_{\text{eff}} = \mathbb{Z}_2 \times \mathbb{Z}_2$. We can then continue to determine its gapped subgroup G_{gap}. This cannot be empty, since it is known that the Ising CFT (without gapped degrees of freedom) does not have a $\mathbb{Z}_2 \times \mathbb{Z}_2$ symmetry at low energies [85]. Moreover, G_{gap} cannot be the full group if we are to have a codimension-one Ising CFT. We thus conclude that $G_{\text{gap}} \cong \mathbb{Z}_2$. There are three choices for this gapped symmetry R_γ ($\gamma = x, y, z$). Note that this implies that σ is odd under the nongapped symmetries. Physically, one side of the Ising transition—where we condense σ—is thus the Ising phase I_γ. The remaining invariant of the G-CFT is the charge of the symmetry fluxes. These symmetry fluxes determine the nearby gapped symmetric phase (where μ is condensed); hence, we know that there are only two distinct choices labeled by whether the symmetry flux of R_γ is even or odd under one of the other symmetries. We thus arrive at the transitions $[1, I_\gamma]$ and $[\text{Hal}, I_\gamma]$, respectively; these are realized by $H_1 + H_\gamma$ and $H_{\text{Hal}} + H_\gamma$.

These nine distinct symmetry-enriched CFTs are summarized in Fig. 6(a). Three of these, namely, $[\text{Hal}, I_\gamma]$ ($\gamma = x, y, z$), are topologically nontrivial with exponentially localized edge modes. We identify the critical spin-1 XXZ chain in Eq. (1) as being in the class $[\text{Hal}, I_z]$. A priori, it could have been that there are additional (codimension-one) Ising CFTs which cannot be smoothly
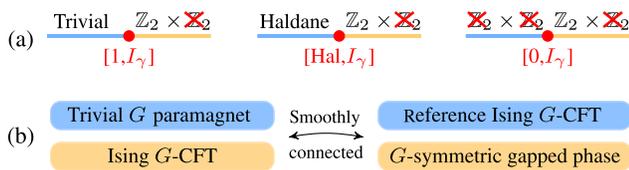

(a) Trivial $\mathbb{Z}_2 \times \mathbb{Z}_2$ [1, I_γ]   Haldane $\mathbb{Z}_2 \times \mathbb{Z}_2$ [Hal, I_γ] $\mathbb{Z}_2 \times \mathbb{Z}_2$ $\mathbb{Z}_2 \times \mathbb{Z}_2$ [0, I_γ]

(b) Trivial G paramagnet   Smoothly   Reference Ising G-CFT
    Ising G-CFT   connected G-symmetric gapped phase

FIG. 6. Classifying ($\mathbb{Z}_2 \times \mathbb{Z}_2$)-enriched Ising CFTs. (a) There are nine distinct $\mathbb{Z}_2 \times \mathbb{Z}_2$ Ising CFTs of codimension one coming in groups of three: One nearby gapped phase is in the trivial or nontrivial SPT phase or the phase that breaks the full $\mathbb{Z}_2 \times \mathbb{Z}_2$; the other side is an Ising phase preserving a $\mathbb{Z}_2$ symmetry R_γ ($\gamma = x, y, z$). All nine can be distinguished by symmetry properties of local operators and/or symmetry fluxes. (b) To see that these nine exhaust all options, we prove that all G-enriched Ising CFTs (Ising G-CFTs, in short) can be obtained by stacking gapped phases on top of a reference Ising G-CFT; the latter is chosen to be a transition between the trivial gapped phase and an Ising phase.

connected to one of these nine, meaning that they would fall outside our proposed set of invariants. However, one can prove (see Appendix D) that once one fixes the unbroken symmetry group G_{eff} and a list of charges for σ, then any G-enriched Ising CFT can be obtained by stacking with (and coupling to) a G-symmetric gapped phase; see Fig. 6(b). Note that the previous list is already closed under this action—e.g., stacking the Haldane phase on top of $[1, I_\gamma]$ gives us $[\text{Hal}, I_\gamma]$—and is hence complete.

To generalize the above discussion to a general symmetry group G, note that the first step involves determining the unbroken symmetry group G_{eff}. The possible choice of gapped symmetries G_{gap} is then constrained by ensuring that our Ising CFT has codimension one. The only remaining nontrivial labels are the charges of symmetry fluxes, which can be related to the topological properties of the nearby gapped phases. Altogether, this straightforwardly leads to a general classification [which is complete due to the bait-and-switch lemma; see Fig. 6(b) and Appendix D]:

> *Classification of symmetry-enriched Ising CFTs of codimension one for a unitary group G*: These CFTs are labeled by a choice of nested subgroups $G_{\text{gap}} \subset G_{\text{eff}} \subset G$ such that $G_{\text{eff}}/G_{\text{gap}} \cong \mathbb{Z}_2$, and by an element $\omega \in H^2(G_{\text{eff}}, \text{U}(1))$, i.e., a class of projective representations of G_{eff}.

Note that the quotient of unbroken symmetries and gapped symmetries $G_{\text{eff}}/G_{\text{gap}}$ can be identified with the $\mathbb{Z}_2$ symmetry that is intrinsic to the Ising CFT, which ensures that the CFT has codimension one (note that σ is odd under any $g \in G_{\text{eff}} - G_{\text{gap}}$). The projective class specifies the symmetry fluxes of G_{eff} such that if we condense μ, we enter the gapped phase labeled by this projective class. If we instead condense σ, we break the symmetry group down to G_{gap}, with the resulting gapped phase identified by $\omega|_{G_{\text{gap}}} \in H^2(G_{\text{gap}}, \text{U}(1))$. Let us illustrate the above general classification for $G = \mathbb{Z}_2 \times \mathbb{Z}_2$. One choice of nested subgroups is $G_{\text{gap}} = \{1\} \subset G_{\text{eff}} = \mathbb{Z}_2 \subset G = \mathbb{Z}_2 \times \mathbb{Z}_2$, with three choices for the unbroken symmetry G_{eff} and no choice for an element in $H^2(\mathbb{Z}_2, \text{U}(1)) \cong \{1\}$. The other choice is $G_{\text{gap}} = \mathbb{Z}_2 \subset G_{\text{eff}} = G$, with three choices for the gapped symmetry G_{gap} and two choices of $\omega \in H^2(\mathbb{Z}_2 \times \mathbb{Z}_2, \text{U}(1)) \cong \mathbb{Z}_2$. We thus recover all $3 + 3 \times 2 = 9$ distinct ($\mathbb{Z}_2 \times \mathbb{Z}_2$)-enriched Ising CFTs of codimension one.

Let us briefly comment on G-enriched Ising CFTs of codimension two. These occur if $G_{\text{gap}} = G_{\text{eff}}$, since then both σ and ε can open up a gap. This is the maximal codimension. Since such an Ising CFT requires the fine-tuning of two parameters, it generically appears in two-dimensional phase diagrams as an isolated point (with a first-order line emanating from it). The symmetry group acts only on gapped degrees of freedom, and the latter can realize any of its phases labeled by a choice of $G_{\text{eff}} \subset G$ and $\omega \in H^2(G_{\text{eff}}, \text{U}(1))$. For $\mathbb{Z}_2 \times \mathbb{Z}_2$, there are thus six such

symmetry-enriched Ising CFTs of codimension two. More generally, for any CFT, one can consider the symmetry enrichment where $G = G_{gap}$. However, this is not a very interesting example: It recovers the gapped classification and the CFT is a mere spectator. In particular, one can apply the usual mechanism of symmetry fractionalization, implying that the degeneracies with open boundary conditions (and their finite-size splitting) exactly coincide with that of the purely gapped case.

C. Gaussian criticality ($c = 1$)

There are six gapped phases for ($\mathbb{Z}_2 \times \mathbb{Z}_2$)-symmetric Hamiltonians, and thus, at least $\binom{6}{2} = 15$ direct transitions to consider. Six of these are Ising transitions of codimension one, such that they are indeed neighboring only two gapped phases; these were considered in Sec. V B and are all found to be distinct. However, we see that the remaining direct transitions are Gaussian CFTs (where the central charge $c = 1$), but there is no codimension-one Gaussian CFT with $\mathbb{Z}_2 \times \mathbb{Z}_2$ symmetry. As we see, the smallest codimension is two, and these phases are proximate to three or four distinct gapped phases. Hence, there are more than the naive $15 - 6 = 9$ remaining direct transitions. Nevertheless, in this section we see that all of these can be smoothly connected. In particular, this means that the set of gapped phases which are proximate to a given (symmetry-enriched) Gaussian CFT are not an invariant: They can change when tuning through the moduli space of CFTs. Relatedly, charge assignments of dominant (local and nonlocal) scaling operators can change when tuning through special points of this moduli space. Note that this phenomenon of level crossing in the universal spectrum is very particular to CFTs with symmetry-allowed marginal deformations.

Proving that all these symmetry-enriched Gaussian CFTs can be connected is somewhat technical—requiring a certain familiarity with these CFTs—and is explained in Appendix E 1. In the main text we focus on illustrative examples which contain all the key ingredients for the general case: For each of the six aforementioned pairs of gapped phases, we consider a Gaussian CFT that separates them. We note that different types of direct transitions can be realized as direct interpolations between the fixed-point Hamiltonians introduced in Sec. V A, as shown in Fig. 7. We first discuss these transitions from the lattice perspective, which has the benefit of being concrete and constructive. Afterward, we rephrase it in the field-theoretic language, which emphasizes the generality of these examples and makes a direct link with established CFT methods.

1. A lattice perspective

One generically needs to tune two parameters to find the direct transitions in Fig. 7, otherwise they split up into two
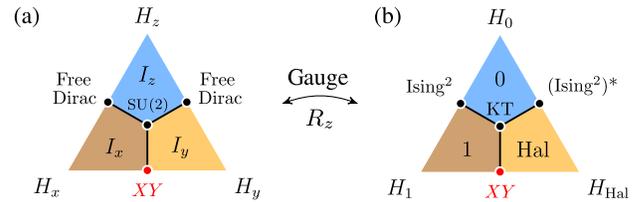

FIG. 7. Classifying ($\mathbb{Z}_2 \times \mathbb{Z}_2$)-enriched Gaussian CFTs. All $\mathbb{Z}_2 \times \mathbb{Z}_2$ CFTs with $c = 1$ can be connected (for $G_{gap} = \{1\}$ and $G_{eff} = G$). The U(1)-symmetric spin-1/2 XY chain appears in both panels (red dot). (a) The black lines are $c = 1$ CFTs whose (dominant) local operators have different symmetry properties; nevertheless, these operators become degenerate at the SU(2)-symmetric point, smoothly connecting these $c = 1$ CFTs. (b) Obtained from the former by a (nonlocal) unitary transformation which can be interpreted as gauging R_z symmetry. Two of the three $c = 1$ lines are described by orbifold CFTs; the dominant symmetry flux is symmetry-even (Ising^2) or symmetry-odd [(Ising^2)*], becoming degenerate at the Kosterlitz-Thouless (KT) point.

separate Ising transitions. Relatedly, each of these transitions is proximate to two other gapped phases, which are not shown. The clearest instance of this is the XY model $H_{XY} = \sum_n (X_n X_{n+1} + Y_n Y_{n+1})$ which appears twice in Fig. 7, once in each panel (red dot); indeed, $H_{XY} = H_x + H_y = H_1 + H_{Hal}$. If one breaks its U(1) symmetry, one flows to one of the I_x or I_y phases (left panel). If one instead dimerizes the chain, one flows to either the trivial or topological Haldane phase (right panel); see also the discussion in Sec. V A. To ensure that the CFT has codimension two, we need the full $\mathbb{Z}_2 \times \mathbb{Z}_2$ symmetry to act nontrivially on the CFT; see Sec. V C 2. In other words, $G_{eff} = \mathbb{Z}_2 \times \mathbb{Z}_2$ and $G_{gap} = \{1\}$. The remaining invariants which we propose are thus the charges of local operators and of symmetry fluxes.

At first glance, such charges seem to indicate distinct Gaussian $\mathbb{Z}_2 \times \mathbb{Z}_2$ CFTs. For instance, let us compare the $[I_x, I_y]$ transition to the $[I_x, I_z]$ transition. The former has a U(1) symmetry in the x-y plane, and indeed, X_n and Y_n have the same scaling dimension $\Delta_\theta = 1/4$ for H_{XY}, whereas Z_n has $\Delta_\varphi = 1$. The roles are reversed in the latter, where Y_n is now the one with larger scaling dimension. Does this not give us a discrete invariant? I.e., for H_{XY} we can say that all local operators of lowest scaling dimension are odd under R_z. This discrete statement is surely true, but not invariant: The Gaussian CFT has a marginal tuning parameter that smoothly connects a whole line of universality classes [59,96]. Indeed, this is well known for the spin-1/2 XXZ chain $H = \sum_n (X_n X_{n+1} + Y_n Y_{n+1} + \tilde{\Delta} Z_n Z_{n+1})$, which is described by a range of Gaussian CFTs for $-1 < \tilde{\Delta} \le 1$. As one tunes $\tilde{\Delta}$ from 0 to 1, the scaling dimensions of X_n, Y_n, and Z_n smoothly evolve toward the same value (this being $1/2$); at $\tilde{\Delta} = 1$, the three operators are related by the SU(2)

symmetry of the model. All three $[I_\gamma, I_{\gamma'}]$ transitions can clearly be connected through this point, as shown in Fig. 7. The takeaway message is that the space of local operators with smallest scaling dimension can change: This two-dimensional space becomes part of a larger-dimensional vector space at the SU(2)-symmetric point. The above attempt at defining a discrete invariant charge is thus not well-founded.

The discussion above demonstrates a subtlety in associating invariant charges with local observables. Something similar happens for the charges of symmetry fluxes. To find a Gaussian CFT whose symmetry fluxes have nontrivial charge, we need to consider transitions which are not invariant under stacking with the gapped Haldane phase: Since the latter comes with charged symmetry fluxes, any transition that is not affected by this could not have had well-defined charges for its symmetry fluxes to begin with. To make clear what we mean, consider [1, Hal], as realized by the XY chain. At this transition, the two distinct symmetry fluxes of R_γ for H_1 and H_{Hal}—as described in Sec. V A—become scaling operators with the same scaling dimension $\Delta = 1/4$. We can thus not associate a unique charge with the symmetry flux of R_γ. This is related to the fact that $[1, \text{Hal}] * \text{Hal} = [1, \text{Hal}]$, since it would merely interchange both sides of the transition. Similarly, the $[I_\gamma, I_{\gamma'}]$ transitions considered above would also absorb such a SPT phase (since $I_\gamma * \text{Hal} = I_\gamma$).

We can, however, find $c = 1$ transitions which are (seemingly) not invariant under such a stacking: Consider the transition between the trivial phase and the phase that completely breaks $\mathbb{Z}_2 \times \mathbb{Z}_2$, i.e., [1,0], realized by $H_1 + H_0$. Conceptually, one can think of this as two separate Ising transitions occurring at the same point. Indeed, the field theory describing this critical point is not a usual Gaussian CFT, but rather the direct product of two Ising CFTs usually denoted by (Ising)². Accordingly, each R_γ has a unique symmetry flux and hence a well-defined charge. For [1,0], these fluxes commute with all symmetries, whereas for [Hal,0], they anticommute. Indeed, stacking with the Haldane phase interchanges these two transitions. However, despite having distinct discrete charge in these two cases, these models can be smoothly connected by tuning to $H_1 + H_{\text{Hal}} + H_0$, as shown in Fig. 7(b). The catch is that at this special point, the space of symmetry fluxes becomes two dimensional, and the aforementioned charge is no longer well defined; this arises naturally from a careful study of the Gaussian universality class (see Sec. V C 2). Note that the novel phase diagram in Fig. 7(b) can be obtained from the known phase diagram in Fig. 7(a) by applying the duality transformation mentioned in Sec. V A.

In conclusion, all $(\mathbb{Z}_2 \times \mathbb{Z}_2)$-enriched CFTs with central charge $c = 1$ can be smoothly connected if they are of codimension two (see Appendix E 1 for further details). For higher codimension, there are distinct symmetry-enriched

CFTs. Examples have already appeared in the literature [11,34], and we touch upon this in Sec. VII.

2. A field-theoretic perspective

We now give a field-theoretic interpretation of Fig. 7, which is complementary to the previous discussion.

Let us recall the compact boson CFT (also known as the one-component Luttinger liquid), which contains a phase field $\theta(x)$ and its conjugate field $\partial_x \varphi(x)$ that generates shifts in $\theta(x)$, i.e., $[\partial_x \varphi(x), \theta(y)] = 2\pi i \delta(x - y)$ [59,96]. Both fields are 2π periodic and the Hamiltonian is given by

$$H = \frac{1}{2\pi} \int \left(\frac{1}{4K} (\partial_x \varphi)^2 + K (\partial_x \theta)^2 \right) dx. \quad (16)$$

Here, K is the stiffness or Luttinger liquid parameter (sometimes one instead speaks of the compactification radius [97] $r_c = \sqrt{K}$). There is thus a one-parameter family of compact boson CFTs with a duality $K \leftrightarrow (1/4K)$ which interchanges the two fields. Particularly important are the primary vertex operators $e^{\pm i(m\varphi + n\theta)}$ which have scaling dimension $\Delta_{m,n} = m^2 K + n^2/(4K)$ (and conformal spin $s_{m,n} = mn$). These vertex operators are local if and only if $n, m \in \mathbb{Z}$.

To see how the $\mathbb{Z}_2 \times \mathbb{Z}_2$ symmetry acts in this field theory, it is useful to use a lattice-continuum correspondence. Let us consider the XY chain $H_{XY} = -\sum_n (X_n X_{n+1} + Y_n Y_{n+1})$: This can be mapped to free fermions, allowing for a straightforward continuum limit of the lattice model, which ends up with the compact boson CFT where $K = r_c = 1$, also called the free Dirac CFT. This route gives a direct relationship between lattice operators and operators of the CFT [98–100]. For instance, the generator of the on-site lattice U(1) symmetry Z_n maps to the generator in the continuum $\partial_x \varphi$. Similarly useful correspondences are $X_n \sim \cos \theta$ and $Y_n \sim \sin \theta$. From such relations—and from knowing how the symmetries act on the lattice operators—we can infer that R_x, R_y, and R_z act in the continuum as

$$R_x : \begin{cases} \varphi \to -\varphi, \\ \theta \to -\theta, \end{cases} \quad R_y : \begin{cases} \varphi \to -\varphi, \\ \theta \to \pi - \theta, \end{cases} \quad R_z : \begin{cases} \varphi \to \varphi, \\ \theta \to \theta + \pi. \end{cases}$$

$$(17)$$

(Note that $R_z = R_x R_y$, as required. Moreover, in Appendix E 1 we show that up to relabeling the CFT fields, this is the only $\mathbb{Z}_2 \times \mathbb{Z}_2$ action on the φ, θ fields of the compact boson CFT.) Enforcing these symmetries constrains the possible perturbations of the CFT. In fact, only two relevant operators commute with this symmetry, namely, the vertex operators $\cos(2\theta)$ and $\cos(\varphi)$ with scaling dimension $\Delta = 1 < 2$ at $K = 1$ [on the lattice, these correspond to $X_n X_{n+1} - Y_n Y_{n+1}$ and $(-1)^n (X_n X_{n+1} + Y_n Y_{n+1})$, respectively]. Hence, this

($\mathbb{Z}_2 \times \mathbb{Z}_2$)-enriched $c = 1$ CFT has codimension two. For example, $\sin(2\theta)$—which is also relevant—is odd under R_x and is thus forbidden [the lattice-continuum correspondence is $X_n Y_{n+1} + Y_n X_{n+1} \sim \sin(2\theta)$]. We note that $\pm\cos(2\theta)$ drives to I_x and I_y, whereas $\pm\cos(\varphi)$ drives to the trivial and Haldane phase; this is consistent with the red dot in Figs. 7(a) and 7(b).

The above action of $\mathbb{Z}_2 \times \mathbb{Z}_2$ is established at $K = 1$, but we see that it must continue to hold for any value of K (since $R_\gamma^2 = 1$). Nevertheless, we obtain other actions when considering, e.g., a transition $[I_x, I_z]$ instead of $[I_x, I_y]$. Indeed, for $H = -\sum_n (X_n X_{n+1} + Z_n Z_{n+1})$ we also arrive at the Dirac CFT in the continuum limit, where we now denote the fields by $\tilde{\varphi}$ and $\tilde{\theta}$ to avoid confusion. The lattice-continuum correspondence including $Y_n \leftrightarrow \partial_x \tilde{\varphi}$ and $Z_n \leftrightarrow \sin(\tilde{\theta})$ implies

$$R_x : \begin{cases} \tilde{\varphi} \to -\tilde{\varphi}, \\ \tilde{\theta} \to -\tilde{\theta}, \end{cases} \quad R_y : \begin{cases} \tilde{\varphi} \to \tilde{\varphi}, \\ \tilde{\theta} \to \tilde{\theta} + \pi, \end{cases} \quad R_z : \begin{cases} \tilde{\varphi} \to -\tilde{\varphi}, \\ \tilde{\theta} \to \pi - \tilde{\theta}. \end{cases}$$
(18)

The same lattice symmetries $R_{\gamma=x,y,z}$ thus act differently in the low-energy compact boson CFTs for these distinct transitions, as evidenced by Eqs. (17) and (18). In particular, this tells us that the local vertex operators of these CFTs (identified by their scaling dimensions) carry seemingly distinct charges, as already observed in the previous subsection.

Nevertheless, these two compact boson CFTs are merely two extremes of a single unified CFT. To see this, we use that tuning K preserves criticality. This corresponds to the black lines in Fig. 7(a) emerging from the phase diagram's edges. As $K \to 1/2$, we reach the center of the phase diagram. To see that the CFTs in terms of φ, θ and $\tilde{\varphi}, \tilde{\theta}$ truly coincide at this point, we use the fact that the self-dual point $K = 1/2$ is known to have an emergent $SU(2) \times SU(2)$ symmetry. As we show in Appendix E 2, this allows us to perform a change of variables that leaves the action invariant:

$$\partial_x \tilde{\theta} = -2 \cos\theta \sin\varphi, \qquad \partial_x \tilde{\varphi} = -2 \sin\theta \cos\varphi. \quad (19)$$

Note that under this correspondence, Eqs. (17) and (18) coincide. The identification in Eq. (19) tells us how these seemingly distinct compact boson CFTs are glued together. This can also be understood from the fact that at $K = 1/2$, the CFT has nine marginal perturbations [96]. Only three of these are compatible with $\mathbb{Z}_2 \times \mathbb{Z}_2$ symmetry, corresponding to the three gapless lines emanating from this point in Fig. 7(a).

Let us now consider the other $c = 1$ transitions shown in Fig. 7(b). As mentioned in the previous subsection, this phase diagram is obtained from Fig. 7(a) by a nonlocal change of variables which maps the XY chain to itself (see Appendix C). In the field theory, this can be interpreted as gauging R_z, the effect of which depends on how R_z acts on the fields. If R_z is a subset of the U(1) rotation $\theta \to \theta + \alpha$—as happens for $[I_x, I_y]$ [see Eq. (17)]—then gauging R_z

amounts [101] to $r_c \to 1/r_c$, or, equivalently, $K \to 1/K$ [96]. This indeed keeps the free Dirac point with $K = 1$ invariant (the red dots in Fig. 7). The self-dual point $K = 1/2$—in the middle of the phase diagram—maps to $K = 2$, which is called the Kosterlitz-Thouless (KT) point since at this point there are no relevant U(1)-symmetric operators. However, if R_z negates the fields—as happens for $[I_x, I_z]$ [see Eq. (18)]—then it is known that gauging this is no longer the usual compact boson CFT. Instead, we obtain a so-called orbifold CFT (this can also be seen as the boson CFT compactified on $S^1/\mathbb{Z}_2$) [96]. In particular, the free Dirac CFT in Fig. 7(a) maps to a stack of two Ising CFTs in Fig. 7(b), usually denoted by (Ising)^2, which is a $c = 1$ orbifold CFT with orbifold radius $r_{\text{orbifold}} = 1$ [96]. This remains critical as one tunes $r_{\text{orbifold}} \to 1/\sqrt{2}$, reaching the center of the phase diagram. Indeed, it is known that at the particular value $r_{\text{orbifold}} = 1/\sqrt{2}$, the $c = 1$ orbifold CFT coincides with the aforementioned KT point of the compact boson CFT [96]. The interpolation between the three models H_1, H_{Hal}, and H_0 thus provides a concrete lattice realization—incidentally solvable by the Bethe ansatz—of the deep fact that the $c = 1$ orbifold CFT and compact boson CFT can be connected by a marginal perturbation, which in this case also preserves $\mathbb{Z}_2 \times \mathbb{Z}_2$.

Lastly, we comment on symmetry fluxes from the perspective of field theory. For the compact boson CFT, the space of symmetry fluxes for R_γ is two dimensional. This is easiest to see for R_z in the case where it acts as $\theta \to \theta + \pi$ [see Eq. (17)]. The two independent fluxes are then $\cos(\varphi/2)$ and $\sin(\varphi/2)$ with dimension $\Delta = K/4$ (on the lattice, these correspond to $\cdots Z_{n-2} Z_{n-1} Z_n$ with n even and odd, respectively). The former (latter) is even (odd) under R_x and R_y. We thus cannot associate a unique charge with the symmetry flux of R_z. The situation is seemingly different for the orbifold CFT, which we illustrate for the (Ising)^{2}CFT as realized by $H = H_1 + H_0$ [appearing in Fig. 7(b)]. Recalling the definition of H_0 in Eq. (15), we see that if σ_i denotes the spin operators of the two copies of the Ising CFT, then σ_1 is odd under R_y and R_z (but even under R_x), and the same is true for σ_2 with R_x and R_y interchanged. From this, we can infer that the symmetry flux for R_z is $\mu_1 \mu_2$ (with dimension $\Delta = 1/4$). Most importantly, this is unique. Indeed, its dimension is well separated from that of $(\mu_1 \mu_2) \times (\sigma_1 \sigma_2) \sim \psi_1 \psi_2$ for which $\Delta = 1$ (similarly, the unique symmetry flux of R_x is μ_2 with $\Delta = 1/8$; its subdominant flux is $\sigma_1 \mu_2$ with $\Delta = 1/4$). As we discuss in Sec. III, we can associate charges with unique symmetry fluxes. For the transition [1,0], it is easy to see that the symmetry flux of R_z is even under R_x and R_y, whereas for [Hal,0] it is odd. Hence, the two orbifold lines in Fig. 7(b) seem topologically distinct. The catch, however, is that both lines connect to the compact boson line, as we discuss above. At that point, the scaling dimensions of $\mu_1 \mu_2$ and $\psi_1 \psi_2$ meet, coinciding with the aforementioned $\cos(\varphi/2)$ and $\sin(\varphi/2)$. Hence, to realize topologically nontrivial

symmetry-enriched $c = 1$ CFTs, one either needs to go to higher codimension or larger symmetry groups; examples for both are discussed in Sec. VII.

VI. OTHER EXAMPLES IN 1 + 1D

Although the framework we introduce is generally applicable, we have thus far shown examples only for symmetry groups $\mathbb{Z}_2 \times \mathbb{Z}_2$ and $\mathbb{Z}_2 \times \mathbb{Z}_2^T$. The purpose of this section is to add two more illustrative examples to this list: a bosonic $\mathbb{Z}_3 \times \mathbb{Z}_3$ and a fermionic $\mathbb{Z}_2^f \times \mathbb{Z}_2^T$. Various other symmetry groups will appear in the next section (Sec. VII on previously studied examples in the literature).

A. $\mathbb{Z}_3 \times \mathbb{Z}_3$ example

We consider a one-dimensional chain where each site consists of a qutrit. For each qutrit, let X and Z denote the analogs of the Pauli matrices (also known as the clock matrices):

$$X = \begin{pmatrix} 0 & 1 & 0 \\ 0 & 0 & 1 \\ 1 & 0 & 0 \end{pmatrix} \quad \text{and} \quad Z = \begin{pmatrix} 1 & 0 & 0 \\ 0 & \omega & 0 \\ 0 & 0 & \omega^2 \end{pmatrix}, \quad (20)$$

where $\omega = e^{2\pi i/3}$. Note that $XZ = \omega ZX$. Subdividing the chain into two sublattices (labeled A and B), we define the Hamiltonian

$$H = \eta_{\text{triv}} H_{\text{triv}} + \eta_{\text{SSB}} H_{\text{SSB}} + \eta_{\text{SPT}} H_{\text{SPT}}, \quad (21)$$

where

$$H_{\text{triv}} = -\sum_n (X_{A,n} + X_{B,n}) + \text{H.c.}, \quad (22)$$

$$H_{\text{SSB}} = -\sum_n Z_{B,n}^\dagger Z_{B,n+1} + \text{H.c.}, \quad (23)$$

$$H_{\text{SPT}} = -\sum_n (Z_{B,n-1}^\dagger X_{A,n} Z_{B,n} + Z_{A,n} X_{B,n} Z_{A,n+1}^\dagger)$$

$$+ \text{H.c.} \quad (24)$$

For all parameters, this Hamiltonian has a $(\mathbb{Z}_3 \times \mathbb{Z}_3)$-symmetry group generated by $P_A = \prod_n X_{A,n}$ and $P_B = \prod X_{B,n}$. The fixed-point Hamiltonian H_{triv} has a product state ground state, whereas H_{SSB} spontaneously breaks P_B such that the remaining symmetry group is $\mathbb{Z}_3$ generated by P_A. More interestingly, H_{SPT} is a generalization of the cluster model encountered in Sec. II and is one of the two nontrivial SPT phases protected by $\mathbb{Z}_3 \times \mathbb{Z}_3$ [102,103] (the other being given by the site-centered inversion of H_{SPT}).

We consider only non-negative tuning parameters in Eq. (21). There are two limiting cases of this model which have been studied before. First, if $\eta_{\text{SPT}} = 0$, then the A sites

remain in a decoupled product state, and the B sites are described by the three-state Potts chain. In particular, the transition between the trivial and SSB phase ($\eta_{\text{triv}} = \eta_{\text{SSB}}$) is known to be described by the three-state Potts CFT with central charge $c = 4/5$ [59,104,105]. Second, if $\eta_{\text{SSB}} = 0$, then we have a direct SPT transition which is known to be described by an orbifold CFT with central charge $c = 8/5$ [106]. This gives us two edges of the phase diagram in Fig. 8(a); we obtain the rest of the phase diagram using DMRG. We observe that the Potts criticality is stable over a whole line; this is consistent with the Potts CFT having only a single relevant perturbation in the presence of $\mathbb{Z}_3$ symmetry (in this case being P_B, which is spontaneously broken on one side of the transition). Note that with periodic boundary conditions, there is a duality [107] that mirrors the phase diagram ($\eta_{\text{triv}} \leftrightarrow \eta_{\text{SPT}}$); hence, the critical line between the SPT phase and the SSB phase is also three-state Potts criticality. Nevertheless, we see that these two Potts criticalities are distinct symmetry-enriched versions, the latter being topologically nontrivial.

Let us focus on the symmetry flux for P_B. In the trivial gapped phase, its end-point operator is trivial, whereas in the gapped SPT phase, we have [108] long-range order in the string

$$\mathcal{S}_n^B = \cdots X_{B,n-2} X_{B,n-1} \mathcal{O}_n^B \quad \text{with} \quad \mathcal{O}_n^B = Z_{A,n}^\dagger. \quad (25)$$

Since $P_A \mathcal{O}_n^B P_A^\dagger = \omega \mathcal{O}_n^B$, long-range order in this charged symmetry flux indeed implies a nontrivial SPT phase.
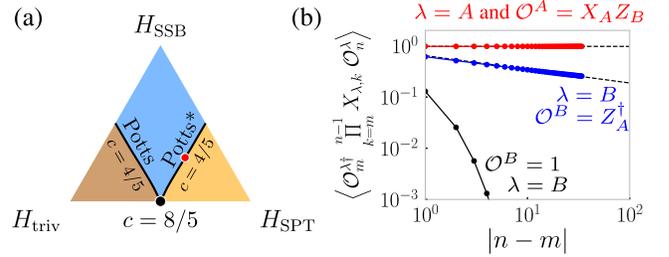

FIG. 8. $(\mathbb{Z}_3 \times \mathbb{Z}_3)$-enriched Potts universality with topological edge modes. (a) Phase diagram of Eq. (21) with $\mathbb{Z}_3 \times \mathbb{Z}_3$ symmetry generated by $\prod_n X_{A,n}$ and $\prod_n X_{B,n}$ obtained with DMRG. The blue phase spontaneously breaks the latter symmetry. The two black lines (despite appearances, these are not straight) are two topologically distinct Potts transitions separated by a CFT with central charge $c = 8/5$. (b) String correlation functions for the red point in (a) given by $(\eta_{\text{triv}}, \eta_{\text{SSB}}, \eta_{\text{SPT}}) \approx (0.8, 1, 1.775)$. The symmetry flux for $\prod_n X_{A,n}$ has long-range order, whereas the one for $\prod_n X_{B,n}$ has algebraic decay; their end-point operators are nontrivially charged under the global symmetries, protecting a threefold degeneracy with open boundaries (see main text). The dashed lines are the analytic predictions; the algebraic decay has dimension $\Delta = 2/15$. Without the charged end-point operator, the decay is exponential (the black line is multiplied $\times 10$ for visibility).

We expect that these symmetry fluxes will still distinguish the two Potts transitions from the trivial or SPT phase to the symmetry-breaking phase. In particular, in Fig. 8(b) we show that at the critical point neighboring the SPT phase, the charged symmetry flux in Eq. (25) has the slowest possible decay: $\Delta = 2/15$ is the smallest scaling dimension of the Potts CFT [59]. If we leave out the charged end-point operator, the correlation function decays exponentially. This is in contrast to the vanilla-flavored Potts criticality between the trivial and symmetry-breaking phases, where it is the uncharged string that has the slowest possible decay ($\Delta = 2/15$). Similar to the Ising CFT, the Potts CFT has a unique nonlocal scaling operator with this dimension [59].

In conclusion, we find two topologically distinct Potts transitions which are enriched by $\mathbb{Z}_3 \times \mathbb{Z}_3$ symmetry; these are distinguished by the symmetry properties of certain nonlocal scaling operators. One consequence is that despite both transitions being a Potts universality with central charge $c = 4/5$, they have to be separated by a different universality class. For instance, in Fig. 8(a) the two phase transitions meet at a multicritical point with central charge $c = 8/5$. Another consequence of this topological invariant is that with open boundaries, the transition between the SPT and symmetry-breaking phases host exponentially localized edge modes, as we explain in Sec. IV.

B. A fermionic example

Thus far, we have discussed examples of bosonic G-CFTs. However, the concept also applies to fermionic systems. We illustrate this by reinterpreting the noninteracting critical chains of Ref. [33] as Majorana CFTs enriched by fermionic parity symmetry $\mathbb{Z}_2^f$ and spinless time-reversal symmetry $\mathbb{Z}_2^T$; this demonstrates that it is stable to interactions. The nontrivial case hosts zero-energy Majorana edge modes. (The models we discuss are related to the spin models encountered in Sec. II by a Jordan-Wigner transformation; however, since this nonlocal mapping changes the physical interpretation, we keep this section self-contained within the fermionic language.)

We consider spinless fermions $\{c_n^\dagger, c_m\} = \delta_{nm}$, where spinless time-reversal symmetry T acts in the occupation basis, i.e., $Tc_nT = c_n$ and $Tc_n^\dagger T = c_n^\dagger$. It is useful to introduce the basis of Majorana modes $\gamma_n = c_n^\dagger + c_n$ and $\tilde{\gamma}_n = i(c_n^\dagger - c_n)$. We see that $T\gamma_nT = \gamma_n$ and $T\tilde{\gamma}_nT = -\tilde{\gamma}_n$. Using these modes, we now define two critical Majorana chains which are symmetric with respect to T and fermionic parity symmetry $P = \prod P_n$ [where $P_n = i\tilde{\gamma}_n\gamma_n = (1 - 2c_n^\dagger c_n)$]:

$$H = i\sum_n \tilde{\gamma}_n(\gamma_n + \gamma_{n+1}),$$

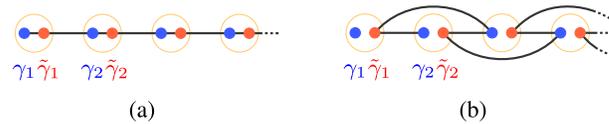$$H'' = i\sum_n \tilde{\gamma}_n(\gamma_{n+1} + \gamma_{n+2}). \quad (26)$$

FIG. 9.   Examples of ($\mathbb{Z}_2^f \times \mathbb{Z}_2^T$)-enriched Majorana CFTs. Both Majorana chains are described by the Majorana CFT ($c = 1/2$) but fall into distinct symmetry-enriched classes. (a) For the standard translation-invariant Majorana chain, the P-even symmetry flux of P is even under spinless time-reversal symmetry T. (b) For this chain, the P-even symmetry flux of P is odd under T; this protects a Majorana edge mode with finite-size splitting of order $1/L^{14}$ (if the system is noninteracting, the finite-size splitting is exponentially small).

These are sketched in Fig. 9 (for a half-infinite chain). In the bulk, both systems are described by the Majorana CFT with central charge $c = 1/2$ [33]. Nevertheless, they show distinct behavior near their boundaries: H'' has a dangling Majorana edge mode, as shown in Fig. 9(b). In Ref. [33], which considered only noninteracting systems, it was proven that as long as we preserve P and T symmetry and keep the bulk in the universality class of the Majorana CFT, then this edge mode remains exponentially localized, despite the absence of well-defined gapped degrees of freedom.

We now illustrate how these two models are distinguished by the charges of the symmetry fluxes of P. Interestingly, for fermionic systems it is possible for a symmetry flux to be charged under itself: The symmetry flux of fermionic parity can itself be fermionic. Indeed, both H and H'' have one symmetry flux of P which is odd under P, and one which is even. The former is the same for both models, being given by $\cdots P_{n-2}P_{n-1}\gamma_n$ (with scaling dimension $\Delta = 1/8$) [61]. Physically, this corresponds to both phases being proximate to the topological Kitaev phase where this symmetry flux has long-range order. The symmetry flux of P which is even under P (with the same scaling dimension) is given by [61]

$$\mathcal{S}_n^P = \cdots P_{n-2}P_{n-1}P_n \quad \text{(for } H\text{)},$$

$$\mathcal{S}_n^P = \cdots P_{n-2}P_{n-1}(i\gamma_n\gamma_{n+1}) \quad \text{(for } H''\text{)}. \quad (27)$$

(The prefactors of the end-point operators are chosen such that the symmetry fluxes are Hermitian; see Sec. III.) We observe that the former is even under T, whereas the latter is odd under T. This defines a discrete bulk invariant. Analogous to the discussion in Sec. IV, the latter protects a Majorana edge mode at each boundary, giving a global twofold degeneracy with a finite-size splitting of order $1/L^{14}$. Indeed, under a Jordan-Wigner transformation—which is exact for open boundary conditions—the models in Eq. (26) are mapped onto the spin chains in Eq. (6) discussed in Sec. II. It would be interesting to work out the analogous case for phase

transitions between distinct SPT phases in parafermionic chains [109,110].

VII. APPLICATION TO PREVIOUS WORKS

In this penultimate section, we demonstrate how previous works on critical systems with edge modes can be placed into the framework of symmetry-enriched CFTs proposed in this work. Considering the extent of the literature on topologically nontrivial gapless phases [11–36], a complete demonstration would constitute a work on its own. Here, we limit ourselves to a few (chronologically ordered) case studies. We point out how these systems can be interpreted as nontrivial symmetry-enriched CFTs, for which we identify bulk invariants.

For clarity, let us mention that in 2011 there were several contemporaneous works discussing algebraically ordered superconductors with topological edge modes [12–14]. However, these are not examples of edge modes protected by a symmetry-enriched CFT. This can be seen from the fact that in these cases, the edge modes have algebraic finite-size splitting of order $1/L^{\beta}$ where the power β is proportional to the Luttinger liquid parameter K. This means that the edge modes can be destroyed by smoothly tuning K to a small enough value. Hence, there cannot be a discrete bulk invariant associated with the $c = 1$ CFT. This is consistent with symmetries not being important to stabilize the edge modes in Refs. [12–14] [aside from the U(1) symmetry stabilizing criticality].

A. Prediction of a gapless topological Haldane liquid phase in a one-dimensional cold polar molecular lattice

In Ref. [11], Kestner *et al.* introduced a gapless analog of the spin-1 Haldane phase. Because of the context of the work (i.e., dipolar gases), long-range interactions were considered. Nevertheless, a nearest-neighbor model is straightforward:

$$H = \sum_{n} [(S_n^x S_{n+1}^x + S_n^y S_{n+1}^y)(S_n^z + S_{n+1}^z)^2 + \Delta S_n^z S_{n+1}^z].$$
$$\tag{28}$$

The Hamiltonian looks similar to the spin-1 XXZ chain, with an extra factor in the spin-hopping term such that $\sum_{n}(S_n^z)^2$ is conserved—this makes all the difference. For $0 < \Delta < 1$, the system is critical with central charge $c = 1$, and using the methods of Ref. [11], it can be shown that the system is topologically nontrivial: There is still long-range order in the Haldane string order parameter $\cdots R_{n-2}^z R_{n-1}^z S_n^z$ and the ground state is twofold degenerate with open boundary conditions.

We note that this model is an example of a $c = 1$ CFT enriched by the $\mathbb{Z}_2 \times \mathbb{Z}_2$ group of π rotations R^x, R^y, and R^z [in fact, the latter symmetry is enhanced to a

full U(1) generated by $\sum_{n}(S_n^z)^2$]. Indeed, the fact that $\cdots R_{n-2}^z R_{n-1}^z S_n^z$ has long-range order, tells us, first, that the symmetry flux of R^z is unique and, second, that it has a nontrivial charge with respect to R^x and R^y. This thus gives us a discrete topological invariant for the critical bulk. In Sec. V C we see that there are no topologically nontrivial ($\mathbb{Z}_2 \times \mathbb{Z}_2$)-enriched CFTs of minimal codimension. Indeed, Eq. (28) is of higher codimension and is not naturally interpreted as a critical point between phases with $\mathbb{Z}_2 \times \mathbb{Z}_2$ symmetry. However, it is a ($\mathbb{Z}_2 \times \mathbb{Z}_2 \times \mathbb{Z}_2^T$)-enriched CFT of minimal codimension. More precisely, it occurs as a direct transition between two gapped phases which are topologically distinct with respect to $T_{\mathrm{spin}} = R^y K$ but which are topologically identical and nontrivial with respect to $\mathbb{Z}_2 \times \mathbb{Z}_2$. To see this, and to shed light on the unusual conservation law, it is useful to consider the unitary $U \equiv \exp[i(\pi/2)\sum_{n}(S_n^z)^2]$. It can be shown that this commutes with $R^{\gamma=x,y,z}$ but not with T_{spin}, i.e., $UT_{\mathrm{spin}}U^{\dagger} = R^x K \neq T_{\mathrm{spin}}$. Hence, if H_{XXZ} is the spin-1 XXZ chain, which is nontrivial with respect to π rotations and time reversal, then $UH_{XXZ}U^{\dagger}$ is still nontrivial with respect to the former, but not the latter. Remarkably, the model in Eq. (28) is exactly the halfway interpolation between these two, $H = \frac{1}{2}(H_{XXZ} + UH_{XXZ}U^{\dagger})$. Indeed, since U toggles between the two gapped phases, the transition must occur at the $\sum(S_n^z)^2$-symmetric point.

Lastly, note that both gapped phases have the same symmetry flux for R^z (this can hence remain long-range ordered at criticality) but have distinct symmetry fluxes for R^x, i.e., $\cdots R_{n-2}^x R_{n-1}^x S_n^x$ and $\cdots R_{n-2}^x R_{n-1}^x (S_n^y S_n^z - S_n^z S_n^y)$. At the critical point, these symmetry fluxes for R^x become algebraically ordered with the same scaling dimension. They are thus degenerate, but both have the same nontrivial charges with respect to R^y and R^z, consistent with this being a nontrivially enriched CFT.

B. Quantum criticality in topological insulators and superconductors: Emergence of strongly coupled Majoranas and supersymmetry

One of the phase transitions considered by Grover and Vishwanath in Ref. [16] is between a topological superconductor in class DIII (protected by an antiunitary symmetry satisfying $T^2 = P$) and an Ising phase which spontaneously breaks T. It was demonstrated that the edge flows to an unusual fixed point, exhibiting itself in unusual fermionic correlations near the boundary (as a function of time).

We point out that this transition is an Ising CFT enriched by T and fermionic parity symmetry P. The clearest way of seeing this is that the symmetry flux of P (which has long-range order for this bosonic transition) can be shown to be odd under T. In an approximate converse, the μ operator of the Ising CFT is odd under fermionic parity symmetry: $P\mu P = -\mu$; see Appendix F 1 for details. As we discuss in

Fig. 4, this nontrivial charge stabilizes the spontaneously fixed boundary condition. According to the analysis in Sec. IV, we thus expect that this class of transition generically has a global twofold degeneracy for open boundaries whose finite-size splitting is exponentially small in system size.

C. Gapless symmetry-protected topological phase of fermions in one dimension

In Ref. [19], Keselman and Berg show that spinful fermions with attractive triplet pairing stabilize a $c = 1$ CFT with exponentially localized edge modes protected by fermionic parity symmetry P [enhanced to a full U(1) in their particular model] and time-reversal symmetry T (obeying $T^2 = P$). In addition to a field-theoretic analysis, this is numerically demonstrated in a simple lattice model:

$$H = -\sum_{n,\sigma}(c_{n,\sigma}^\dagger c_{n+1,\sigma} + \text{H.c.}) + U\sum_n \Delta_n^\dagger \Delta_n, \quad (29)$$

where $\sigma \in \{\uparrow, \downarrow\}$ and $\Delta_n = c_{n,\uparrow}c_{n+1,\downarrow} + c_{n,\downarrow}c_{n+1,\uparrow}$ [on the lattice, the symmetries are given by $P = \prod_j P_j$ where $P_j = e^{i\pi(n_{j,\uparrow}+n_{j,\downarrow})}$ and $T = \prod_j e^{i\pi S_j^y}K$ with $S_j^y = (i/2) \times (c_{j,\downarrow}^\dagger c_{j,\uparrow} - c_{j,\uparrow}^\dagger c_{j,\downarrow})$]. For $U < 0$, the spin sector is gapped, whereas charges remain gapless. The stability of the edge mode was argued to be a consequence of the gap to single-fermion excitations (which moreover implies that the phenomenon persists upon adding spin-orbit coupling). Moreover, in Ref. [19] it was shown that fermionic parity symmetry anticommutes with T near the edges, implying edge modes.

We remark that this $c = 1$ CFT is nontrivially enriched by P and T. We find that for $U < 0$, the symmetry flux of P has long-range order and is given by $\mathcal{S}_j^P = \cdots P_{j-2}P_{j-1}(n_{j,\uparrow} - n_{j,\downarrow})$, which obeys $T\mathcal{S}^P T^{-1} = -\mathcal{S}^P$. See Appendix F 2 for numerical details. This generalizes the observation of Ref. [19] that P and T anticommute near the boundary to a topological invariant in the bulk. This moreover confirms that the phase is protected by virtue of P being a gapped symmetry. The fact that the nontrivial symmetry flux is for a gapped symmetry is naturally related to the exponentially small finite-size splitting observed in Ref. [19].

D. Gapless symmetry-protected topological order

In Refs. [28,34], Scaffidi *et al.* extended the well-known mechanism of creating gapped SPT phases by decorating domain walls [111] to critical systems. The idea is illustrated straightforwardly with an example (their mechanism also applies to higher dimensions, but here we limit ourselves to one dimension). Let U be the unitary which maps the gapped $\mathbb{Z}_2 \times \mathbb{Z}_2$ paramagnet to the $(\mathbb{Z}_2 \times \mathbb{Z}_2)$-SPT phase. As a starting point, take a Hamiltonian H which consists of trivial gapped degrees of freedom decoupled

from a critical bulk; moreover, presume that one of the $\mathbb{Z}_2 \subset \mathbb{Z}_2 \times \mathbb{Z}_2$ acts only on the former gapped chain. The claim is then that $UHU^\dagger$, which is clearly still critical, is topologically nontrivial. This was diagnosed in terms of edge properties. In particular, in the above case, the ground state will be twofold degenerate for open boundary conditions (with exponentially small finite-size splitting). Through a combination of perturbative arguments and numerical calculations, this topological phenomenon was shown to be stable.

The above procedure, which can be applied for any symmetry group G, indeed creates nontrivial G-enriched CFTs. This can be seen from the perspective of symmetry fluxes: By construction, part of the symmetry group will be gapped, which ensures that the associated symmetry fluxes are unique. This means that the nontrivial charge endowed by the SPT entangler U will be a well-defined topological invariant, even at criticality, as we discuss in Sec. III. Using the boundary RG analysis of Sec. IV, this nontrivial symmetry flux can be used to argue the presence of edge modes. The notion of charged symmetry flux thus gives a topological bulk invariant for the cases studied in Refs. [28,34]. We note that the presence of gapped degrees of freedom is not essential to make domain-wall decoration work at criticality (which goes beyond the scope of Ref. [28]): The models H and H'' in Sec. II are related by the SPT entangler $U = \prod_n (CZ)_{n,n+1}$; in this case, we find the finite-size splitting to be algebraic.

The one-dimensional system which Ref. [28] focuses on is the cluster SPT model with an Ising coupling which preserves $\mathbb{Z}_2 \times \mathbb{Z}_2$ symmetry. We identify its bulk topological invariant in Appendix F 3. We note that Ref. [28] also presented a $2 + 1d$ example, which we revisit in Sec. VIII where we generalize our topological invariants to higher dimensions.

E. Topology and edge modes in quantum critical chains

In Ref. [33], a subset of the current authors showed that exponentially localized edge modes can exist in critical systems without gapped degrees of freedom. This work was restricted to noninteracting fermions, where arbitrary models with fermionic parity symmetry P and spinless time-reversal symmetry T ($T^2 = 1$)—realizing the so-called BDI class—could be described in terms of a complex function $f(z)$. The number of roots of this function on the unit circle tells us the central charge of the bulk CFT. The number (and norm) of roots strictly within the unit disk tell us about the number of topological edge modes (and their individual localization lengths). In particular, this shows that in this noninteracting setup, one can have edge modes for an arbitrary (half-integer) central charge c.

These critical systems can indeed be seen as CFTs enriched by P and T symmetry. Since there are no additional gapped degrees of freedom, all symmetry fluxes are

algebraic. Nevertheless, these can still have nontrivial charges. In particular, as we show in Sec. III, the Ising CFT ($c = 1/2$) has unique symmetry fluxes. And indeed, as we discuss in Sec. VI B, this allows us to extend some of the nontrivial CFTs considered in Ref. [33] to the interacting case, where the finite-size splitting becomes algebraic, scaling as $1/L^{14}$ (the algebraic splitting does not show up in the noninteracting limit since the descendant responsible for the splitting is intrinsically interacting). For more general CFTs ($c \geq 1$), a case-by-case study is necessary: Some remain nontrivial with interactions, while others do not; this can be determined by examining the symmetry action on the higher-dimensional space of symmetry fluxes. We leave an exhaustive discussion of these more general situations to future work.

VIII. ON TWISTED SECTORS AND HIGHER DIMENSIONS

Thus far, we have discussed topological invariants and edge modes in one-dimensional critical systems in great detail. The purpose of this last section is to give some higher-dimensional generalizations. A complete characterization of gapless topological phases is a challenging endeavor, since—as we will argue—it would require the knowledge of topological defects in conformal field theories, which in higher dimensions is itself a nascent field with a great promise for rich physics [112–125]. We first give an equivalent reformulation of our one-dimensional invariant (restricted to unitary symmetry groups) in Sec. VIII A, which is then extended to higher dimensions in Sec. VIII B.

A. Reformulation in terms of twisted sectors

Let us first explain why a reformulation is natural when trying to generalize to higher dimensions. In Sec. III, topological invariants at criticality are defined in terms of the symmetry charges of (slowest-decaying) string operators. Since these strings consist of a symmetry $\prod_n U_n$, one possible generalization to 2D would be to consider membrane operators corresponding to a symmetry $\prod_{m,n} U_{m,n}$. One could thus attempt to define a "slowest-decaying" membrane operator and study its symmetry properties. However, this is a less natural object to define and study than in 1D since the boundary of an $L \times L$ membrane grows like L. This means that generically the expectation value of the membrane operator will decay exponentially in both the gapped [126] and gapless case [127,128], making the notion of slowest decaying less practical and straightforward compared to 1D.

Fortunately, we can avoid this subtlety by instead working with static or external symmetry defects, which are more natural objects in CFTs (in arbitrary dimensions). In 1D, this will turn out to be equivalent to what we have already discussed. To define a symmetry defect (or

equivalently, symmetry twist) in 1D, consider a local Hamiltonian $H = \sum_n h_n$ and an on-site unitary symmetry $U^g = \prod_n U_n^g$ (i.e., $U^g h_n U^{g\dagger} = h_n$). A system with a g defect or twist at site n_0 in an infinite chain is defined as the Hamiltonian $H_{\text{twist}} := V_{n_0} H V_{n_0}^\dagger$ with $V_{n_0} = \prod_{n \leq n_0} U_n^g$. Crucially, since H is local and symmetric, H_{twist} differs from H only near the defect $n \approx n_0$. (See also the discussion in Ref. [77].) This thus also defines a g defect for a finite system on a ring (as long as the system size is larger than the support or range of the terms in the Hamiltonian). One can refer to H_{twist} as the twisted sector, since a periodic system with a g defect can be interpreted as having a boundary condition which has been twisted by g.

A key claim is that the topological invariant which we define in Sec. III, i.e., the charge under U^h of the symmetry flux $\mathcal{S}^g$ associated with U^g is identical to the charge under U^h of the ground state of the g-twisted sector H_{twist} (reminder: we take $g, h \in G$ to be two commuting symmetries). Indeed, this is a direct consequence of the operator-state correspondence. To see this, note that this correspondence, which involves conformally mapping the (punctured) plane to the spacetime cylinder [59,129], relates the scaling dimensions of local operators to the finite-size energy spectrum on a circle [59]. Similarly, as illustrated in Fig. 10, scaling dimensions of nonlocal string operators whose string consists of a symmetry operator are in 1-to-1 correspondence with the finite-size energy spectrum on a circle with a twisted boundary condition, i.e., the spectrum of H_{twist}. In particular, the leading scaling dimension (i.e., the slowest-decaying string operator) then naturally corresponds to the ground state of H_{twist}. The claimed identification of their charges thus follows. Note that the symmetry twist on a ring can equivalently be interpreted as threading a flux through the ring; this explains our nomenclature of symmetry flux in Sec. III. Indeed, in the case of gapped SPT phases it is well known that SPT invariants are encoded in the charges attached to external fluxes [5,6,57,58,73–82].

Let us illustrate this equivalence for the cluster model with a single-sublattice Ising coupling [28]:

$$
\begin{aligned}
H = -\sum_n (Z_{A,n} X_{B,n} Z_{A,n+1} + Z_{B,n-1} X_{A,n} Z_{B,n}) \\
- J \sum_n Z_{A,n} Z_{A,n+1}.
\end{aligned}
\tag{30}
$$

This has a $\mathbb{Z}_2 \times \mathbb{Z}_2$ symmetry generated by $P_A = \prod_n X_{A,n}$ and $P_B = \prod_n X_{B,n}$. Reference [28] showed that the edges mode of the cluster SPT phase ($|J| < 1$) persist at the Ising critical point at $|J| = 1$ (beyond which there is a phase that spontaneously breaks P_A), although no bulk invariant was identified. Using the methods introduced in Sec. III, one can straightforwardly derive a bulk topological invariant for these two cases (i.e., $|J| \leq 1$): We find that the symmetry
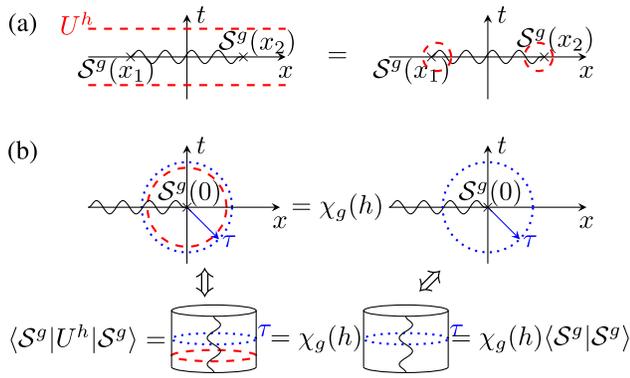
FIG. 10.　Operator-state correspondence for symmetry fluxes. (a) The black wiggly line represents a two-point function of a symmetry flux operator $\mathcal{S}^g$ as defined in Sec. III. The red dashed lines represent a commuting symmetry U^h; the figure shows how $U^h \mathcal{S}^g U^{h\dagger}$ can be represented in spacetime as $\mathcal{S}^g$ with a U^h loop wrapped around its end point. (b) The first equality is simply the definition of the charge $\chi_g(h)$ of the symmetry flux, as defined in Sec. III. For operator-state correspondence [59], we perform radial quantization (i.e., the new time τ runs radially; the blue dotted line is a spatial slice); by conformally mapping the plane to the cylinder, the operator $\mathcal{S}^g$ acts at $\tau = -\infty$, such that on the dashed line we have a state denoted by $|\mathcal{S}^g\rangle$, which is defined for g-twisted boundary conditions. Because of the symmetry flux being the slowest decaying string operator, $|\mathcal{S}^g\rangle$ is the ground state of the twisted sector. We see that $U^h|\mathcal{S}^g\rangle = \chi_g(h)|\mathcal{S}^g\rangle$, i.e., $\chi_g(h)$ can be obtained by considering a lattice model with g-twisted boundary conditions and measuring the h charge of its ground state.

flux of P_A is odd under P_B (and vice versa); the derivation can be found in Appendix F 3.

We now demonstrate how to obtain the same nontrivial invariant using symmetry twists. Twisting Eq. (30) by P_A gives us

$$H_{\text{twist}} = -\sum_n (-1)^{\delta_{n,n_0}} Z_{A,n}(X_{B,n} + J)Z_{A,n+1}$$
$$- \sum_n Z_{B,n-1} X_{A,n} Z_{B,n}. \qquad (31)$$

Note that $Z_{A,n} X_{B,n} Z_{A,n+1}$ is a local integral of motion. We thus read off that the ground state is in the sector $Z_{A,n} X_{B,n} Z_{A,n+1} = (-1)^{\delta_{n,n_0}}$ implying a quantum number

$$P_B = \prod_n X_{B,n} = \prod_n Z_{A,n} X_{B,n} Z_{A,n+1} = -1. \qquad (32)$$

This is in contrast to a trivial decoupled case [for instance, a unitary mapping can disentangle Eq. (30) into $H = -\sum_n (X_{A,n} + X_{B,n} + JZ_{A,n}Z_{A,n+1})$], where the ground state in the P_A-twisted sector satisfies $P_B = +1$. These quantum numbers are robust invariants on the condition that level crossings are not possible without leaving the

phase. For a gapped symmetric phase, this follows from having a unique ground state in the twisted sector (this property in turn follows from symmetry fractionalization). For a CFT, the noncrossing follows from the low-energy spectrum being universal [130]. E.g., for the Ising criticality under consideration, for asymptotically large system sizes the finite-size energy gap in the twisted sector can be related (by the operator-state correspondence) to the difference in scaling dimension between the disorder operator ($\Delta_\mu = 1/8$) and the fermion ($\Delta_\psi = 1/2$), preventing a crossing [see, e.g., Eq. (7.25) in Ref. [96]]. We thus arrive at a nontrivial topological invariant for $|J| = 1$. In contrast, in the Ising phase ($|J| > 1$) the ground-state manifold of the twisted sector is extensively degenerate and not universal; this can be understood by noting that it traps a domain wall whose energy (relative to the untwisted sector) becomes infinite when flowing to an RG fixed point. Thus, in the symmetry-breaking case, it does not provide an invariant [e.g., $H = -\sum_n [Z_{A,n}Z_{A,n+1} + X_{B,n}(1 - \lambda + \lambda Z_{A,n}Z_{A,n+1})]$ is in an Ising phase for all λ, but the P_A-twisted sector has a crossing at $\lambda = 1/2$ where its P_B charge swaps].

B. Generalizations to two dimensions

The idea that charges of twisted sectors provide topological invariants naturally generalizes to arbitrary dimensions, as has already been well explored in the gapped case [5,6,57,58,73–82]. First, the notion of the symmetry twist or defect is entirely analogous to what we see in 1D: Consider a local Hamiltonian H which is periodic along, say, the y direction, and infinite along x. If $U^g = \prod_{x,y} U^g_{x,y}$ is an on-site unitary symmetry, then its twist along the y direction is defined as $H_{\text{twist}} := V_{x_0} H V^\dagger_{x_0}$ with $V_{x_0} = \prod_{x \leq x_0} \prod_y U_{x,y}$. Because of U^g being a symmetry and H being local, we see that H_{twist} differs only from H for terms $x \approx x_0$. Hence, this also defines the meaning of a symmetry twist on a torus geometry (even though in that case, H_{twist} is not necessarily unitarily equivalent to H).

In 2D, if we have two defect lines (say, a U^g twist in the x direction and a U^h twist in the y direction), then their intersection is a point in space, and it is thus natural to measure "its" charge (i.e., the charge of the ground state in this twisted sector) with respect to a third symmetry. For gapped symmetric phases of matter, the ground state in the twisted sector is unique (indeed, symmetry fractionalization implies that the twisted sector is unitarily equivalent to the untwisted sector, and the latter is gapped by definition) such that its charge is a quantized topological invariant. Our contribution is to point out that this can also work for symmetry-preserving gapless systems: The low-energy spectrum (be it in a twisted sector or not) is universal, which in particular means that there can be no level crossings (except for the case where there are marginal operators, whose existence is known for a typical CFT). Hence, the charge of the ground state(s) in twisted

sectors can serve as a topological invariant for gapless systems.

We note that the low-energy spectrum for $2+1$D CFTs has been studied before on a torus geometry where the claim of universality was numerically confirmed [131–135]. We are not aware of similar numerical explorations for the case with a symmetry twist (although an epsilon expansion was studied in Ref. [133]), but it is a natural extension; in particular, the symmetry twist is expected to flow to a conformal defect of the CFT. We numerically confirm this for the transverse-field Ising model $H = -\sum_{\langle n,m \rangle} Z_n Z_m + g \sum_n X_n$; we set g to achieve $2+1d$ Ising criticality, whose value is known for a variety of lattices [136]. In Ref. [131], the universal finite-size spectrum on a torus geometry was studied. In the present work, we rescale the spectrum such that the finite-size gap (in this untwisted sector) is asymptotically $E_1 - E_0 \sim 1/L$. We can now twist one of the periodic directions with the $\mathbb{Z}_2$ symmetry (this involves flipping the sign of $Z_n Z_m$ on certain bonds). In Fig. 11(a), we show the finite-size energy gap in this twisted sector for the square, triangular, and honeycomb lattices. First, up to a global prefactor of $1/L$, we observe that the gap tends to a finite value; i.e., the ground state is unique also in the twisted sector. Second, its asymptotic value coincides for the triangular and honeycomb lattices: This confirms our claim of universality
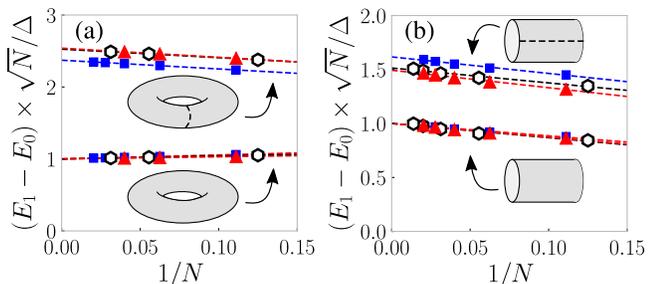

FIG. 11. Symmetry defect in the $2+1$D Ising CFT. We consider the critical ferromagnetic Ising model in a transverse field on the square, triangular, and honeycomb lattices, respectively, denoted by (blue) squares, (red) triangles, and (white) hexagons. (a) The bottom curve shows the finite-size energy gap for periodic boundary conditions (i.e., the torus); since this is a CFT, $E_1 - E_0 \sim \Delta/\sqrt{N}$ (for total number of sites $N = L \times L$). For each lattice, we rescale the y axis such that the extrapolated prefactor Δ is unity. The other data are for a torus twisted by the $\mathbb{Z}_2$ symmetry of the Ising model; again we extract the finite-size energy gap in this twisted sector. With the aforementioned rescaled y axis, we find the universal y intercepts approximately equal to 2.4 (for square lattice, i.e., modular parameter $\tau = e^{i\pi/2}$) and 2.5 (for triangular and honeycomb lattices, i.e., $\tau = e^{i\pi/3}$). (b) Similar setup for the cylinder geometry (i.e., open in one direction, periodic in the other). Here too we find that the twisted sector has a unique ground state with the finite-size energy splitting in this rescaled y axis giving the universal intercepts approximately equal to 1.6 (for $\tau = e^{i\pi/2}$) and 1.5 (for $\tau = e^{i\pi/3}$).

(since in the scaling limit, only the information of the modular parameter remains, which for both lattices is $\tau = e^{\pi i/3}$). In Fig. 11(b), we confirm that the universality also appears for the cylinder geometry. Hence, as we explain above, the charge of its ground state can serve as a robust topological invariant, as we illustrate in the next subsection.

In fact, one can argue that the following stronger property holds: a conformal symmetry defect or twist is automatically also a topological defect [137]; i.e., the universal finite-size energy spectrum is independent of deformations of the line defect. This property is not needed to define the topological invariant, but it is key in arguing that a nontrivial value of the invariant implies edge modes, as we discuss in Sec. VIII B 2.

1. Examples in 2D

Let us illustrate the above 2D topological invariant in a variety of examples. For simplicity, all of these will focus on the symmetry group $\mathbb{Z}_2 \times \mathbb{Z}_2 \times \mathbb{Z}_2$. As a natural setting for this symmetry, we consider the triangular lattice with the three sublattices shown in Fig. 12(a); for each sublattice, we define the $\mathbb{Z}_2$-symmetry operator $P_\lambda = \prod_n X_{\lambda,n}$ with $\lambda = A, B, C$. For any symmetric Hamiltonian H, we can twist by P_A and P_B along the two dashed lines in Fig. 12(a), leading to H_{twist}. If the ground state of H_{twist} is unique, it must have a well-defined charge under P_C, providing a topological invariant [138]. This can also apply in the case of degeneracy, e.g., if all ground states have the same charge under P_C.

Before we discuss examples of concrete Hamiltonians H satisfying the above condition, let us note that topological invariants are interesting only if we can also realize a phase with a different value of the invariant. Fortunately, we have a general result to this end: defining the SPT entangler $U_{2D} = \prod_\triangle CCZ$ (applying the control-control-Z gate [this three-site gate is defined as
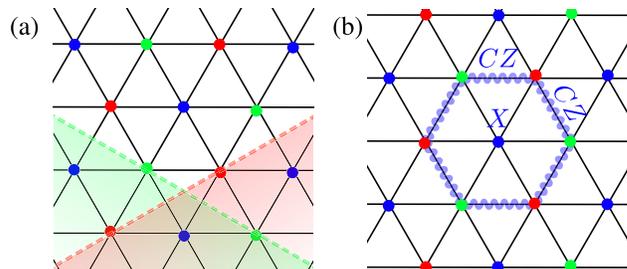

FIG. 12. Triangular lattice, twists, and the Yoshida SPT model. (a) The triangular lattice with A (green), B (red), and C (blue) sublattices. The dashed lines denote possible ways of twisting by P_A and P_B symmetry (e.g., the latter corresponds to conjugating H by $\prod X_{B,n}$ on the shaded red area). (b) An elementary term in the Yoshida SPT model protected by $\mathbb{Z}_2^3$ symmetry; the wiggly line represents a product of control-Z gates.

$CCZ|\sigma_1\sigma_2\sigma_3\rangle = (-1)^{\delta_{\sigma_1\sigma_2\sigma_3,\uparrow\uparrow\uparrow}}|\sigma_1\sigma_2\sigma_3\rangle$] on every triangle of the triangular lattice), we derive the following in Appendix G.

Different topological invariants in 2D.—Let H be a (gapped or gapless) model on the triangular lattice commuting with P_A, P_B, and P_C, and suppose it has a well-defined topological invariant as described above (e.g., all ground states in the twisted sector have the same P_C charge). Then H and $H' := U_{2D}HU_{2D}^\dagger$ have distinct topological invariants. More precisely, if H_{twist} is defined as above, then its ground-state charge under P_C is opposite that of $(H')_{\text{twist}}$.

The simplest example is the trivial gapped paramagnet, e.g., $H = -\sum_n (X_{A,n} + X_{B,n} + X_{C,n})$. In this case, $H_{\text{twist}} = H$, such that we read off that the ground-state charge is $P_C = 1$ (since $X_{C,n} = 1$). The SPT-entangled Hamiltonian $H' = U_{2D}HU_{2D}^\dagger$ is Yoshida's $\mathbb{Z}_2^3$ SPT model [139,140]. The terms in H' are of the form $U_{2D}X_{\lambda,n}U_{2D}^\dagger = X_{\lambda,n} \times \prod_{\text{hex}} CZ$ where the product runs around the six neighboring sites as shown in Fig. 12(b). By the above general result, we see that in the twisted sector of the Yoshida model, the ground-state charge is $P_C = -1$, giving a nontrivial value of the topological invariant. (This particular case is calculated explicitly in Appendix G 1.) This confirms that these two models cannot be adiabatically connected while preserving the symmetry and the universality class (in this case, the finite-energy gap). Note that we even obtain a stronger condition: Any critical point between the trivial and nontrivial SPT phase must have a degeneracy in the twisted sector (labeled by opposite charges $P_C = \pm 1$).

Let us discuss topological invariants in gapless examples. First note that in the above gapped example, to derive $P_C = 1$ (for the twisted sector) we do not actually use that P_A and P_B are gapped symmetries (i.e., that the A and B degrees of freedom are gapped). The argument relied only on H not coupling the sublattices. Hence, the same conclusion follows as long as at least one of the three symmetries is gapped; without loss of generality, let this be P_C. In particular, let $H = H_C + H_{AB}$ with $H_C = -\sum_n X_{C,n}$ and H_{AB} an arbitrary (symmetry-preserving) Hamiltonian on the A and B sublattices. Twisting by P_A and P_B will clearly not affect the C degrees of freedom, such that the ground state satisfies $X_n = +1$ and thus $P_C = 1$ in the twisted sector. Note that the ground-state subspace is not necessarily unique: Twisting by P_A and P_B could introduce a degeneracy, but this argument shows that $P_C = 1$ for all ground states. This charge acts as a topological invariant, with $H' = U_{2D}HU_{2D}^\dagger$ giving a model with $P_C = -1$. Let us stress that although we obtain the invariant in a fine-tuned limit where the C sites satisfy $X_{C,n} = 1$, by virtue of universality the resulting topological invariant is well defined and robust as long as one does not leave the universality class.

This simple insight applies to a whole array of examples, including the 2D example discussed by Scaffidi *et al.* [28] where H is decoupled such that the A sites formed a gapless U(1) spin liquid and the B and C sites were gapped. In that work, it was demonstrated that $H' = U_{2D}HU_{2D}^\dagger$ has topologically protected edge excitations. Here, we derive a bulk topological invariant distinguishing the models H and H' studied in Ref. [28]. The invariant is well defined by virtue of having a gapped sector; it is not sensitive to the particular choice of gapless degrees of freedom. Another interesting by-product is that any continuous phase transition between the trivial phase and the $\mathbb{Z}_2^3$ SPT phase must necessarily be gapless for all three symmetries (otherwise, its remaining gapped degrees of freedom would remember the topological invariant, preventing the required self-duality of a SPT transition).

Our topological invariant can also apply to systems with no gapped symmetries. As a concrete example, let us consider $\text{Ising}^3 = \text{Ising} \times \text{Ising} \times \text{Ising}$ criticality, where we define H as having a copy of the critical Ising model on each of the three sublattices of the triangular lattice. Twisting by P_A and P_B again does not affect the C sites. From Ref. [131], we learn that the ground state of the critical Ising model on the torus is unique and satisfies $P_C = 1$. We can thus already conclude that H has a well-defined topological invariant, with all the ground states in the twisted sector satisfying $P_C = 1$. In fact, from Fig. 11 we see that this ground state is unique (although this is strictly speaking not necessary to have a well-defined invariant). Using our general result above, we see that $H' = U_{2D}HU_{2D}^\dagger$ gives a version of the Ising^3 criticality which has the opposite invariant $P_C = -1$ in the twisted sector. As long as one preserves Ising^3 criticality, these two symmetry-enriched versions cannot be connected. Moreover, as we see in the next subsection, H' must host nontrivial edge phenomena, which are protected by this bulk topological invariant.

The above Ising^3 example is a good proof of principle for the existence of topologically distinct symmetry-enriched versions of the same universality class (even in the absence of gapped degrees of freedom). However, to some extent the example is academic in nature: If one does not enforce the Ising^3 criticality by hand, then energy-energy perturbations between the distinct sublattices are expected to trigger a flow to O(3) criticality with cubic anisotropy [141]; see also Refs. [142–146]. Fortunately, our general result above still applies: If the O(3) criticality has the property that all ground states in the sector twisted by P_A and P_B have the same P_C charge (in particular, it is sufficient to show that the ground state in the twisted sector is unique), then the SPT entangler U_{2D} gives a topologically nontrivial version of O(3) criticality [this reasoning applies to both the standard O(3) fixed point as well as its cubic perturbation]. While we expect this property of O(3) criticality to hold, its numerical

confirmation goes beyond the scope of the present work such that we leave it to future studies. Moreover, it could be explored via ε expansion using the methods of Ref. [133]. If true, this means that the two O(3) critical lines that appeared in Ref. [147] are in fact topologically distinct and must be separated by a multicritical point where the twisted sector becomes degenerate. (The particular model studied in Ref. [147] instead has an intermediate symmetry-breaking phase, suggesting that such a multicritical point requires more fine-tuning.)

2. Implications for the edge

In this last section, we sketch an argument for why a nontrivial value of the topological invariant (i.e., the charge in the twisted sector is different from the untwisted case) implies a nontrivial boundary theory. This generalizes the bulk-boundary correspondence to cases with a gapless bulk. The idea is to consider the above charge not as a property of the system as whole, but rather as being associated with the intersection of two symmetry defects. This intuitive idea is consistent with two facts: First, as we discuss above, the symmetry defect is actually topological, which means the charge is unchanged when we arbitrarily deform the defect lines, and second, if one repeats the above arguments and calculations for nonintersecting defect lines, one finds that the charge remains trivial; i.e., the presence of intersecting defects is crucial in the examples we discuss.

Using this basic idea, one can infer a nontrivial constraint on the edge theory. Indeed, for a closed spatial manifold—like the torus considered above—the intersection cannot be removed by deforming the defect lines. In contrast, for a manifold with a boundary, such intersections can be undone. For concreteness, let us consider the situation in Fig. 13(a), where the bulk has two intersecting symmetry defects. If the boundary theory also preserves the symmetries, then the defects are topological both in the bulk and the boundary, such that we can freely move the defect lines. In particular, nothing prevents us from sliding the
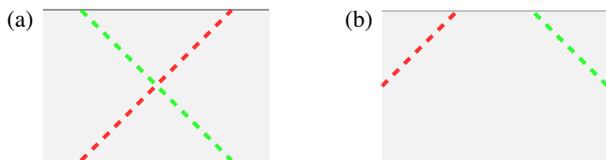

FIG. 13. Edge modes from 2D topological invariant. (a) We start with two intersecting symmetry defects (red and green dashed lines) in a system with a boundary (solid gray line). (b) If the boundary is symmetry preserving, the defect is topological and can be moved upward such that the intersection can be "slid off" the system. If the intersection carried a nontrivial charge (i.e., the bulk is topologically nontrivial), then consistency demands that the intersections of the defect line at the boundary are themselves nontrivial, excluding a trivial boundary condition (see main text for details).

intersection upward, such that it eventually disappears as in Fig. 13(b). We end up with an apparent paradox if the original intersection carried a nontrivial charge, since the final configuration has no more intersection to host a nontrivial charge (seemingly violating the topological nature of these defects). The resolution is that the localized points where the symmetry defect intersects the boundary must themselves be nontrivial. In particular, if these localized points carry a degeneracy with opposite charges, then it can freely absorb the bulk topological invariant without causing an inconsistency. Note that this nontrivial property excludes a trivial boundary condition.

Let us illustrate this for the Ising^3 CFT discussed in Sec. VIII B 1. For the nontopological case of three decoupled copies of the Ising CFT on each of the three sublattices of the triangular lattice, we find that the intersection of the P_A and P_B symmetry defects hosts a trivial charge $P_C = 1$. In this case, one can freely slide off the intersection without obtaining a condition on the boundary theory. In contrast, for the SPT-entangled version, we find a charge $P_C = -1$. Hence, the above argument implies that either the boundary spontaneously breaks P_A or P_B, or where the P_A (or P_B) defect intersects the boundary it must host a degeneracy with charges $P_C = \pm 1$. This excludes the free boundary condition: Fig. 11(b) shows that an Ising CFT with a symmetry defect intersecting the free boundary condition has a unique ground state. We thus conclude that the topologically nontrivial $\mathbb{Z}_2^3$-enriched Ising^3 CFT cannot have a free boundary condition. Possible alternatives are symmetry-breaking or fine-tuned gapless edges; we leave a study of concrete lattice models to future work. Note that a trivial Ising CFT can also have a symmetry-breaking edge, but in that case, one can drive a boundary phase transition into a free boundary condition: Here that is impossible without also driving the bulk into a different universality class.

IX. OUTLOOK

Similar to how gapped degrees of freedom can realize a multitude of distinct phases of matter in the presence of a global symmetry G [1–4], a given universality class has many distinct symmetry-enriched versions. This forms the concept of G-enriched quantum criticality. We introduce various invariants to characterize this, the crucial one being the symmetry flux associated with a global symmetry in the 1D case. In the simplest case, this has a well-defined charge which then serves as a topological invariant. We relate this to the presence of edge modes, whose finite-size splitting depends on whether the flux is charged under a gapped symmetry. A particularly novel aspect to come out is that the Ising CFT enriched by an antiunitary symmetry can host an edge mode whose finite-size splitting scales as $1/L^{14}$. The aforementioned invariants also allow us to broach the classification of G-CFTs, giving a complete picture for the

Ising CFT and a partial understanding for the Gaussian CFT. The latter serves to discuss various subtleties, such as how the $c = 1$ orbifold CFT seemingly has a nontrivial topological invariant. We also demonstrate how the concept of symmetry-enriched quantum criticality allows us to unify previous works into a single picture. Lastly, we show how these novel topological invariants can be generalized to higher dimensions by studying symmetry charges of CFTs in twisted sectors.

Examples of topologically nontrivial symmetry-enriched CFTs are presumably rather ubiquitous, once one knows where to look. For example, one can expect them to occur—although not exclusively—at transitions between gapped SPT phases and symmetry-breaking phases where the ground-state degeneracies (for open boundaries) have compatible symmetry properties. Indeed, this guideline suggests that it should occur for the spin-1 XXZ chain, as we confirm in Fig. 1. Moreover, as we establish in Sec. VII, various known examples of critical systems with edge modes can be reinterpreted as phase transitions between distinct nontrivial gapped phases of matter (see also Ref. [72]). It would hence be interesting to uncover more experimentally relevant examples of this sort. It is likely that these are already present—but overlooked—in known phase diagrams (the critical spin-1 XXZ chain illustrates this).

Related to finding more physical realizations of this phenomenon, is the question of what its practical use could be. The unique phenomenology of topologically nontrivial symmetry-enriched quantum criticality is that it allows for a localized topological edge modes which is apparently oblivious to long-range correlations in the bulk. Relatedly, it allows for quantum information to remain localized while the bulk is tuned through a quantum critical point. Such surprising stability of quantum information could conceivably prove to be useful.

On the theoretical front, an obvious—and important—challenge is the complete classification of G-enriched CFTs for which we give partial results in one spatial dimension. Such a task is vast, as it contains the classification of all CFTs as a subset. A more realistic question is thus, what is the classification for G-CFTs where the CFT is already known and understood in the absence of additional symmetries? In this work, we provide the answer for the Ising CFT. Despite making progress for the case of the symmetry-enriched $c = 1$ CFT, its classification is still an open issue for general symmetry groups, as it is for all remaining CFTs. As a first step, it is conceivable that our classification for the Ising CFT can be extended to all minimal unitary models. Moreover, in our classification we presume a unitary group G for convenience, even though we discuss antiunitary examples. It would hence be useful to extend this to include the case of time-reversal symmetry, and perhaps even spatial or anomalous symmetries, which we do not touch upon. An equally exciting question is whether our topological invariants can be efficiently detected in a tensor-network representation of the ground

state, such as the multiscale entanglement renormalization ansatz (MERA) [148].

Finally, while the last section of this paper already touches upon generalizations of these topological invariants to higher dimensions, many exciting open questions remain. The most nontrivial setting is the one where there are no gapped degrees of freedom to appeal to. An interesting case study beyond the Ising[3] discussed in the present work is O(3) criticality in $2 + 1d$: As we discuss in Sec. VIII, it admits a topological invariant if twisting the x (y) direction by, say, a π rotation around the internal x (y) axis gives rise to a unique ground state. [Indeed, the $\mathbb{Z}_2^3$ subgroup discussed in Sec. VIII can be identified—as a subgroup of O(3)—with the $\mathbb{Z}_2 \times \mathbb{Z}_2$ subgroup of π rotations and the $\mathbb{Z}_2$ subgroup generated by $-\mathbb{I} \in O(3)$.] In fact, this will give a nontrivial topological invariant for the O(3) criticality between the Néel phase and 2D Affleck-Kennedy-Lieb-Tasaki state found in Ref. [149]. More generally, one can revisit well-studied CFTs in $2 + 1d$ from the perspective of studying their twisted sectors. As we discuss above, the invariants embedded in these twisted sectors can put nontrivial constraints on the possible boundary fixed points, which also deserves further study. We suspect that the tools presented in this work are timely considering the recent foray into higher-dimensional gapless topological phases [28,149–154] which have thus far been lacking a unifying framework.

APPENDIX A: SYMMETRY FLUXES AND THEIR CHARGES

1. Symmetry properties of unique symmetry fluxes

For any $g \in G$ and $h \in C(g)$, we define $\chi_g(h)$ through $U^h \mathcal{S}^g U^{h\dagger} = \chi_g(h)\mathcal{S}^g$ [presuming we choose the end-point operator $\mathcal{O}^g$ such that $C(g)$ acts nicely on it; see the discussion in Sec. III]. From this definition, it directly follows that $\chi_g(hk) = \chi_g(h)\chi_g(k)$, i.e., $\chi_g : C(g) \to \mathrm{U}(1)$ is a one-dimensional representation. Other useful properties, which hold for bosonic systems which are gapped or described by a CFT, are $\chi_g(h) = \chi_h(g)^{-1}$ and $\chi_g(g) = 1$. In the gapped case, these can be derived from the concept of symmetry fractionalization. More generally, these can be argued based on modular invariance of the partition function. Note that $\chi_g(g) = 1$ need not be true for fermionic systems: The Kitaev chain is a paradigmatic example where the symmetry flux of P is charged under itself.

2. From Abelian charges to cocycles

Here we show how specifying the above charge χ_g for any $g \in G$ is equivalent to specifying a projective representation of G if G is Abelian.

Because of the structure theorem, we have $G \cong \mathbb{Z}_{r_1} \times \cdots \mathbb{Z}_{r_n}$ (for convenience, we take G to be finite). Let $g_1, \ldots, g_n$ be a set of generators. We now define a central extension of G, which is a group $\tilde{G}$ generated by the symbols $\hat{g}_1, \ldots, \hat{g}_n$, and complex phases. To define the relations between these generating elements, it is useful to introduce the shorthand $[a, b] \equiv aba^{-1}b^{-1}$. The relations of $\tilde{G}$ are then $\hat{g}_j^{r_j} \equiv 1$ and $[\hat{g}_j, \hat{g}_k] \equiv \chi_{g_k}(g_j)$. *A priori*, it is not trivial that this definition is consistent, since there are nontrivial relationships between commutators. In particular, $[a, b] = [b, a]^{-1}$ and $[a, bc] = [a, b][b, [a, c]][a, c]$ and $[g, g^{-1}] = 1$. However, the properties of χ_g mentioned in the previous subsection indeed show that the consistency relations are satisfied.

We thus define a central extension $\mathrm{U}(1) \to \hat{G} \to G$. This short exact sequence simply means that $G \cong \tilde{G}/\mathrm{U}(1)$,

as one can readily verify. This is equivalent to defining a projective representation of G. The latter is often characterized in terms of a cocycle $\omega(g, h)$. The standard way of obtaining this from the extension is by first defining a section $s : G \to \hat{G}$, i.e., an embedding of the original group into the extended one. It is sufficient to define this on the products of the generating elements: $s(g_1^{k_1} \cdots g_n^{k_n}) \equiv \hat{g}_1^{k_1} \cdots \hat{g}_n^{k_n}$. The cocycle is then determined via $\omega(g, h) = s(g)s(h)s(gh)^{-1}$.

3. Gapped symmetries

In this subsection, we focus on symmetries which act only on gapped degrees of freedom.

a. Symmetry flux from symmetry fractionalization: String order parameter

For gapped symmetries, there is the notion of symmetry fractionalization [1,2]. This says that if one acts with the symmetry operator on a finite but large region, it effectively acts nontrivially only near the edges: $U_m^g U_{m+1}^g \cdots U_{n-1}^g = U_L^g U_R^g$. These obey a projective representation $U_R^g U_R^h = e^{i\omega(g,h)} U_R^{gh}$; here, $\omega(\cdot, \cdot)$ characterizes the so-called second group cohomology class. These fractional symmetries U_L^g and U_R^g might have nontrivial symmetry properties which force their expectation value to be zero. A string order parameter is then usually defined by finding an operator $\mathcal{O}^g$ that cancels these symmetry properties such that $\langle \mathcal{O}_m^{g\dagger} U_L^g \rangle \neq 0$ and $\langle U_R^g \mathcal{O}_n^g \rangle \neq 0$. The resulting string order parameter is then $\mathcal{O}_m^{g\dagger} U_m^g U_{m+1}^g \cdots U_{n-1}^g \mathcal{O}_n^g$, which has long-range order by construction. Note that this exactly satisfies the condition for the symmetry flux of g as defined in Sec. III A.

b. Uniqueness of symmetry flux

Suppose one has a second operator $\tilde{\mathcal{O}}$ that satisfies the same properties. In particular, $\langle \tilde{\mathcal{O}}_m^{g\dagger} U_L^g \rangle \neq 0$ and $\langle U_R^g \tilde{\mathcal{O}}_n^g \rangle \neq 0$. Then the linear combination $\mathcal{T}_n^g := \langle U_R^g \tilde{\mathcal{O}}_n^g \rangle \times \mathcal{S}_n^g - \langle U_R^g \mathcal{O}_n^g \rangle \times \tilde{\mathcal{S}}_n^g$ no longer has long-range order, and thus by the definition of the equivalence class in Sec. III, the symmetry fluxes $\mathcal{S}^g$ and $\tilde{\mathcal{S}}^g$ generate the same class; i.e., the symmetry flux is unique. To prove the above claim:

$$\langle \mathcal{T}_m^{g\dagger} \mathcal{T}_n^g \rangle = \langle ((\langle U_R^g \tilde{\mathcal{O}}_n^g \rangle \mathcal{O}_m^g - \langle U_R^g \mathcal{O}_n^g \rangle \tilde{\mathcal{O}}_m^g)^\dagger U_m^g U_{m+1}^g \cdots U_{n-1}^g (\langle U_R^g \tilde{\mathcal{O}}_n^g \rangle \mathcal{O}_n^g - \langle U_R^g \mathcal{O}_n^g \rangle \tilde{\mathcal{O}}_n^g) \rangle \tag{A1}$$

$$= \langle \cdots \rangle \times \langle U_R^g (\langle U_R^g \tilde{\mathcal{O}}_n^g \rangle \mathcal{O}_n^g - \langle U_R^g \mathcal{O}_n^g \rangle \tilde{\mathcal{O}}_n^g) \rangle = \langle \cdots \rangle \times (\langle U_R^g \tilde{\mathcal{O}}_n^g \rangle \langle U_R^g \mathcal{O}_n^g \rangle - \langle U_R^g \mathcal{O}_n^g \rangle \langle U_R^g \tilde{\mathcal{O}}_n^g \rangle) = 0. \tag{A2}$$

c. Charges from the cocycle

Having shown the uniqueness of the symmetry flux of $g \in G$, we can now consider its symmetry properties. For any $h \in C(g)$ (i.e., the elements of commuting with g), we

can consider $U^h \mathcal{S}^g (U^h)^\dagger = \chi_g(h)\mathcal{S}^g$ with $\chi_g(h) \in \mathrm{U}(1)$. As noted before, the function $\chi_g : C(g) \to \mathrm{U}(1) : h \mapsto \chi_g(h)$ is a one-dimensional representation of the stabilizer of g. We now show that $\chi_g(h) = e^{-i(\omega(h,g)+\omega(hg,h^{-1}))}$. By definition of

$\mathcal{O}^g$, it has the opposite symmetry property of U_R^g (indeed, otherwise $\mathcal{O}^g U_R^g$ could not have a nonzero expectation value), hence, $U^h U_R^g U^{h\dagger} = \chi_g^*(h) U_R^g$. The left-hand side equals $U_R^h U_R^g U_R^{h\dagger} = e^{i\omega(h,g)} U_R^{hg} U_R^{h-1} = e^{i(\omega(h,g)+\omega(hg,h^{-1}))} U_R^g$. ∎

Note that in Sec. A 2, we prove that this relationship can be inverted if G is Abelian.

APPENDIX B: SYMMETRY-ENRICHED ISING CFT IN AN EXACTLY SOLVABLE MODEL

Here we solve the Hamiltonian $H = J_1 H_1 + J_{\mathrm{Hal}} H_{\mathrm{Hal}} + J_x H_x$ by mapping it to free fermions. We use the formalism of Ref. [33] to obtain a simple solution that straightforwardly allows us to extract bulk correlation lengths and edge mode localization lengths from zeros of holomorphic functions.

After a Jordan-Wigner transformation, we have a quadratic fermionic chain. More generally, when there is a two-site unit cell, it is useful to write the Hamiltonian as follows:

$$H = -i \sum_{n\in\mathrm{sites}} \sum_{\alpha\in\mathbb{Z}} (\tilde{\gamma}_{2n-1}, \tilde{\gamma}_{2n}) T_\alpha \begin{pmatrix} \gamma_{2(n+\alpha)-1} \\ \gamma_{2(n+\alpha)} \end{pmatrix}. \quad (B1)$$

In particular, for the above Hamiltonian, we obtain

$$T_{-1} = \begin{pmatrix} 0 & J_H \\ 0 & 0 \end{pmatrix}, \quad T_0 = \begin{pmatrix} 0 & J_1 + J_x \\ J_1 & 0 \end{pmatrix}, \quad T_1 = \begin{pmatrix} 0 & 0 \\ J_H + J_x & 0 \end{pmatrix}. \quad (B2)$$

As in Ref. [33], it is useful to consider

$$F(z) := \sum_\alpha T_\alpha z^\alpha = \begin{pmatrix} 0 & J_1 + J_x + J_H/z \\ (J_H + J_x)z + J_1 & 0 \end{pmatrix} = \begin{pmatrix} 0 & h(z) \\ g(z) & 0 \end{pmatrix}, \quad (B3)$$

where we define $h(z) = (J_1 + J_x/z)[z + (J_H/J_1 + J_x)]$ and $g(z) = (J_H + J_x)[z + (J_1/J_H + J_x)]$ (written in such a way that their zeros can be read off). In the style of Ref. [33], we can associate a correlation length with both functions (the extra factor of 2 in the numerator is due to the two-site unit cell):

$$\xi_h = \frac{2}{\left|\ln\left|\frac{J_H}{J_1+J_x}\right|\right|} \quad \text{and} \quad \xi_g = \frac{2}{\left|\ln\left|\frac{J_1}{J_H+J_x}\right|\right|}. \quad (B4)$$

The correlation length of the system is then given by $\xi = \max\{\xi_h, \xi_g\}$.

For edge modes and topological invariants, it is useful to consider the winding number $\omega = N_z - N_p$ associated with $h(z)$ and $g(z)$ denoted by ω_h and ω_g, respectively. Their values are shown in the phase diagrams in Fig. 14. This figure clarifies that the topological phase transition is driven by $h(z)$, whereas the topology of $g(z)$ is stable

throughout that same region. It is hence natural to conclude that $\xi_{\mathrm{loc}} = \xi_g$. (This is also confirmed with numerics.)

In Fig. 3(b) of the main text, the red path is parametrized by $J_x = 2\lambda J_1$ and $J_H = 2(1-\lambda)J_1$ (for $\lambda \in [0,1]$). Hence, $(J_1/J_H + J_x) = \frac{1}{2}$ and $(J_H/J_1 + J_x) = [1 - \lambda/(1/2+\lambda)]$ From Eq. (B4), we conclude that the edge mode has constant localization length $\xi_{\mathrm{loc}} = 2/\ln 2$, whereas the bulk correlation length is

$$\xi = \begin{cases} \frac{2}{\left|\ln\left(\frac{1-\lambda}{1/2+\lambda}\right)\right|} & \text{for } \lambda \in [0, 1/2], \\ \frac{2}{\ln 2} & \text{for } \lambda \in [1/2, 1]. \end{cases} \quad (B5)$$

APPENDIX C: DUALITY MAPPING $(I_x, I_y, I_z) \leftrightarrow (1, \mathrm{Hal}, 0)$

One can define the following unitary mapping (ignoring boundary conditions):
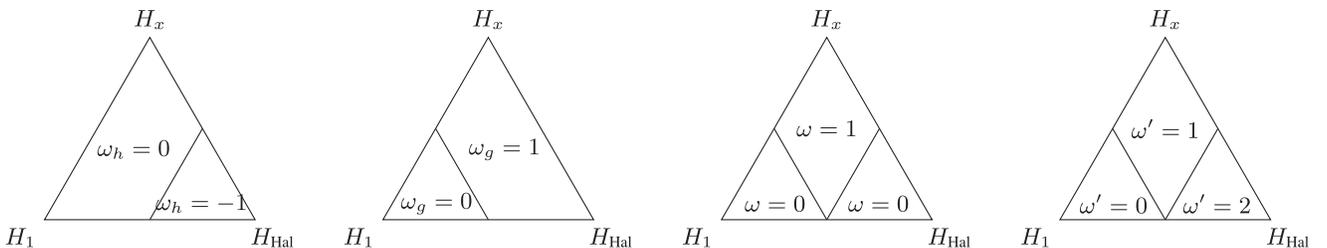

FIG. 14. The first two plots show the topological invariant associated with $h(z)$ and $g(z)$. The third plot shows the BDI topological invariant which can be expressed as $\omega = \omega_h + \omega_g$. In the last plot, we show $\omega' := |\omega_h| + |\omega_g|$, which is the one to consider in this case.

$$X_{2n+1} = (-1)^n \tilde{Z}_1 \cdots \tilde{Z}_{2n-1} \tilde{Z}_{2n}, \tag{C1}$$

$$Y_{2n+1} = (-1)^n \tilde{Z}_1 \cdots \tilde{Z}_{2n-1} \tilde{Y}_{2n} \tilde{Y}_{2n+1}, \tag{C2}$$

$$Z_{2n+1} = -\tilde{X}_{2n} \tilde{Y}_{2n+1}, \tag{C3}$$

$$X_{2n+2} = (-1)^n \tilde{Z}_1 \cdots \tilde{Z}_{2n-1} \tilde{Z}_{2n} \tilde{X}_{2n+1} \tilde{X}_{2n+2}, \tag{C4}$$

$$Y_{2n+2} = (-1)^{n+1} \tilde{Z}_1 \cdots \tilde{Z}_{2n-1} \tilde{Z}_{2n} \tilde{Z}_{2n+1}, \tag{C5}$$

$$Z_{2n+2} = \tilde{Y}_{2n+1} \tilde{X}_{2n+2}. \tag{C6}$$

One can check that as thus defined, the operators satisfy the relevant algebra: Operators on different sites commute, and on the same site they form a representation of the Pauli algebra.

From the above correspondences, one can derive

$$X_{2n} X_{2n+1} = \tilde{Y}_{2n-1} \tilde{Y}_{2n}, \tag{C7}$$

$$Y_{2n} Y_{2n+1} = \tilde{Y}_{2n} \tilde{Y}_{2n+1}, \tag{C8}$$

$$X_{2n+1} X_{2n+2} = \tilde{X}_{2n+1} \tilde{X}_{2n+2}, \tag{C9}$$

$$Y_{2n+1} Y_{2n+2} = \tilde{X}_{2n} \tilde{X}_{2n+1}. \tag{C10}$$

This directly implies that $H_x \leftrightarrow H_1$ and $H_y \leftrightarrow H_{\mathrm{Hal}}$.

Similarly, one can check

$$Z_{2n} Z_{2n+1} = -\tilde{Y}_{2n-1} \tilde{Y}_{2n+1}, \tag{C11}$$

$$Z_{2n+1} Z_{2n+2} = -\tilde{X}_{2n} \tilde{X}_{2n+2}, \tag{C12}$$

$$-Y_{2n} Y_{2n+2} = \tilde{Z}_{2n} \tilde{Z}_{2n+1}, \tag{C13}$$

$$-X_{2n+1} X_{2n+3} = \tilde{Z}_{2n+1} \tilde{Z}_{2n+2}. \tag{C14}$$

Hence, $H_z \leftrightarrow H_0$. [Caveat: Depending on which direction of the mapping one takes, H_0 has XX couplings on even or odd sites. However, since all five other Hamiltonians are

inversion symmetric (when inverting along bonds between two-site unit cells), we can always concatenate with spatial inversion to obtain the desired variant.]

APPENDIX D: THE BAIT-AND-SWITCH LEMMA

Consider two G-enriched Ising CFTs, which we refer to as the A and B systems. Suppose that each has the same charge for their σ operator. We now prove that if we stack the A system which has been perturbed into its gapped symmetry-preserving phase on top of the critical B system, then we can smoothly connect this to the B system in its gapped symmetry-preserving phase stacked on top of the critical A system. Conceptually, this says that all (non-symmetry-breaking) G-enriched Ising CFTs with the same charges for local operators can be realized by stacking gapped SPT phases on top of a reference Ising CFT. (Note that in the presence of symmetry breaking, one can apply this lemma to the remaining symmetry group.) This lemma can be seen as a generalization of Corollary 1 in the Appendix of Ref. [33] to the interacting case.

It is convenient to use the representation of the Ising CFT as a ϕ^4 theory. In particular, for a decoupled stack of the above two critical Ising CFTs, the Lagrangian would be

$$\mathcal{L}_0 = \sum_{i=A,B} [(\partial \phi_i)^2 - \phi_i^4 - m_c^2 \phi_i^2]. \tag{D1}$$

The parameter m_c is taken such that we are at the Ising fixed point. (This is roughly $m_c^2 \approx 0.5$ according to Ref. [155], but its precise value is not important to the argument.) We now show that the situation where (only) the A system is gapped, i.e., $\mathcal{L} = \mathcal{L}_0 - m^2 \phi_A^2$, can be smoothly connected to where (only) the B system is gapped, i.e., $\mathcal{L} = \mathcal{L}_0 - m^2 \phi_B^2$, preserving both the Ising universality class and the G symmetry throughout.

Since by assumption the ϕ_A and ϕ_B fields have the same charges under each element of G, we can consider the following symmetric coupling (where $\theta \in [0, \pi/2]$ is a free parameter):

$$\mathcal{L} = \mathcal{L}_0 - m^2 \underbrace{((\cos \theta) \phi_A + (\sin \theta) \phi_B)}_{\equiv \varphi_1}{}^2 + f(m, \theta) \underbrace{[-(\sin \theta) \phi_A + (\cos \theta) \phi_B]}_{\equiv \varphi_2}{}^2. \tag{D2}$$

For $\theta = 0$ [taking $f(m, 0) = 0$], the A d.o.f. are indeed gapped out and decoupled from the critical B d.o.f., whereas for $\theta = \pi/2$ the roles are reversed. We now show how to define $f(m, \theta)$ to keep the system Ising critical for intermediate values of θ.

If we express the Lagrangian in terms of the new fields φ_1 and φ_2 which are defined in Eq. (D2), we obtain

$$\mathcal{L} = \sum_{i=1,2} \left[(\partial \varphi_i)^2 - \left(\frac{3 + \cos(4\theta)}{4} \right) \varphi_i^4 - m_c^2 \varphi_i^2 \right] - m^2 \varphi_1^2 + f(m, \theta) \varphi_2^2 - V, \tag{D3}$$

where the coupling V arises due to the quartic term $V = \frac{3}{2}[1 - \cos(4\theta)]\varphi_1^2 \varphi_2^2 + \sin(4\theta)(\varphi_1 \varphi_2^3 - \varphi_1^3 \varphi_2)$. If we work in the limit of large m^2, then φ_1 will be pinned to $\varphi_1 = 0$, such that

$$\mathcal{L} = (\partial\varphi_2)^2 - \left(\frac{3+\cos(4\theta)}{4}\right)\varphi_2^4 - \left(m_c^2 + \frac{3}{2}[1-\cos(4\theta)]\langle\varphi_1^2\rangle_{m,\theta} - f(m,\theta)\right)\varphi_2^2. \tag{D4}$$

Here $\langle\varphi_1^2\rangle_{m,\theta}$ depends on the UV (lattice) scale a. (Note that there is no effective coupling through $\langle\varphi_1\rangle$ or $\langle\varphi_1^3\rangle$ since symmetry forces this to be zero.) The Lagrangian in Eq. (D4) is at the Ising critical point if we enforce the ratio

$$m_c^2 = \frac{m_c^2 + \frac{3}{2}[1-\cos(4\theta)]\langle\varphi_1^2\rangle_{m,\theta} - f(m,\theta)}{\frac{3+\cos(4\theta)}{4}} \Rightarrow f(m,\theta) \equiv \sin^2(2\theta)\left(\frac{m_c^2}{2} + \langle\varphi_1^2\rangle_{m,\theta}\right). \tag{D5}$$

Note that when integrating out φ_1, higher-order corrections can be generated; these can be included, leading to a slight shift in $f(m,\theta)$. The main conceptual point is that we can reach (or better yet, stay on) criticality by tuning a single parameter.

APPENDIX E: THE CURIOUS CASE OF $c=1$

1. The ($\mathbb{Z}_2 \times \mathbb{Z}_2$)-enriched $c=1$ CFTs of codimension two

We consider the compact boson CFT and the $c=1$ orbifold CFT; These constitute the main component of the moduli space of $c=1$ theories [96,156–158]. Focusing on CFTs of codimension two, we show that any two ($\mathbb{Z}_2 \times \mathbb{Z}_2$)-enriched versions of the aforementioned CFTs can be smoothly connected without abruptly having to change the universality class at some intermediate point (i.e., they are connected by a path of symmetric marginal perturbations). More precisely, we characterize all possible symmetry assignments of local operators and nonlocal symmetry fluxes and demonstrate that these form a connected moduli space. For the case of the Ising CFT, we prove that it is sufficient to consider such symmetry assignments (see the bait-and-switch lemma in Appendix D); while we do not have a proof for the analogous statement for these $c=1$ CFTs, we suspect it to be true.

Let us first consider the compact boson CFT, with fields $[\partial\varphi(x), \theta(y)] = 2\pi i\delta(x-y)$ (see also Sec. V C of the main text). To achieve the lowest possible codimension (i.e., two) with a $\mathbb{Z}_2 \times \mathbb{Z}_2$ symmetry, the symmetry needs to act within the CFT (i.e., it cannot act on only gapped degrees of freedom). The symmetry group of the compact boson (which is generically $\mathrm{U}(1) \times \mathrm{U}(1) \rtimes \mathbb{Z}_2$, although our discussion is not limited to generic cases) admits various $\mathbb{Z}_2 \times \mathbb{Z}_2$ subgroups. However, there are only two such subgroups which are not related by conjugation; equivalently, by appropriately redefining our fields, the only two $\mathbb{Z}_2 \times \mathbb{Z}_2$ subgroups to consider are those generated by $\mathcal{C}, \mathcal{S}$ and those generated by $\mathcal{C}, \tilde{\mathcal{S}}$, where

$$\mathcal{C}:\begin{cases}\theta \rightarrow -\theta, \\ \varphi \rightarrow -\varphi,\end{cases} \mathcal{S}:\begin{cases}\theta \rightarrow \theta+\pi, \\ \varphi \rightarrow \varphi,\end{cases} \tilde{\mathcal{S}}:\begin{cases}\theta \rightarrow \theta, \\ \varphi \rightarrow \varphi+\pi.\end{cases} \tag{E1}$$

We refer to $\mathcal{C}$ as charge conjugation and to $\mathcal{S}, \tilde{\mathcal{S}}$ as shift symmetries (one could also consider the shift symmetry $\mathcal{S}\tilde{\mathcal{S}}$ which shifts both fields, but this is anomalous and thus cannot arise from an on-site $\mathbb{Z}_2$ symmetry on the lattice). Moreover, by applying T duality (which corresponds to defining the new fields $\tilde{\varphi} := \theta$ and $\tilde{\theta} := \varphi$), one can interchange $\mathcal{S}$ and $\tilde{\mathcal{S}}$ at the cost of changing the Luttinger liquid parameter $K \rightarrow 1/(4K)$. Since such dual points are connected along the compact boson line (by tuning K) [96], it is sufficient to consider the case where our $\mathbb{Z}_2 \times \mathbb{Z}_2$ symmetry is generated by charge conjugation $\mathcal{C}$ and shift symmetry $\mathcal{S}$.

With regard to symmetry assignments of symmetry fluxes, note that this corresponds to the charges of states in twisted sectors. If two symmetry-enriched CFTs have the same charges for local operators, then the charges of twisted sectors can differ only by a relative global charge (otherwise, one can argue that there exists a local operator with a different charge in the two CFTs). By standard arguments, as in Appendix A 2, these charge assignments naturally form a group cocycle in $H^2(G, \mathrm{U}(1))$. Hence, we need only to consider stacking the CFT with gapped SPT phases. However, as we discuss in the main text (see Sec. V C), the compact boson CFT is invariant under stacking with the $\mathbb{Z}_2 \times \mathbb{Z}_2$ Haldane SPT phase.

In conclusion, a ($\mathbb{Z}_2 \times \mathbb{Z}_2$)-enriched compact boson CFT is unique up to matching the physical symmetries (say, R_x, R_y, R_z) to the continuum symmetry $\mathbb{Z}_2 \times \mathbb{Z}_2$ generated by $\mathcal{C}$ and $\mathcal{S}$. Since $\mathcal{C}$ and $\mathcal{CS}$ are related by conjugation (i.e., there is no observable or absolute difference between them), the only real choice is in which of the three symmetries corresponds to $\mathcal{S}$. This thus gives us three copies of the compact boson line, as shown in Fig. 15 (two of which are shown in gray). These naturally join at the SU(2)-invariant point (where the Luttinger liquid parameter $K=1$), where R_x, R_y, and R_z are all symmetry equivalent (see Appendix E 2 where this is discussed in more detail, as well as the related discussion in the main text in Sec. V C).

Let us now focus on the cases with only two relevant symmetry-allowed perturbations. Since $e^{i(m\varphi+n\theta)}$ has dimension $m^2K + n^2/(4K)$, this region is $2/9 < K < 9/2$. Along this line, we show the nearby two-parameter phase diagram in Fig. 15. In particular, region I corresponds to $2 < K < 9/2$, where the relevant operators are $\cos(2\theta)$
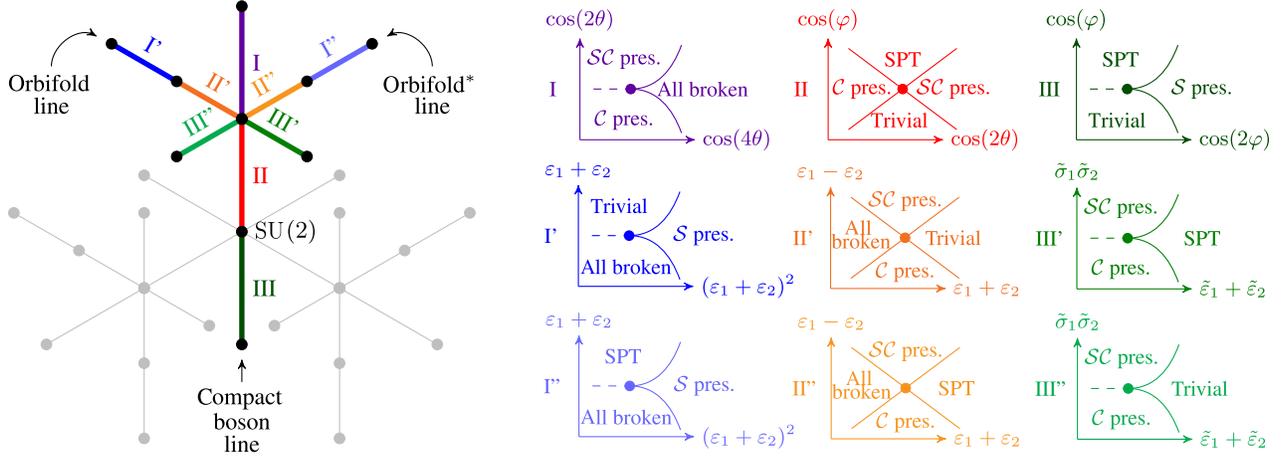
FIG. 15. The moduli space of $(\mathbb{Z}_2 \times \mathbb{Z}_2)$-enriched $c = 1$ CFTs of codimension two (containing the compact boson and its $\mathbb{Z}_2$ orbifold). The compact boson line appears thrice (twice in gray), corresponding to different identifications of the $\mathbb{Z}_2 \times \mathbb{Z}_2$ subgroup generated by charge conjugation $\mathcal{C}$ and shift symmetry $\mathcal{S}$; these lines are joined at the SU(2)-invariant point ($K = 1/2$). Each compact boson line sprouts two orbifold lines at the KT point ($K = 2$) which are pairwise related by a SPT entangler. Together, there are $3 \times 3 \times 3 = 27$ distinct regions which are all smoothly connected; for each region, the nearby phase diagram is sketched.

and $\cos(4\theta)$; the latter can lead to a first-order transition (dashed line in Fig. 15). When a nearby phase has spontaneous symmetry breaking, we denote which symmetry is preserved (if any). Region II has $1/2 < K < 2$, containing the free-fermion point at $K = 1$; this corresponds to the XY chain in Fig. 7 [where Fig. 7(a) corresponds to the $\cos(2\theta)$ perturbation and Fig, 7(b) to the $\cos(\varphi)$ perturbation]. Finally, region III has $2/9 < K < 1/2$, which also contains a dual free-fermion point at $K = 1/4$ (however, unlike the $K = 1$ above, the symmetry-allowed perturbations are no longer quadratic in the fermionic representation).

The discussion of the orbifold CFT is quite similar. One way of viewing this CFT is as a marginal perturbation of $(\text{Ising})^2$, with Ising fields σ_1 and σ_2 and marginal perturbation $\varepsilon_1 \varepsilon_2$. Now the symmetry group is D_8, the symmetry group of the square, which admits the representation $\langle r, s | r^4 = s^2 = srsr = 1 \rangle$ (geometrically, r is rotation and s is reflection) where

$$r : \begin{cases} \sigma_1 & \to & -\sigma_2, \\ \sigma_2 & \to & \sigma_1, \end{cases} \qquad s : \begin{cases} \sigma_1 & \to & \sigma_1, \\ \sigma_2 & \to & -\sigma_2. \end{cases} \qquad (E2)$$

As before, there are two inequivalent choices of a $\mathbb{Z}_2 \times \mathbb{Z}_2$ subgroup generated by r^2, s or r^2, sr. And, as before, these two different choices are in fact related by T duality and lie on the same orbifold line. The self-dual point is where the orbifold line meets the compact boson line [96]. E.g., if one passes from II' to III' (in Fig. 15), the roles of s and sr are reversed. In particular, coming from one side (II'), we can equate $s = \mathcal{C}$ (by identifying $\sigma_1 = \cos\theta$ and $\sigma_2 = \sin\theta$, where the latter are the compact boson fields at the KT point) and from the other side, $sr = \mathcal{C}$ (by identifying $\tilde{\sigma}_{1,2} = \cos\theta \pm \sin\theta$); we see that in both cases $r^2 = \mathcal{S}$. Note that either side of the KT point has an $(\text{Ising})^2$ point

(i.e., in II' and in III'), and for conceptual simplicity, we denote the fields in terms of the respective Ising operators (using tilde variables in III' to avoid confusion); these are related under T duality, in particular: $\tilde{\sigma}_{1,2} = \sigma_1 \pm \sigma_2$.

As we argue above, the nonlocal charges can be toggled by stacking with G-SPTs. Stacking with the unique $\mathbb{Z}_2 \times \mathbb{Z}_2$ SPT, we obtain the twisted "orbifold*" line in Fig. 15. Indeed, note that in the nearby phase diagrams, the roles of trivial and SPT are reversed in I", II", III" relative to I', II', III'. In all cases, these nearby phase diagrams can be obtained by a direct inspection of the symmetric relevant operators, but a shortcut for the two orbifold lines is by noting how these CFTs (and their nearby phase diagrams) can be obtained by gauging charge-conjugation symmetry of the compact boson CFT [96]. Note that as in the case of the compact boson, we consider only the part of the orbifold branch where there are two relevant symmetry-preserving perturbations.

2. SU(2) symmetry at the self-dual radius

At the self-dual radius of the compact boson CFT (i.e., $K = 1/2$ or $r_c = 1/\sqrt{2}$), we have an emergent SU(2) × SU(2) symmetry generated by the following operators with dimensions (1,0) and (0,1), respectively,

$$J^x = \cos(\theta + \varphi), \quad J^y = \sin(\theta + \varphi), \quad J^z = \frac{1}{2} i \partial_z(\theta + \varphi),$$

$$\bar{J}^x = \cos(\theta - \varphi), \quad \bar{J}^y = \sin(\theta - \varphi), \quad \bar{J}^z = \frac{1}{2} i \partial_{\bar{z}}(\theta - \varphi).$$

$$(E3)$$

For clarity, we are using a convention such that $\theta + \varphi$ is holomorphic and $\theta - \varphi$ is antiholomorphic at $K = 1/2$.

We can define a change of variables which corresponds to a rotation generated by J^x, such that $\tilde{J}^x \equiv J^x$ but $\tilde{J}^z \equiv J^y$ and $\tilde{J}^y \equiv -J^z$ (and similar for the antiholomorphic sector). Note that this transformation is a symmetry only at the self-dual radius (i.e., at that point the theory is identical in these new variables). We thus find

$$\partial_x \tilde{\theta} = -2\cos\theta\sin\varphi, \qquad \partial_x \tilde{\varphi} = -2\sin\theta\cos\varphi,$$

$$\cos\tilde{\theta}\cos\tilde{\varphi} = \cos\theta\cos\varphi, \qquad \sin\tilde{\theta}\sin\tilde{\varphi} = \sin\theta\sin\varphi.$$

$$(E4)$$

APPENDIX F: RELATION TO THE LITERATURE

1. Quantum criticality in topological insulators and superconductors: Emergence of strongly coupled Majoranas and supersymmetry (Grover, Vishwanath)

In this subsection, we discuss a model appearing in Ref. [16], reinterpreting certain aspects in terms of symmetry-enriched quantum criticality. For that reason, we closely follow the notation used in that paper. To start, let us consider a model which does not directly appear in Ref. [16], but which will aid our analysis:

$$H = \sum_{n\geq 1} \left(J_{n \bmod 2}\, \chi_{2n-1}\chi_{2n}\chi_{2n+1}\chi_{2n+2} \right.$$

$$\left. - \frac{g}{2} i\chi_{4n-1}\chi_{4n+1} + \frac{g}{2} i\chi_{4n}\chi_{4n+2} \right). \qquad (F1)$$

The Hamiltonian is pictorially represented in Fig. 16. It has an antiunitary symmetry T_- defined by $(\chi_{2n-1}, \chi_{2n}) \overset{T_-}{\mapsto} (\chi_{2n}, -\chi_{2n-1})$ satisfying $T_-^2 = -1$. If we set $J_0 = J_1 = 0$ (but $g \neq 0$), then in Fig. 16 we directly see that we are in a topological phase with two zero-energy Majorana edge modes at a edge, χ_1 and χ_2, which T_- prevents us from gapping out. This is the only nontrivial class in DIII. Oppositely, if we make J_0 and J_1 positive and large, then the ground state wants to occupy vertical bonds, spontaneously breaking T_-.

Note that—similar to the SSH model—the above model is only nontrivial if we fix our convention of the physical unit cells to be $(1234)(5678)\cdots$, i.e., the blue boxes in Fig. 16.
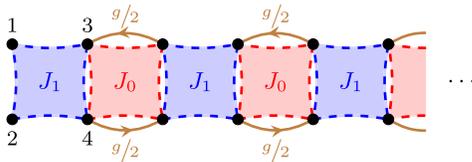

FIG. 16. A strongly interacting Majorana model [see Eq. (F1)] in the DIII class.

a. Deriving an effective (almost-)spin model (as $J_0 \to +\infty$)

Note that the J_0 term is an integral of motion. In fact, it is already minimized in the above phase, so we can adiabatically ramp up the term J_0 such that $J_0 \gg \max\{|J_1|, |g|\}$. We can then work in the subspace $\mathcal{H}_0$ where for all n, we have $\chi_{4n-1}\chi_{4n}\chi_{4n+1}\chi_{4n+2} = -1$. In this subspace, we can define the following bosonic operators:

$$\sigma_n^z := i\chi_{4n-1}\chi_{4n} = i\chi_{4n+1}\chi_{4n+2}, \qquad (F2)$$

$$\sigma_n^x := i\chi_{4n-1}\chi_{4n+1} = -i\chi_{4n}\chi_{4n+2}. \qquad (F3)$$

In this sector, we then obtain

$$H_{\text{eff}} = \sum_{n\geq 1}(J_1\chi_{4n-3}\chi_{4n-2}\chi_{4n-1}\chi_{4n} - gi\chi_{4n-1}\chi_{4n+1}) \qquad (F4)$$

$$= -J_1\sigma_1^z i\chi_1\chi_2 - \sum_{n\geq 1}(J_1\sigma_n^z\sigma_{n+1}^z + g\sigma_n^x). \qquad (F5)$$

The model in Eq. (F5) is the one appearing Ref. [16] [Eq. (1) of that work]. The antiunitary symmetries acts the following way on the bosonic operators: $(\sigma_n^x, \sigma_n^y, \sigma_n^z) \overset{T_-}{\mapsto} (\sigma_n^x, \sigma_n^y, -\sigma_n^z)$. In other words, for the spin variables, we can write $T_{-,\text{eff}} = (\prod \sigma_n^x)K$. Note that this implies $T_{-,\text{eff}}^2 = +1$.

We see that the antiunitary symmetry in H_{eff} is spontaneously broken for $|J_1| > |g|$, whereas for $|J_1| < |g|$ we have two protected Majorana modes (per edge).

b. Symmetry fluxes

Let us first obtain the symmetry flux for fermionic parity symmetry $P = \prod_n P_n$ where $P_n = \gamma_{4n-3}\gamma_{4n-2}\gamma_{4n-1}\gamma_{4n}$ is the fermionic parity per unit cell (i.e., per blue box in Fig. 16). Since we work in the limit where $J_0 \to +\infty$, we have that the product of red boxes has long-range order. We conclude that the symmetry flux of P is $\mathcal{S}_n^P = \cdots P_{n-2}P_{n-1}(i\gamma_{4n-3}\gamma_{4n-2})$ [note that the i is there to ensure that $\langle(\mathcal{S}_n^P)^2\rangle > 0$]. We observe that $T_-\mathcal{S}^P T_- = -\mathcal{S}^P$; i.e., the symmetry flux of P is odd under T. This gives us a discrete label which is moreover topologically nontrivial.

By the reciprocal nature of charges of symmetry fluxes, we expect that the symmetry flux of T should be odd under P. However, in this work we do not study the notion of symmetry fluxes for antiunitary symmetries. Nevertheless, a closely related statement is that we expect that $P\mu P = -\mu$. To make this precise, we can consider a lattice $\mathbb{Z}_2$ symmetry which we can relate to the unitary $\mathbb{Z}_2$ symmetry of the Ising CFT. This is of course $\prod_n \sigma_n^x$, or in the original fermionic model, the fermionic parity symmetry of a single leg, $P_{\text{odd}} = \prod_n(\chi_{4n-1}\chi_{4n+1})$. Indeed, for $J_0 \to +\infty$, one can derive that $P_{\text{odd}} = \prod_n \sigma_n^x$ (at least without boundaries). Similar to P, the symmetry flux of P_{odd} has an extra Majorana mode: $\mathcal{S}^{P_{\text{odd}}} = \cdots (P_{\text{odd}})_{n-2}(P_{\text{odd}})_{n-1}\chi_{4n-1}$. Hence, we conclude that the

symmetry flux of P_{odd} is odd under fermionic parity symmetry. Equivalently, the symmetry flux of $\prod_n \sigma_n^x$ is $\cdots \sigma_{n-2}^x \sigma_{n-1}^x \chi_{4n-1}$; we thus conclude that $P\mu P = -\mu$.

If we do not enforce the lattice $\mathbb{Z}_2$ symmetry $\prod_n \sigma_n^x$, then it becomes subtle to claim that $P\mu P = -\mu$ is well defined. However, in this particular case, we expect that due to T_- symmetry being enforced, this invariant remains well defined even in the absence of explicit $\prod_n \sigma_n^x$ symmetry; the methods developed in this paper do not allow us to prove this.

c. Edge modes

Since μ is charged under P, we know that by the general arguments in Sec. IV, the Ising CFT will have a degeneracy with open boundaries. This is in fact easy to

$$H = -\sum_{n,\sigma}(c_{n,\sigma}^\dagger c_{n+1,\sigma} + \text{H.c.}) + U\sum_n(-c_{n,\uparrow}^\dagger c_{n,\downarrow} c_{n+1,\uparrow} c_{n+1,\downarrow}^\dagger + \text{H.c.} + n_{i,\uparrow}n_{i+1,\downarrow} + n_{i,\downarrow}n_{i+1,\uparrow}). \tag{F6}$$

If we relabel the indices as $2j-1 \equiv (j,\uparrow)$ and $2j \equiv (j,\downarrow)$, then one can straightforwardly apply the Jordan-Wigner transformation to obtain the following spin-1/2 chain:

$$H = \frac{1}{2}\sum_i(X_{i-1}Z_iX_{i+1} + Y_{i-1}Z_iY_{i+1}) + U\sum_i(S_{2i-1}^+ S_{2i}^- S_{2i+1}^- S_{2i+2}^+ + \text{H.c.} + n_{2i-1}n_{2i+2} + n_{2i}n_{2i+1}), \tag{F7}$$

where $S^\pm = (X_i \pm iY_i)/2$ and $n_i = (1 + Z_i)/2$. In this bosonic language, we have the symmetries $P = \prod_i P_i$ (where $P_i = Z_{2i-1}Z_{2i}$) and $T = \prod_j e^{i(\pi/4)(S_{2j-1}^x S_{2j}^y - S_{2j-1}^y S_{2j}^x)}K$. Note that $T^2 = P$.

We consider the two string operators $(\mathcal{O}_\pm^P)_i \equiv \cdots Z_{2i-3}Z_{2i-2}(Z_{2i-1} \pm Z_{2i})$. Note that $T\mathcal{O}_\pm^P T^{-1} = \pm\mathcal{O}_\pm^P$. If $U = 0$, the bulk is a $c = 2$ CFT and both operators have the same scaling dimension $\Delta = 1/2$. For $U \neq 0$, the bulk gaps out the spin sector (of the original spinful fermions), stabilizing a $c = 1$ CFT. We confirm this in Fig. 17(a) for $U = -0.9$. Moreover, we find that $\mathcal{O}_+^P$ remains critical, whereas $\mathcal{O}_-^P$ now has long-range order;
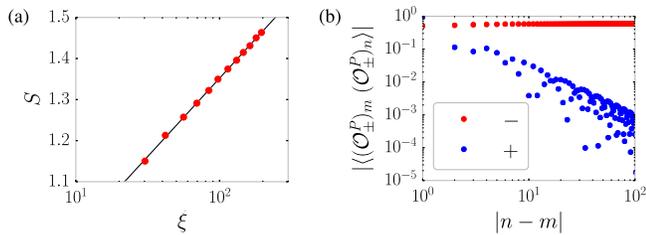

FIG. 17. Spinful fermions with triplet pairing: The model of Ref. [19] as shown in Eq. (F6) [or Eq. (F7)] with $U = -0.9$. (a) Confirmation that the bulk (which has central charge $c = 2$ for $U = 0$) has flown to central charge $c = 1$. The black line is a fit $S \sim (c_{\text{fit}}/6)\ln\xi$ with $c_{\text{fit}} \approx 0.994$. (b) Correlation function for $\mathcal{O}_\pm^P$ (where $T\mathcal{O}_\pm^P T = \pm\mathcal{O}_\pm^P$). We find that the T-odd string operator has long-range order; this is thus the unique symmetry flux of P.

see in Eqs. (F1) and (F5). In both cases, we see that $i\chi_1\chi_2$ and $\chi_1\sigma_2^x\sigma_3^x\cdots$ are symmetries of the Hamiltonian, whereas they mutually anticommute. The half-infinite geometry thus has a twofold degeneracy labeled by the occupation $i\chi_1\chi_2 = \pm 1$. Remarkably, this degeneracy is protected by the bulk CFT being enriched nontrivially by P and T_-. Even with generic symmetry-preserving perturbations, the system will have a global twofold degeneracy whose splitting is exponentially small in system size.

2. Gapless symmetry-protected topological phase of fermions in one dimension (Keselman, Berg)

Let us recall the model in Eq. (29) of the main text:

this is shown in Fig. 17(b). We conclude that the system has flown to a $c = 1$ CFT which is nontrivially enriched by P and T; in particular, the (unique) symmetry flux of P is odd under T.

3. Gapless symmetry-protected topological order (Scaffidi, Parker, Vasseur)

We consider the cluster model with an Ising term on one of the two sublattices [28]:

$$H = -\sum_n(Z_{A,n}X_{B,n}Z_{A,n+1} + Z_{B,n-1}X_{A,n}Z_{B,n} + JZ_{A,n}Z_{A,n+1}). \tag{F8}$$

This model has a $\mathbb{Z}_2 \times \mathbb{Z}_2$ symmetry generated by $P_A = \prod_n X_{A,n}$ and $P_B = \prod_n X_{B,n}$. To obtain its phase diagram, note that the unitary $U = \prod_n(CZ)_{A,n;B,n}(CZ)_{B,n;A,n+1}$ maps H to two decoupled chains. In particular, if we define

$$\begin{cases} \tilde{X}_{A,n} := UX_{A,n}U^\dagger = Z_{B,n-1}X_{A,n}Z_{B,n}, \\ \tilde{X}_{B,n} := UX_{B,n}U^\dagger = Z_{A,n}X_{B,n}Z_{A,n+1}, \\ \tilde{Z}_{A,n} := UZ_{A,n}U^\dagger = Z_{A,n}, \\ \tilde{Z}_{B,n} := UZ_{B,n}U^\dagger = Z_{B,n}, \end{cases} \tag{F9}$$

then for periodic boundary conditions, Eq. (F8) becomes an Ising chain on A sites and a fixed-point paramagnet on B sites:

$$H = -\sum_n \tilde{X}_{B,n} - \sum_n (\tilde{X}_{A,n} + J\tilde{Z}_{A,n}\tilde{Z}_{A,n+1}). \quad \text{(F10)}$$

Hence, from this we infer that Eq. (F8) is in the SPT cluster phase for $|J| < 1$, spontaneously breaks P_A for $|J| > 1$, and is at an Ising critical point for $|J| = 1$. In Ref. [28], it was pointed out that for Eq. (F8) with open boundary conditions, the edge modes of the SPT phase (partially) survive at the Ising critical point (even upon including arbitrary ($\mathbb{Z}_2 \times \mathbb{Z}_2$)-symmetric perturbations).

Using the concepts introduced in Sec. III, we can identify a nontrivial bulk topological invariant explaining the aforementioned edge modes. It is straightforward to obtain the symmetry flux associated with P_B: We see that Eq. (F10) has long-range order in $\prod_{m\leq n} \tilde{X}_{B,m} = (\prod_{m\leq n} X_{B,m})Z_{A,n+1}$, which is odd under P_A. This charge thus gives us a topological invariant whenever P_A is preserved [159]: I.e., in the gapped SPT phase ($|J| < 1$) or at the critical point ($|J| = 1$). The fact that it has long-range order is due to the symmetry being gapped; it is thus also instructive to consider the other symmetry, which is more representative of the purely gapless case. In particular, at criticality ($|J| = 1$), the Ising chain Eq. (F10) has an algebraically decaying disorder parameter $\mu \sim \prod_{m\leq n} \tilde{X}_{A,n} = (\prod_{m\leq n} X_{A,n})Z_{B,n}$ with scaling dimension $\Delta = 1/8$ (e.g., see the discussion in Sec. II). We thus see that the Ising critical point of Eq. (F8) has a disorder operator μ which is odd under P_B, encoding the nontrivial topological invariant.

APPENDIX G: DETAILS ABOUT THE CONSTRUCTION OF 2D EXAMPLES

Let H be a spin-1/2 model on the triangular lattice which is symmetric with respect to the $\mathbb{Z}_2 \times \mathbb{Z}_2 \times \mathbb{Z}_2$ symmetry generated by $P_A = \prod_n X_{A,n}$, $P_B = \prod_n X_{B,n}$, and $P_C = \prod_n X_{C,n}$ (here A, B, C denote the three sublattices which are, respectively, colored green, red, and blue in Fig. 18). Denote $U_{2D} = \prod_\triangle CCZ$ which applies the CCZ gate on every triangle of the triangular lattice, and define $H' = UHU$ (note that all unitary operators considered in this section will square to unity, so we will not distinguish U from $U^\dagger$). We now show that the twisted sectors of H and H' twisted by P_A and P_B are unitarily equivalent in such a way that eigenstates with well-defined P_C have opposite quantum numbers.

1. Warm-up: The fixed-point case

It is instructive to first consider the simpler case where $H = -\sum_r X_r$ [here r is shorthand for (λ, n) with $\lambda = A, B, C$]. In this case, $H' = UHU$ corresponds to the Yoshida model which is a $\mathbb{Z}_2^3$ SPT phase [139,140]. Using the property that $(CCZ)_{1,2,3}X_1(CCZ)_{1,2,3} = X_1(CZ)_{2,3}$, we see that $UX_rU = X_r \prod_{\text{hex}(r)} CZ$ where the product of CZ gates runs along the hexagon surrounding the site r; see Fig. 12(b).
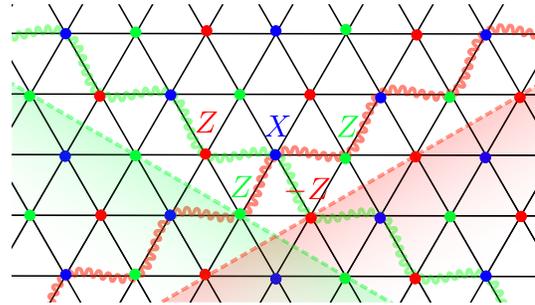

FIG. 18. If one starts with the trivial paramagnet on the triangular lattice, and then SPT entangles using U_{2D}, twists by P_A along the green dashed line, and SPT entangles back, then the resulting model is a trivial paramagnet except for the sites along the green wiggly line, where it is in a 1D cluster model. Similar for twisting by P_B along the red dashed line. If one twists by both symmetries at the same time, then the blue site near the defect intersection is mapped to the five-site operator as shown, with a minus sign due to the Z operator on the green wiggly line anticommuting with the P_B twist. After a global unitary transformation ($V = U_{0D}U_{1D}U_{2D}$ in the text), the system can be mapped back to the original trivial paramagnet, at the cost of flipping the sign of P_C.

Since each term in H commutes with P_A and P_B, twisting has no effect on the trivial Hamiltonian, i.e., $H_{\text{twist}} = H$. In particular, since the ground state satisfies $X_r = 1$, the ground-state parity in the twisted sector is $P_C = \prod_n X_{C,n} = 1$. (This signifies that we are in a trivial $\mathbb{Z}_2^3$ SPT phase.)

In contrast, the terms in the Yoshida model H' are affected whenever they overlap with the defect line. Let us first twist by P_A, which corresponds to conjugating the Hamiltonian term with a product of $X_{A,n}$ operators if n lies below or on the green dashed line in Fig. 18. Using the fact that $X_1(CZ)_{1,2}X_1 = (CZ)_{1,2}Z_2$, we see that Hamiltonian terms that intersect the defect line will acquire extra factors of $Z_{B,n}$ or $Z_{C,n}$ after twisting with P_A. The net result can be phrased as follows: If after twisting with P_A we conjugate the term again with U_{2D} (i.e., removing the $\prod CZ$ around the hexagon), we end up with a trivial X_r except along the green wiggly line in Fig. 18 where the Hamiltonian is the 1D cluster chain.

Twisting by P_B is analogous, with one exception: The blue site at the intersection of the two twist lines (indicated in Fig. 18) also obtains a minus sign since only one of the two $Z_{B,n}$ operators is acted on by the P_B twist (and $Z_{B,n}$ of course anticommutes with $X_{B,n}$). In summary, twisting by P_A and P_B for the Yoshida model is equivalent to conjugating by $U_{1D}U_{0D}$ where $U_{1D} = \prod CZ$ with the product running along the green and red wiggly lines in Fig. 18 and where $U_{0D} = Z_{C,n_0}$ with n_0 being the (blue) site at the intersection of the two defect lines. More precisely, $H'_{\text{twist}} = U_{1D}U_{0D}H'U_{1D}U_{0D} = VHV$ with $V = U_{2D}U_{1D}U_{0D}$. We thus obtain that the ground state of H'_{twist} satisfies $VX_{C,n}V = 1$, such that

$$P_C = \prod_{\boldsymbol{n}} X_{C,\boldsymbol{n}} = -\prod_{\boldsymbol{n}} U_{0D} X_{C,\boldsymbol{n}} U_{0D} = -\prod_{\boldsymbol{n}} U_{0D} \left(\prod_{\boldsymbol{m} \in l \cup l'} Z_{B,\boldsymbol{m}}^2 \right) X_{C,\boldsymbol{n}} \left(\prod_{\boldsymbol{m} \in l \cup l'} Z_{B,\boldsymbol{m}}^2 \right) U_{0D} \tag{G1}$$

$$= -\prod_{\boldsymbol{n}} U_{0D} U_{1D} X_{C,\boldsymbol{n}} U_{1D} U_{0D} = -\prod_{\boldsymbol{n}} U_{0D} U_{1D} \left(\prod_{\triangle} (CCZ)^2 \right) X_{C,\boldsymbol{n}} \left(\prod_{\triangle} (CCZ)^2 \right) U_{1D} U_{0D} = -\prod_{\boldsymbol{n}} V X_{C,\boldsymbol{n}} V = -1. \tag{G2}$$

Here we use the aforementioned properties that $(CZ)_{1,2} X_1 (CZ)_{1,2} = X_1 Z_2$ and $(CCZ)_{1,2,3} X_1 (CCZ)_{1,2,3} = X_1 (CZ)_{2,3}$, and l and l' denote the sites along the green and red wiggly lines in Fig. 18.

2. The general case

In the simple case above, we see that the twisted sector of H' (i.e., H'_{twist}) is in fact unitarily equivalent to H' (which is in turn unitarily equivalent to H). The above derivation directly extends to Hamiltonians which contain only products of $X_{\boldsymbol{r}}$ operators. However, H' and H'_{twist} are no longer unitarily equivalent when there are also terms containing $Z_{\boldsymbol{r}}$ (or $Y_{\boldsymbol{r}}$, but this need not be discussed separately since one can rewrite this as the product $iX_{\boldsymbol{r}} Z_{\boldsymbol{r}}$). Fortunately, it is still true that H_{twist} and H'_{twist} are unitarily equivalent. The idea is simple: For any $X_{\boldsymbol{r}}$ that appears, we apply the previous unitary mapping, whereas for any $Z_{\boldsymbol{r}}$ that appears, the twisting by P_A and P_B is the same for both H and H'.

Let us now confirm that the details work out. Without loss of generality, we can write (note that α is just a label and need not be interpreted as a spatial index) $H = \sum h_\alpha$ where each h_α is a product of Pauli operators: $h_\alpha = a_\alpha \prod_{\boldsymbol{r} \in S_{\alpha,x}} X_{\boldsymbol{r}} \prod_{\boldsymbol{r} \in S_{\alpha,z}} Z_{\boldsymbol{r}}$ where a_α is a number and $S_{\alpha, \gamma = x, z}$ are unspecified sets of indices (note that $S_{\alpha,x} \cap S_{\alpha,z}$ could be nonzero, corresponding to a Pauli-Y operator; hence, Hermiticity requires $a_\alpha \in i^{|S_{\alpha,x} \cap S_{\alpha,z}|} \mathbb{R}$).

The twisted sector of H can then be written as $H_{\text{twist}} = \sum_\alpha h_{\text{twist}, \alpha}$ with $h_{\text{twist}, \alpha} = a_\alpha \prod_{\boldsymbol{r} \in S_{\alpha,x}} X_{\boldsymbol{r}} \mathcal{T}(\prod_{\boldsymbol{r} \in S_{\alpha,z}} Z_{\boldsymbol{r}})$. Here $\mathcal{T}(\cdot)$ simply denote the twisting operation; the result of twisting the $Z_{\boldsymbol{r}}$ operators could be written out more explicitly but we do not need such detailed expressions to establish the unitary equivalence.

We now turn to $H' = UHU = \sum_\alpha h'_\alpha$ with $h'_\alpha = a_\alpha \prod_{\boldsymbol{r} \in S_{\alpha,x}} (UX_{\boldsymbol{r}} U) \prod_{\boldsymbol{r} \in S_{r,z}} Z_{\boldsymbol{r}}$. Twisting this gives $H'_{\text{twist}} = \sum_\alpha h'_{\text{twist}, \alpha}$ and $h'_{\text{twist}, \alpha} = a_\alpha (\prod_{\boldsymbol{r} \in S_{\alpha,x}} \mathcal{T}(UX_{\boldsymbol{r}} U)) \times \mathcal{T}(\prod_{\boldsymbol{r} \in S_{\alpha,z}} Z_{\boldsymbol{r}})$. From the discussion in Sec. G 1 we learn that $\mathcal{T}(UX_{\boldsymbol{r}} U) = VX_{\boldsymbol{r}} V$ with $V = U_{2D} U_{1D} U_{0D}$. Hence, if we define the new variables under the unitary mapping, $\tilde{X} = VX_{\boldsymbol{r}} V$ and $\tilde{Z} = VZ_{\boldsymbol{r}} V = Z_{\boldsymbol{r}}$, then we see that the twisted sector of H and H' is unitarily equivalent. However,

$$\tilde{P}_C = \prod_{\boldsymbol{n}} \tilde{X}_{C,\boldsymbol{n}} = \prod_{\boldsymbol{n}} VX_{C,\boldsymbol{n}} V = -\prod_{\boldsymbol{n}} X_{C,\boldsymbol{n}} = -P_C. \tag{G3}$$

In other words, the unitary mapping between H_{twist} and H'_{twist} toggles the eigenvalue of P_C (for each eigenstate).

[1] L. Fidkowski and A. Kitaev, *Topological Phases of Fermions in One Dimension*, Phys. Rev. B **83**, 075103 (2011).

[2] A. M. Turner, F. Pollmann, and E. Berg, *Topological Phases of One-Dimensional Fermions: An Entanglement Point of View*, Phys. Rev. B **83**, 075102 (2011).

[3] X. Chen, Z.-C. Gu, and X.-G. Wen, *Classification of Gapped Symmetric Phases in One-Dimensional Spin Systems*, Phys. Rev. B **83**, 035107 (2011).

[4] N. Schuch, D. Pérez-García, and J. I. Cirac, *Classifying Quantum Phases Using Matrix Product States and Projected Entangled Pair States*, Phys. Rev. B **84**, 165139 (2011).

[5] X. Chen, Z.-C. Gu, Z.-X. Liu, and X.-G. Wen, *Symmetry Protected Topological Orders and the Group Cohomology of Their Symmetry Group*, Phys. Rev. B **87**, 155114 (2013).

[6] A. Kapustin, *Symmetry Protected Topological Phases, Anomalies, and Cobordisms: Beyond Group Cohomology*, arXiv:1403.1467.

[7] A. Kapustin, R. Thorngren, A. Turzillo, and Z. Wang, *Fermionic Symmetry Protected Topological Phases and Cobordisms*, J. High Energy Phys. 12 (2015) 052.

[8] T. Senthil, *Symmetry-Protected Topological Phases of Quantum Matter*, Annu. Rev. Condens. Matter Phys. **6**, 299 (2015).

[9] I. Affleck, T. Kennedy, E. H. Lieb, and H. Tasaki, *Valence Bond Ground States in Isotropic Quantum Antiferromagnets*, Commun. Math. Phys. **115**, 477 (1988).

[10] T. Kennedy, *Exact Diagonalisations of Open Spin-1 Chains*, J. Phys. Condens. Matter **2**, 5737 (1990).

[11] J. P. Kestner, B. Wang, J. D. Sau, and S. D. Sarma, *Prediction of a Gapless Topological Haldane Liquid Phase in a One-Dimensional Cold Polar Molecular Lattice*, Phys. Rev. B **83**, 174409 (2011).

[12] M. Cheng and H.-H. Tu, *Majorana Edge States in Interacting Two-Chain Ladders of Fermions*, Phys. Rev. B **84**, 094503 (2011).

[13] L. Fidkowski, R. M. Lutchyn, C. Nayak, and M. P. A. Fisher, *Majorana Zero Modes in One-Dimensional Quantum Wires without Long-Ranged Superconducting Order*, Phys. Rev. B **84**, 195436 (2011).

[14] J. D. Sau, B. I. Halperin, K. Flensberg, and S. D. Sarma, *Number Conserving Theory for Topologically Protected Degeneracy in One-Dimensional Fermions*, Phys. Rev. B **84**, 144509 (2011).

[15] J. Ruhman, E. G. Dalla Torre, S. D. Huber, and E. Altman, *Nonlocal Order in Elongated Dipolar Gases*, Phys. Rev. B **85**, 125121 (2012).

[16] T. Grover and A. Vishwanath, *Quantum Criticality in Topological Insulators and Superconductors: Emergence of Strongly Coupled Majoranas and Supersymmetry*, arXiv:1206.1332.

[17] C. V. Kraus, M. Dalmonte, M. A. Baranov, A. M. Läuchli, and P. Zoller, *Majorana Edge States in Atomic Wires Coupled by Pair Hopping*, Phys. Rev. Lett. **111**, 173004 (2013).

[18] G. Ortiz, J. Dukelsky, E. Cobanera, C. Esebbag, and C. Beenakker, *Many-Body Characterization of Particle-Conserving Topological Superfluids*, Phys. Rev. Lett. **113**, 267002 (2014).

[19] A. Keselman and E. Berg, *Gapless Symmetry-Protected Topological Phase of Fermions in One Dimension*, Phys. Rev. B **91**, 235309 (2015).

[20] J. Ruhman, E. Berg, and E. Altman, *Topological States in a One-Dimensional Fermi Gas with Attractive Interaction*, Phys. Rev. Lett. **114**, 100401 (2015).

[21] N. Kainaris and S. T. Carr, *Emergent Topological Properties in Interacting One-Dimensional Systems with Spin-Orbit Coupling*, Phys. Rev. B **92**, 035139 (2015).

[22] F. Iemini, L. Mazza, D. Rossini, R. Fazio, and S. Diehl, *Localized Majorana-Like Modes in a Number-Conserving Setting: An Exactly Solvable Model*, Phys. Rev. Lett. **115**, 156402 (2015).

[23] N. Lang and H. P. Büchler, *Topological States in a Microscopic Model of Interacting Fermions*, Phys. Rev. B **92**, 041118(R) (2015).

[24] G. Ortiz and E. Cobanera, *What is a Particle-Conserving Topological Superfluid? The Fate of Majorana Modes beyond Mean-Field Theory*, Ann. Phys. (Amsterdam) **372**, 357 (2016).

[25] A. Montorsi, F. Dolcini, R. C. Iotti, and F. Rossi, *Symmetry-Protected Topological Phases of One-Dimensional Interacting Fermions with Spin-Charge Separation*, Phys. Rev. B **95**, 245108 (2017).

[26] Z. Wang, Y. Xu, H. Pu, and K. R. A. Hazzard, *Number-Conserving Interacting Fermion Models with Exact Topological Superconducting Ground States*, Phys. Rev. B **96**, 115110 (2017).

[27] J. Ruhman and E. Altman, *Topological Degeneracy and Pairing in a One-Dimensional Gas of Spinless Fermions*, Phys. Rev. B **96**, 085133 (2017).

[28] T. Scaffidi, D. E. Parker, and R. Vasseur, *Gapless Symmetry-Protected Topological Order*, Phys. Rev. X **7**, 041048 (2017).

[29] K. Guther, N. Lang, and H. P. Büchler, *Ising Anyonic Topological Phase of Interacting Fermions in One Dimension*, Phys. Rev. B **96**, 121109(R) (2017).

[30] N. Kainaris, R. A. Santos, D. B. Gutman, and S. T. Carr, *Interaction Induced Topological Protection in One-Dimensional Conductors*, Fortschr. Phys. **65**, 1600054 (2017).

[31] H.-C. Jiang, Z.-X. Li, A. Seidel, and D.-H. Lee, *Symmetry Protected Topological Luttinger Liquids and the Phase Transition between Them*, Sci. Bull. **63**, 753 (2018).

[32] R.-X. Zhang and C.-X. Liu, *Crystalline Symmetry-Protected Majorana Mode in Number-Conserving Dirac Semimetal Nanowires*, Phys. Rev. Lett. **120**, 156802 (2018).

[33] R. Verresen, N. G. Jones, and F. Pollmann, *Topology and Edge Modes in Quantum Critical Chains*, Phys. Rev. Lett. **120**, 057001 (2018).

[34] D. E. Parker, T. Scaffidi, and R. Vasseur, *Topological Luttinger Liquids from Decorated Domain Walls*, Phys. Rev. B **97**, 165114 (2018).

[35] A. Keselman, E. Berg, and P. Azaria, *From One-Dimensional Charge Conserving Superconductors to the Gapless Haldane Phase*, Phys. Rev. B **98**, 214501 (2018).

[36] C. Chen, W. Yan, C. S. Ting, Y. Chen, and F. J. Burnell, *Flux-Stabilized Majorana Zero Modes in Coupled One-Dimensional Fermi Wires*, Phys. Rev. B **98**, 161106(R) (2018).

[37] F. D. M. Haldane, *Continuum Dynamics of the 1-D Heisenberg Antiferromagnet: Identification with the $O(3)$ Nonlinear Sigma Model*, Phys. Lett. **93A**, 464 (1983).

[38] T. Kennedy and H. Tasaki, *Hidden Symmetry Breaking and the Haldane Phase in $S = 1$ Quantum Spin Chains*, Commun. Math. Phys. **147**, 431 (1992).

[39] Z.-C. Gu and X.-G. Wen, *Tensor-Entanglement-Filtering Renormalization Approach and Symmetry-Protected Topological Order*, Phys. Rev. B **80**, 155131 (2009).

[40] F. Pollmann, A. M. Turner, E. Berg, and M. Oshikawa, *Entanglement Spectrum of a Topological Phase in One Dimension*, Phys. Rev. B **81**, 064439 (2010).

[41] W. Chen, K. Hida, and B. C. Sanctuary, *Ground-State Phase Diagram of $S = 1$ XXZ Chains with Uniaxial Single-Ion-Type Anisotropy*, Phys. Rev. B **67**, 104401 (2003).

[42] C. Vafa, *Modular Invariance and Discrete Torsion on Orbifolds*, Nucl. Phys. **B273**, 592 (1986).

[43] C. Vafa and E. Witten, *On Orbifolds with Discrete Torsion*, J. Geom. Phys. **15**, 189 (1995).

[44] M. R. Douglas, *D-Branes and Discrete Torsion*, arXiv:hep-th/9807235.

[45] E. Sharpe, *Discrete Torsion*, Phys. Rev. D **68**, 126003 (2003).

[46] T. Senthil, A. Vishwanath, L. Balents, S. Sachdev, and M. P. A. Fisher, *Deconfined Quantum Critical Points*, Science **303**, 1490 (2004).

[47] S. Jiang and O. Motrunich, *Ising Ferromagnet to Valence Bond Solid Transition in a One-Dimensional Spin Chain: Analogies to Deconfined Quantum Critical Points*, Phys. Rev. B **99**, 075103 (2019).

[48] B. Roberts, S. Jiang, and O. I. Motrunich, *Deconfined Quantum Critical Point in One Dimension*, Phys. Rev. B **99**, 165143 (2019).

[49] F. Pollmann and A. M. Turner, *Detection of Symmetry-Protected Topological Phases in One Dimension*, Phys. Rev. B **86**, 125441 (2012).

[50] M. Suzuki, *Relationship among Exactly Soluble Models of Critical Phenomena. I*)2D Ising Model, Dimer Problem and the Generalized XY-Model*, Prog. Theor. Phys. **46**, 1337 (1971).

[51] R. Raussendorf and H. J. Briegel, *A One-Way Quantum Computer*, Phys. Rev. Lett. **86**, 5188 (2001).

[52] J. P. Keating and F. Mezzadri, *Random Matrix Theory and Entanglement in Quantum Spin Chains*, Commun. Math. Phys. **252**, 543 (2004).

[53] W. Son, L. Amico, R. Fazio, A. Hamma, S. Pascazio, and V. Vedral, *Quantum Phase Transition between Cluster and Antiferromagnetic States*, Europhys. Lett. **95**, 50001 (2011).

[54] R. Verresen, R. Moessner, and F. Pollmann, *One-Dimensional Symmetry Protected Topological Phases and Their Transitions*, Phys. Rev. B **96**, 165124 (2017).

[55] D. V. Else, S. D. Bartlett, and A. C. Doherty, *Hidden Symmetry-Breaking Picture of Symmetry-Protected Topological Order*, Phys. Rev. B **88**, 085114 (2013).

[56] Depending on the charge of these long-range-ordered strings, they lead to distinct symmetry-breaking phases after gauging, and they incorporate the "correct" way of terminating a gauge string.

[57] M. Levin and Z.-C. Gu, *Braiding Statistics Approach to Symmetry-Protected Topological Phases*, Phys. Rev. B **86**, 115109 (2012).

[58] C. Wang and M. Levin, *Topological Invariants for Gauge Theories and Symmetry-Protected Topological Phases*, Phys. Rev. B **91**, 165119 (2015).

[59] P. Di Francesco, P. Mathieu, and D. Senechal, *Conformal Field Theory*, Graduate Texts in Contemporary Physics (Springer-Verlag, New York, 1997).

[60] Throughout this paper, we use the notation "CFT operator~lattice operator" to express which lattice operator contains which dominant scaling operator (as evidenced by, e.g., correlation functions).

[61] N. G. Jones and R. Verresen, *Asymptotic Correlations in Gapped and Critical Topological Phases of 1D Quantum Systems*, J. Stat. Phys. **175**, 1164 (2019).

[62] This can be reached by perturbing with $\varepsilon(x) \sim -\mu(x) \times \mu(x + a) + \sigma(x)\sigma(x + a)$.

[63] E.g., consider a gapped SPT phase with long-range order in a string order parameter $\mathcal{A}_n$ which is odd under T. If this is stacked on top of a critical chain, then μ and $\mu\mathcal{A}$ have the same scaling dimension $\Delta = 1/8$ yet distinct charges. Fortunately, they are distinguished by their string; i.e., they are symmetry fluxes for distinct symmetries.

[64] G. M. T. Watts, *On the Boundary Ising Model with Disorder Operators*, Nucl. Phys. **B596**, 513 (2001).

[65] J. L. Cardy, *Effect of Boundary Conditions on the Operator Content of Two-Dimensional Conformally Invariant Theories*, Nucl. Phys. **B275**, 200 (1986).

[66] D. Vodola, L. Lepori, E. Ercolessi, A. V. Gorshkov, and G. Pupillo, *Kitaev Chains with Long-Range Pairing*, Phys. Rev. Lett. **113**, 156402 (2014).

[67] D. Vodola, L. Lepori, E. Ercolessi, and G. Pupillo, *Long-Range Ising and Kitaev Models: Phases, Correlations and Edge Modes*, New J. Phys. **18**, 015001 (2015).

[68] K. Patrick, T. Neupert, and J. K. Pachos, *Topological Quantum Liquids with Long-Range Couplings*, Phys. Rev. Lett. **118**, 267002 (2017).

[69] S. B. Jäger, L. Dell'Anna, and G. Morigi, *Edge States of the Long-Range Kitaev Chain: An Analytical Study*, Phys. Rev. B **102**, 035152 (2020).

[70] In the noninteracting case, a stronger property will hold: An edge mode means that $[\gamma_L, H] = 0$ such that all energy levels are degenerate. This is not generic for interacting systems.

[71] A. Kitaev, *Unpaired Majorana Fermions in Quantum Wires*, Phys. Usp. **44**, 131 (2001).

[72] D. E. Parker, R. Vasseur, and T. Scaffidi, *Topologically Protected Long Edge Coherence Times in Symmetry-Broken Phases*, Phys. Rev. Lett. **122**, 240605 (2019).

[73] L.-Y. Hung and X.-G. Wen, *Quantized Topological Terms in Weak-Coupling Gauge Theories with a Global Symmetry and Their Connection to Symmetry-Enriched Topological Phases*, Phys. Rev. B **87**, 165107 (2013).

[74] M. Barkeshli, C.-M. Jian, and X.-L. Qi, *Theory of Defects in Abelian Topological States*, Phys. Rev. B **88**, 235103 (2013).

[75] X.-G. Wen, *Symmetry-Protected Topological Invariants of Symmetry-Protected Topological Phases of Interacting Bosons and Fermions*, Phys. Rev. B **89**, 035147 (2014).

[76] M. Cheng and Z.-C. Gu, *Topological Response Theory of Abelian Symmetry-Protected Topological Phases in Two Dimensions*, Phys. Rev. Lett. **112**, 141602 (2014).

[77] M. P. Zaletel, *Detecting Two-Dimensional Symmetry-Protected Topological Order in a Ground-State Wave Function*, Phys. Rev. B **90**, 235113 (2014).

[78] J. C. Y. Teo, A. Roy, and X. Chen, *Unconventional Fusion and Braiding of Topological Defects in a Lattice Model*, Phys. Rev. B **90**, 115118 (2014).

[79] D. V. Else and C. Nayak, *Classifying Symmetry-Protected Topological Phases through the Anomalous Action of the Symmetry on the Edge*, Phys. Rev. B **90**, 235137 (2014).

[80] A. Kapustin, *Bosonic Topological Insulators and Paramagnets: A View from Cobordisms*, arXiv:1404.6659.

[81] N. Tarantino, N. H. Lindner, and L. Fidkowski, *Symmetry Fractionalization and Twist Defects*, New J. Phys. **18**, 035006 (2016).

[82] A. Tiwari, X. Chen, K. Shiozaki, and S. Ryu, *Bosonic Topological Phases of Matter: Bulk-Boundary Correspondence, Symmetry Protected Topological Invariants, and Gauging*, Phys. Rev. B **97**, 245133 (2018).

[83] Since U^h is a symmetry, this string order still has scaling dimension Δ_g. This shows that $\Delta_{hgh^{-1}} \leq \Delta_g$. By similarly starting from a symmetry flux of hgh^{-1}, we derive $\Delta_{hgh^{-1}} \geq \Delta_g$. Hence, $\Delta_{hgh^{-1}} = \Delta_g$.

[84] Indeed, $\mathcal{O}^g = (A + iB)/2$ with Hermitian operators $A = \mathcal{O}^g + (\mathcal{O}^g)^\dagger$ and $B = i((\mathcal{O}^g)^\dagger - \mathcal{O}^g)$. If neither A nor B give rise to symmetry fluxes, then also their linear combination $\mathcal{O}^g$ cannot.

[85] P. Ruelle and O. Verhoeven, *Discrete Symmetries of Unitary Minimal Conformal Theories*, Nucl. Phys. **B535**, 650 (1998).

[86] In principle, we should label it by μ_{R_x}, since the symmetry flux of R_y also has scaling dimension $\Delta = 1/8$ and may be denoted by μ_{R_y}.

[87] S. R. White, *Density Matrix Formulation for Quantum Renormalization Groups*, Phys. Rev. Lett. **69**, 2863 (1992).

[88] J. A. Kjäll, M. P. Zaletel, R. S. K. Mong, J. H. Bardarson, and F. Pollmann, *Phase Diagram of the Anisotropic Spin-2 XXZ Model: Infinite-System Density Matrix Renormalization Group Study*, Phys. Rev. B **87**, 235106 (2013).

[89] M. Yamanaka, Y. Hatsugai, and M. Kohmoto, *Phase Diagram of the S = 1/2 Quantum Spin Chain with Bond Alternation*, Phys. Rev. B **48**, 9555 (1993).

[90] S. Ejima, T. Yamaguchi, F. H. L. Essler, F. Lange, Y. Ohta, and H. Fehske, *Exotic Criticality in the Dimerized spin-1 XXZ Chain with Single-Ion Anisotropy*, SciPost Phys. **5,** 59 (2018).

[91] J. L. Cardy, *Boundary Conditions, Fusion Rules and the Verlinde Formula*, Nucl. Phys. **B324**, 581 (1989).

[92] Consider, for example, $H = -\sum_{n=1}^{\infty} Z_n Z_{n+1} - \sum_{n=2}^{\infty} X_n$ with its spontaneous boundary magnetization $Z_1 = \pm 1$. This is unstable against the perturbation $X_1 \sim \mu(0)$ flowing to a unique ground state.

[93] R. Blumenhagen and E. Plauschinn, *Introduction to Conformal Field Theory: With Applications to String Theory*, Lecture Notes in Physics (Springer, Berlin, 2009).

[94] All N_{2m} descendants generate independent rotations since otherwise a linear combination of descendants would be conserved—in conflict with the nonzero scaling dimension Δ_{2m}.

[95] K. Hida, *Crossover between the Haldane-Gap Phase and the Dimer Phase in the Spin-1/2 Alternating Heisenberg Chain*, Phys. Rev. B **45**, 2207 (1992).

[96] P. Ginsparg, in *Applied Conformal Field Theory, Proceedings of the Les Houches Summer School, Session XLIX*, edited by E. Brezin and J. Zinn-Justin (Elsevier, New York, 1990).

[97] This name arises due to the rescaled field $\tilde{\theta} \equiv \sqrt{K}\theta$ being $2\pi r_c$ periodic.

[98] I. Affleck, in *Field Theory Methods and Quantum Critical Phenomena, Proceedings of the Les Houches Summer School, Session XLIX*, edited by E. Brezin and J. Zinn-Justin (Elsevier, New York, 1990).

[99] S. Sachdev, *Quantum Phase Transitions* (Cambridge University Press, Cambridge, England, 2001).

[100] T. Giamarchi, *Quantum Physics in One Dimension*, International Series of Monographs on Physics (Clarendon Press, Oxford, 2004).

[101] This can be seen as a concatenation of halving the compactification radius and a duality transform: $r_c \rightarrow r_c/2 \rightarrow [1/2(r_c/2)] = 1/r_c$.

[102] S. D. Geraedts and O. I. Motrunich, *Exact Models for Symmetry-Protected Topological Phases in One Dimension*, arXiv:1410.1580.

[103] L. H. Santos, *Rokhsar-Kivelson Models of Bosonic Symmetry-Protected Topological States*, Phys. Rev. B **91**, 155150 (2015).

[104] A. B. Zamolodchikov and V. A. Fateev, *Nonlocal (Parafermion) Currents in Two-Dimensional Conformal Quantum Field Theory and Self-Dual Critical Points in Z_N-Symmetric Statistical Systems*, Sov. Phys. JETP **62**, 215 (1985).

[105] G. von Gehlen and V. Rittenberg, *Operator Content of the Three-State Potts Quantum Chain*, J. Phys. A **19**, L625 (1986).

[106] L. Tsui, Y.-T. Huang, H.-C. Jiang, and D.-H. Lee, *The Phase Transitions between $Z_n \times Z_n$ Bosonic Topological Phases in $1 + 1$D, and a Constraint on the Central Charge for the Critical Points between Bosonic Symmetry Protected Topological Phases*, Nucl. Phys. **B919,** 470 (2017).

[107] Under the antiunitary $\mathbb{Z}_2^T$ mapping $\tilde{X}_{A,n} := Z_{B,n-1}^\dagger X_{A,n} Z_{B,n}$, $\tilde{X}_{B,n} = Z_{A,n} X_{B,n} Z_{A,n+1}^\dagger$, $\tilde{Z}_{A,n} := Z_{A,n}^\dagger$, and $\tilde{Z}_{B,n} := Z_{B,n}^\dagger$, we have $H_{\text{triv}} \leftrightarrow H_{\text{SPT}}$ with H_{SSB} being invariant.

[108] As in the $\mathbb{Z}_2 \times \mathbb{Z}_2$ case in Sec. II, this follows from noting that the limiting Hamiltonian H_{SPT} is a stabilizer code such that $Z_{A,n} X_{B,n} Z_{A,n+1}^\dagger = +1$ in the ground state.

[109] J. Motruk, E. Berg, A. M. Turner, and F. Pollmann, *Topological Phases in Gapped Edges of Fractionalized Systems*, Phys. Rev. B **88**, 085115 (2013).

[110] D. Meidan, E. Berg, and A. Stern, *Classification of Topological Phases of Parafermionic Chains with Symmetries*, Phys. Rev. B **95**, 205104 (2017).

[111] X. Chen, Y.-M. Lu, and A. Vishwanath, *Symmetry-Protected Topological Phases from Decorated Domain Walls*, Nat. Commun. **5**, 3507 (2014).

[112] D. M. McAvity and H. Osborn, *Energy-Momentum Tensor in Conformal Field Theories near a Boundary*, Nucl. Phys. **B406**, 655 (1993).

[113] D. M. McAvity and H. Osborn, *Conformal Field Theories near a Boundary in General Dimensions*, Nucl. Phys. **B455**, 522 (1995).

[114] P. Liendo, L. Rastelli, and B. C. van Rees, *The Bootstrap Program for Boundary* CFT$_d$, J. High Energy Phys. 07 (2013) 113.

[115] M. Bill, M. Caselle, D. Gaiotto, F. Gliozzi, M. Meineri, and R. Pellegrini, *Line Defects in the 3d Ising Model*, arXiv:1304.4110.

[116] D. Gaiotto, D. Mazac, and M. F. Paulos, *Bootstrapping the 3d Ising Twist Defect*, J. High Energy Phys. 03 (2014) 100.

[117] F. Gliozzi, P. Liendo, M. Meineri, and A. Rago, *Boundary and Interface CFTs from the Conformal Bootstrap*, J. High Energy Phys. 05 (2015) 036.

[118] M. Billò, V. Gonçalves, E. Lauria, and M. Meineri, *Defects in Conformal Field Theory*, J. High Energy Phys. 04 (2016) 091.

[119] M. Fukuda, N. Kobayashi, and T. Nishioka, *Operator Product Expansion for Conformal Defects*, J. High Energy Phys. 01 (2018) 013.

[120] E. Lauria, M. Meineri, and E. Trevisani, *Spinning Operators and Defects in Conformal Field Theory*, J. High Energy Phys. 08 (2019) 066.

[121] M. A. Metlitski, *Boundary Criticality of the O(N) Model in $d = 3$ Critically Revisited*, arXiv:2009.05119.

[122] P. Dey and A. Söderberg, *On Analytic Bootstrap for Interface and Boundary CFT*, J. High Energy Phys. 07 (2021) 013.

[123] A. Antunes, *Conformal Bootstrap near the Edge*, arXiv:2103.03132.

[124] E. Lauria, P. Liendo, B. C. van Rees, and X. Zhao, *Line and Surface Defects for the Free Scalar Field*, J. High Energy Phys. 01 (2021) 060.

[125] C. P. Herzog and A. Shrestha, *Two Point Functions in Defect CFTs*, J. High Energy Phys. 04 (2021) 226.

[126] By symmetry fractionalization, gapped phases admit a fine-tuned choice of unitary string operator which would give the membrane operator long-range order—indeed, it gives one route to the classification of 2D gapped SPT phases [5]—but this object is exceedingly difficult to access in practice (away from fixed-point limits).

[127] J. Zhao, Z. Yan, M. Cheng, and Z. Y. Meng, *Higher-Form Symmetry Breaking at Ising Transitions*, Phys. Rev. Research **3**, 033024 (2021).

[128] X.-C. Wu, C.-M. Jian, and C. Xu, *Universal Features of Higher-Form Symmetries at Phase Transitions*, SciPost Phys. **11**, 033 (2021).

[129] J. L. Cardy, *Operator Content of Two-Dimensional Conformally Invariant Theories*, Nucl. Phys. **B270**, 186 (1986).

[130] One should be mindful of marginal perturbations when these exist. See the discussion in Sec. V C where charge assignments can swap when tuning along the moduli space of $c = 1$ CFTs. This does not occur for the Ising CFT.

[131] M. Schuler, S. Whitsitt, L.-P. Henry, S. Sachdev, and A. M. Läuchli, *Universal Signatures of Quantum Critical Points from Finite-Size Torus Spectra: A Window into the Operator Content of Higher-Dimensional Conformal Field Theories*, Phys. Rev. Lett. **117**, 210401 (2016).

[132] A. Thomson and S. Sachdev, *Spectrum of Conformal Gauge Theories on a Torus*, Phys. Rev. B **95**, 205128 (2017).

[133] S. Whitsitt, M. Schuler, L.-P. Henry, A. M. Läuchli, and S. Sachdev, *Spectrum of the Wilson-Fisher Conformal Field Theory on the Torus*, Phys. Rev. B **96**, 035142 (2017).

[134] A. Belin, J. de Boer, and J. Kruthoff, *Comments on a State-Operator Correspondence for the Torus*, SciPost Phys. **5**, 60 (2018).

[135] M. Schuler, S. Hesselmann, S. Whitsitt, T. C. Lang, S. Wessel, and A. M. Läuchli, *Torus Spectroscopy of the Gross-Neveu-Yukawa Quantum Field Theory: Free Dirac versus Chiral Ising Fixed Point*, Phys. Rev. B **103**, 125128 (2021).

[136] H. W. J. Blöte and Y. Deng, *Cluster Monte Carlo Simulation of the Transverse Ising Model*, Phys. Rev. E **66**, 066110 (2002).

[137] This is a direct consequence from noting that since it is derived from a symmetry, the defect line commutes with the stress-energy tensor; remembering how the latter encodes the dependence of the action on the metric, the claim follows.

[138] Similar to the discussion in Sec. VIII A, this works only in the absence of spontaneous symmetry breaking: If P_C is broken, then there are ground states with opposite charge, whereas if P_A or P_B is broken, the twisted sector can have level crossings without leaving the phase.

[139] B. Yoshida, *Topological Phases with Generalized Global Symmetries*, Phys. Rev. B **93**, 155131 (2016).

[140] B. Yoshida, *Gapped Boundaries, Group Cohomology and Fault-Tolerant Logical Gates*, Ann. Phys. (Amsterdam) **377**, 387 (2017).

[141] More precisely, it will flow to the cubic fixed point if we preserve the symmetry between the three sublattices, otherwise, it will flow to Ising × O(2); nevertheless, the critical exponents of both CFTs are very similar to those of the O(3) CFT, differing only beyond the third decimal [142].

[142] S. M. Chester, W. Landry, J. Liu, D. Poland, D. Simmons-Duffin, N. Su, and A. Vichi, *Bootstrapping Heisenberg Magnets and their Cubic Instability*, Phys. Rev. D **104**, 105013 (2021).

[143] A. Aharony, *Critical Behavior of Anisotropic Cubic Systems*, Phys. Rev. B **8**, 4270 (1973).

[144] J. M. Carmona, A. Pelissetto, and E. Vicari, *N-Component Ginzburg-Landau Hamiltonian with Cubic Anisotropy: A Six-Loop Study*, Phys. Rev. B **61**, 15136 (2000).

[145] M. Hasenbusch and E. Vicari, *Anisotropic Perturbations in Three-Dimensional* O(N)-*Symmetric Vector Models*, Phys. Rev. B **84**, 125136 (2011).

[146] L. T. Adzhemyan, E. V. Ivanova, M. V. Kompaniets, A. Kudlis, and A. I. Sokolov, *Six-Loop Expansion Study of Three-Dimensional n-Vector Model with Cubic Anisotropy*, Nucl. Phys. **B940**, 332 (2019).

[147] M. Dupont, S. Gazit, and T. Scaffidi, *From Trivial to Topological Paramagnets: The Case of $\mathbb{Z}_2$ and $\mathbb{Z}_2^3$ Symmetries in Two Dimensions*, Phys. Rev. B **103**, 144437 (2021).

[148] G. Vidal, *Class of Quantum Many-Body States That Can Be Efficiently Simulated*, Phys. Rev. Lett. **101**, 110501 (2008).

[149] L. Zhang and F. Wang, *Unconventional Surface Critical Behavior Induced by a Quantum Phase Transition from the Two-Dimensional Affleck-Kennedy-Lieb-Tasaki Phase to a Néel-Ordered Phase*, Phys. Rev. Lett. **118**, 087201 (2017).

[150] L. Weber, F. P. Toldin, and S. Wessel, *Nonordinary Edge Criticality of Two-Dimensional Quantum Critical Magnets*, Phys. Rev. B **98**, 140403(R) (2018).

[151] Y. Xu, X.-C. Wu, C.-M. Jian, and C. Xu, *Topological Edge and Interface States at Bulk Disorder-to-Order Quantum Critical Points*, Phys. Rev. B **101**, 184419 (2020).

[152] X.-C. Wu, Y. Xu, H. Geng, C.-M. Jian, and C. Xu, *Boundary Criticality of Topological Quantum Phase Transitions in Two-Dimensional Systems*, Phys. Rev. B **101**, 174406 (2020).

[153] R. Verresen, *Topology and Edge States Survive Quantum Criticality between Topological Insulators*, arXiv:2003.05453.

[154] R. Thorngren, A. Vishwanath, and R. Verresen, *Intrinsically Gapless Topological Phases*, Phys. Rev. B **104**, 075132 (2021).

[155] N. Anand, V. X. Genest, E. Katz, Z. U. Khandker, and M. T. Walters, *RG Flow from φ^4 Theory to the 2D Ising Model*, J. High Energy Phys. 08 (2017) 056.

[156] R. Dijkgraaf, E. Verlinde, and H. Verlinde, *$c = 1$ Conformal Field Theories on Riemann Surfaces*, Commun. Math. Phys. **115**, 649 (1988).

[157] P. Ginsparg, *Curiosities at $c = 1$*, Nucl. Phys. **B295**, 153 (1988).

[158] E. B. Kiritsis, *Proof of the Completeness of the Classification of Rational Conformal Theories with $c = 1$*, Phys. Lett. B **217**, 427 (1989).

[159] This charge is not well defined in the symmetry-breaking phase. E.g., if $J = +\infty$, then $Z_{A,n} = \pm 1$, so both $(\prod_{m \leq n} X_{B,m}) Z_{A,n+1}$ and $\prod_{m \leq n} X_{B,m}$ have long-range order.